NTNU
Norwegian University of
Science and Technology

Characterization of a combined downward jet for protected zone ventilation reducing exposure risk of occupants to indoor pollutants

Jonas Stokkeland Fuglseth

Preface

This thesis is written at the Department of Energy and Process Engineering at NTNU Trondheim. Laboratory experiments and the writing of the report was done during autumn of 2016 and winter 2017.

This thesis concludes my status as a student.

I would like to thank Guangyu Cao for being flexible in defining the ramifications of this thesis considering I started during the spring semester.

I would also like to thank Marie Steffensen, Hanne Trydal and Amar Aganovic for their help and cooperation discussing possible solutions, helping with practical issues and flexibility in the setup and completion of my experiments. A special thank you to Håkon Kiær for support in statistical error calculations and Inge Håvard Rekstad and Reidar Tellebon in the construction of the experimental diffuser.

Completing the thesis proved challenging, but through extended literature research, scrutinizing experimental results and possible theoretical models, I am satisfied the main goal has been achieved.

I hope you enjoy reading this.

Jonas Fuglseth
Molde, March 12th, 2017

Sammendrag

Målet med avhandlingen er å karakterisere luftdistribusjonen fra en kombinert jet og modellere hastighetsfordelingen. Målet oppnås ved å analysere utgangshastighetene fra luftventilene, hastighetstapet fra de to strømmene sammenlignet med teoretiske formler, måle defleksjonen av strømningen, og til slutt modellere den dimensjonsløse hastighetsprofilen for strømningen ved bruk av «Excess velocity method». Den kombinerte jetten er en mulig forbedring av «Protected occupied zone ventilation» (beskyttet sone ventilasjon), som tar sikte på å redusere eksponering av forurensninger for personer. Urbanisering og strengere regulering på energibruk av ventilasjonsanlegg øker risikoen for innendørs eksponering av miljøgifter og luftbårne patogener. Ventilasjonssystemer som håndterer problemet er nødvendig. En kombinert jet dannes ved å danne en luftgardin fra en spalte-diffuser og en parallelstrømning fra en perforert plate. Vindmålere og en røykmaskin brukes til å måle og analysere strømningen. Den kombinerte jetten avbøyes bort fra parallelstrømningen og avbøyningsvinkelen øker med høyere hastighet på parallelstrømningen, mens hastighetstapet reduseres. Ekspansjonshastigheten av hastighetsprofilen, målt ved $y_{1/2}$ er opp til 2,5 ganger så stor sammenlignet med en luftgardin uten parallelstrømning. Det er sannsynlig at luftgardinen stjeler moment fra parallelstrømningen, og denne effekten øker jo større hastigheten til parallelstrømmen er. «Excess velocity method» er lovende i å skape en modell for den kombinerte jetten, men med ubesvarte potensielle begrensninger. Videre arbeid må analysere samspillet mellom luftgardinen og parallelstrømningen, og strømninger fra perforerte plater behøver mer nøyaktige modeller for hastighetstap.

Abstract

The objective of the dissertation is to characterize the air distribution of a combined downward jet and to obtain a model of the velocity distribution. The objective is achieved through analyzing the initial outlet conditions of the diffusers, the velocity decay from the two flows, measuring the deflection of flow and finally modelling the dimensionless velocity profile of the flow using the excess velocity method on the co-flow. The combined downward jet is a possible improvement of the protected occupied zone ventilation, which aim to lower the exposure of contaminants to the occupant. Urbanization and stricter regulation on energy use of ventilation systems increase the risk of indoor exposure to pollutants and airborne pathogens. Ventilation systems that address the problem are needed. A combined downward jet is formed by introducing a plane jet from a slot diffuser and a co-flow from a perforated plate diffuser. Anemometers and a smoke machine is used to measure and analyze the flow. The combined downward jet deflects away from the co-flow and the deflection angle increase with higher co-flow velocity, while the velocity decay decrease. The expansion rate of the velocity profile, measured at $y_{1/2}$, increase up to 2.5 times that of a plane jet without co-flow. There is likely the plane jet steal momentum from the co-flow, and the rate increase with the co-flow velocity. The excess velocity method show promise in creating a model for the combined downward jet, however with unanswered potential limitations. Future work need to analyze the interaction the plane jet has on the co-flow, and the co-flow needs accurate models for its velocity decay.

Contents

Abbreviations

ACH	Air Change Hourly
ATD	Air Terminal Device
UN	United Nations
HVAC	Heating, Ventilation and Air Conditioning
LAF	Laminar Air Flow
LEV	Local Exhaust Ventilation
OR	Operating Room
PIV	Particle Image Velocimetry
POV	Protected Occupied zone Ventilation
PV	Personal Ventilation
SBS	Sick Building Syndrome
USB	Universal Serial Bus

Nomenclature

Latin symbols

A_0	$[m^2]$	Effective area of diffuser opening
A	$[m^2]$	Gross area of diffuser
b_0	$[m]$	Height of the half plane of a slot opening
C_0	$[-]$	Velocity decay constant
C_1	$[-]$	Velocity decay constant
C_d	$[-]$	Discharge coefficient
D_0	$[-]$	Dimensionless distance from plane jet outlet
h_0	$[m]$	Height of slot opening
K-factor	$[-]$	Velocity decay constant
K_v	$[-]$	Velocity decay constant
R_a	$[-]$	Degree of perforation, factor between 0 and 1
Re	$[-]$	Reynolds number
u	$[m/s]$	Specific velocity
u_{excess}	$[m/s]$	Excess velocity, velocity when removing co-flow velocity
$u_{co-flow}$	$[m/s]$	Velocity of co-flow
U_0	$[m/s]$	Outlet velocity of primary flow diffuser
U_1	$[m/s]$	Outlet velocity of co-flow diffuser
U_c	$[m/s]$	Maximum velocity, velocity at flow centerline
U_m	$[m/s]$	Maximum velocity, velocity at flow centerline
V_r	$[-]$	Velocity ratio, primary flow velocity divided by co-flow velocity
$\overline{x}_0$	$[m]$	Length of potential core
x	$[m]$	Distance from normal plane of diffuser outlet
$y_{1/2}$	$[m]$	Distance from the point of maximum velocity to its half velocity
y	$[m]$	Distance in the plane normal to its velocity vector

Greek symbols

η	$[-]$	Dimensionless distance, $[y/y_{1/2}]$
σ_1	$[-]$	Velocity decay constant
α	$[-]$	Velocity ratio, equal to "V_r"
α_1	$[°]$	Angle of inner sheer layer of plane compound jets
φ_1	$[-]$	Sheer layer constant of compound plane jets
φ_2	$[-]$	Sheer layer constant of compound plane jets

Chapter 1 - Introduction

1.1 Problem statement

In society today the majority of people live in cities. According to the UN, urbanization is expected to continue further into the century. Energy standards in countries across the globe trend to lower the energy consumption of HVAC, the effect of which is lower ventilation rates [1]. Traditional air distribution systems rely on the principle of dilution to eliminate contaminants. In an article by Bolashikov et al. [2] it is pointed out that the mixing effect might actually increase the occupants exposure to contaminants. In order to not get infected by airborne pathogens the ventilation system need to supply sufficient contaminant free air to the occupant.

Protected occupied zone ventilation address this problem by introducing an air curtain to divide the room into sub-zones. Experiments by Cao et al. [3] and Xu et al. [4] show that the use of an air curtain has the ability to significantly improve protection from pollutants and cross-infection. In this thesis the air curtain is examined with a co-flow on one side, similarly to solutions used in many operating theaters [5]. Introducing a secondary flow in parallel with an air curtain, the combined jet has potential to improve pollutant protection. Precise characterization of the flow from the combined jet is lacking in the literature.

1.2 Objective of this study

The goal of this thesis is to characterize the air distribution of a combined downward jet. The characteristics considered are initial flow conditions, velocity decay, velocity distribution and flow expansion. The tasks are to conduct a literature review of air distribution methods for protected occupied zone ventilation and to obtain a model for the velocity distribution of the combined downward jet.

The objectives are reached by doing a literature review of all relevant literature of protective ventilation systems and to obtain the theoretical foundation needed to evaluate the characteristics of the flow from the combined downward jet. When the characteristics are analyzed, attempts to model the flow can be done.

The thesis is organized with a literature review in chapters 2 and 3. Chapter 2 reviews the current protective ventilation solutions, and chapter 3 reviews the theory of plane jet flow, flow from perforated plates, co-flow and combined downward jet flow. Chapter 4 explain the methodology of the experimental work. Chapter 5 presents the results from the experiments with plane jet flow, flow from a perforated plate ATD and the combined downward jet at different velocity ratios, $V_r=U_0/U_1$, ranging from 1.5 to 7.5. The excess velocity method is an attempt to model the flow from the combined downward jet with the use of dimensionless velocity profiles known from co-flow theory. The method simplify the combined jet flow to fit well established

theory. In chapter 6 the results from the experiments are discussed and compared with theory and chapter 7 has the conclusion and recommendations of future work.

Chapter 2 - Protection by ventilation

The task of ventilation is to heat or cool air and exchange used air [6]. In Norway the current housing standard "TEK 10" define ventilation as "The building should have ventilation adapted to the pollution- and moisture load to ensure satisfying air quality." In other words, not especially specific with regards to which degree of protection the occupant can expect from pollution such as airborne pathogens. Carrier et al. [7] summarize existing research into the correlation between ventilation rates, disease spread and SBS. The article conclude there is some correlation, but results are not consistent. A review article by Li et al. [8] show a correlation between the directions of airflow movement and spread of infectious diseases. The reason for non-conclusive results when comparing ventilation rates to disease spread Li et al. suggest that studies for the most part tunnelvision toward rates alone, without considering the direction of airflow movement. With increasing focus on minimizing the spread of disease, air distribution methods addressing the problem has been developed. This chapter will go on to summarize air distribution methods that focus on exposing the occupants to pollution free air.

2.1 Local Exhaust Ventilation

LEV reduce the occupants risk of exposure to contaminants by extracting the pollutant directly from its source. The solution is good in an environment where the source of pollution is easily detected and stationary. The solution is widely used in industrial processes and there is a new solution that extract air from hospital beds, which reduce exposure to contaminants by up to 70% with ventilation only and 96% together with local air cleaning [9]. While the solution has a high efficiency, it has a limited scope of operation. In office environments the solution is not applicable, since occupants move around.

2.2 Piston Ventilation

Piston ventilation is used as an "overkill" option to avoid contamination. Supply air often use directional tubes to create "laminar" airflow, or more correctly, low turbulence airflow. For hospital applications, the most common configuration is LAF ATD's in the ceiling with extract on the side walls or directly underneath the operating table. It is mostly used in operating theaters where contaminants must be kept to a minimum to avoid infections in operating wounds. LAF ATD's are a popular choice, but the supply air velocity needs to be high to overcome thermal plumes and disturbances in airflow from surgeons moving around. Piston ventilation is based on brute-force to function and an ACH of 100 and even higher is typical [10]. A review by Memarzadeh et al. [11] show that of 12 ventilation strategies for protecting a patient in an operating theatre, a downward LAF array with extract on the side walls is the most successful in protecting the patient.The results suggest that the most important part is the flow pattern, once the optimal air pattern is obtained a further increase in airflow does not increase protection efficiency.

2.3 Personal Ventilation

PV protects the occupant by supplying a high degree of fresh air directly to the breathing zone. Traditional PV deliver air from ATD's mounted in a variety of positions on a office desk, however multiple articles by Yang et al. [12][13] present a solution which can be classified as PV, but with the ATD mounted in the ceiling. A big issue with PV is the challenge of placing the feed lines for supply air to the workstation, which is overcome when it is ceiling mounted. Although the studies of Yang et al. on this solution do not include an analysis of how ceiling-mounted PV affect the degree of contaminants the occupant is subject to, the principle is interesting.

2.4 Protected Occupied zone Ventilation

The aim of POV is to create a personal zone for an occupant, whether it is at a work space, clean room, hospital ward, operating theater or any imaginable suitable space. The basic principle is to use air curtains alone or together with physical separators to divide an occupied zone into subzones for one or multiple occupants. The air curtain can be described as a plane free jet, which is explained in chapter 3.1. Air curtains or "air doors" as it may also be called is widely used in commercial buildings to avoid high heat loss from entrances. In industry it is used in clean rooms to create protected zones for delicate processes and in operating theaters to create a protected zone around the operating table. In mines it is used to control air movement and it is used in emergency pathways to block out smoke from fire while leaving full access to the emergency exits [14]. A relative new development is to use the air curtain in offices to protect workers from cross-infection from airborne pathogens. In a study by Cao et al. [3] the air curtain is evaluated with and without a partition wall to measure the "protection effectiveness". In the study a partition wall increase the protection efficiency, but the protection efficiency seem more related to the supply air velocity than other parameters. In the study the air curtain agrees with the well established plane jet models.

In an office environment the air curtain alone is not likely to be able to supply a high enough rate of fresh air, and need to be used in co-operation with a whole-space ventilation principle as well. In a study by Cao et al. [15] the cross-infection risk due to exhaled airflows is evaluated using POV with swirl-diffusers as whole-space ventilation. In the study the swirl-diffusers are placed 1.3m from the air curtain diffuser, and the study demonstrate that the air curtain indeed can break the risk of cross-infection between people, although it require people being on either side of the air curtain to work.

In principle, the air curtain can be used in together with any whole-room air distribution system. The whole room ventilation must be chosen so it does not disrupt the flow pattern of the air curtain, and such analysis are not yet done.

Chapter 3 - Airflow distribution theory

This chapter summarize the theory needed to obtain an understanding of the main characteristics of airflow distribution. Chapter 3.1 summarizes air curtain theory, or plane jet theory as it is often called. Chapter 3.2 summarizes theory regarding flow from a perforated plate diffuser. Chapter 3.3 represent co-flow or parallel flow theory and chapter 3.4 goes through theory regarding a combined jet.

3.1 Downward plane jet

A slot with aspect ratio greater than 40 (w/h_0) can be approximated as a plane jet. The flow from a plane jet can be divided into four zones, starting with the potential core. The potential core is the zone immediately downstream from the supply opening. In this zone the centerline velocity of the jet remain constant and equal to the initial velocity, U_0. The length of the potential core depends on nozzle shape and turbulence intensity, but usually extends between 5-10 opening diameters, $D_0 = x/h_0$ [16]. The transition zone, or "characteristic decay region" as it is in called in some literature, follow the potential core zone. As its name suggest, this is the part where the flow transition to become developed. The length of the transition zone can be neglected for low aspect ratio supply openings such as square and circular openings [16]. For high aspect ratio openings, as a slot is, the length of the transition zone can last up to $20\,D_0$ [14]. According to Guyonnaud et al. [14] the velocity distribution in the potential core and transition zone can be expressed as

Figure 3.1 - Schematic of a plane jet

$$\frac{U(x,y)}{U_0} = \frac{1}{2}[1 + erf(\sigma_1 \frac{y+\frac{h_0}{2}}{x})] \qquad (1)$$

Where σ_1 is a constant of value 13.5.

The developed zone start at about $20\,D_0$, and is dominated by highly turbulent flow. The decay of the centerline velocity in this region according to Schlichting et al. [17] can be expressed as

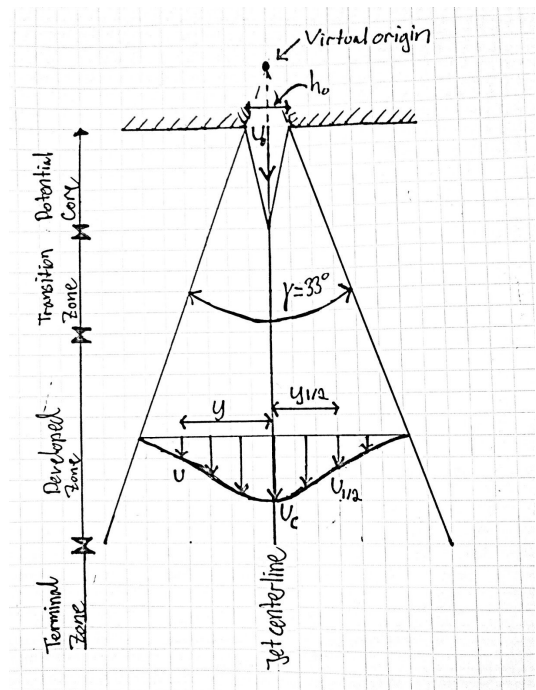$$\frac{U_c(x)}{U_0} = C_1(\frac{x}{h_0} - C_2)^{-1/2} \qquad (2)$$

Other authors have developed similar equations for the centerline velocity decay, which Awbi summarize as

$$\frac{U_c}{U_0} = K_v / \sqrt{x/h_0} \tag{3}$$

Eqn. 2 and 3 are the same as long as $C_2=0$. The value of C_1 in eqn. 2 and K_v in eqn. 3 are equal. The value of C_1 or K_v, depending on the chosen equation are according to the Goertler solution 2.4. In the Tollmien solution it is 2.67 and Rajaratnam recommend a value of 2.47, which all are similar. The velocity distribution in the developed zone is expressed by Awbi as an Gaussian error curve where

$$u/U_c = exp(-0.693\eta^2) \tag{4}$$

Where $\eta = y/y_{1/2}$ and $y_{1/2} = 0.1x$ and x is the distance from the diffuser.

Schlichting et al. [17] describe the velocity distribution as

$$\frac{U(x,y)}{U_0} = \frac{\sqrt{3}}{2}\sqrt{\frac{7.67h_0}{x}}[1 - tanh^2(7.67\frac{y}{x})] \tag{5}$$

Equation 4 and 5 describe the same, the velocity distribution. Eqn. 4 expresses the velocity distribution by dimensionless means, while equation 5 expresses the specific velocity distribution. An example of the velocity distribution of eqn. 5 is found in figure 3.2.
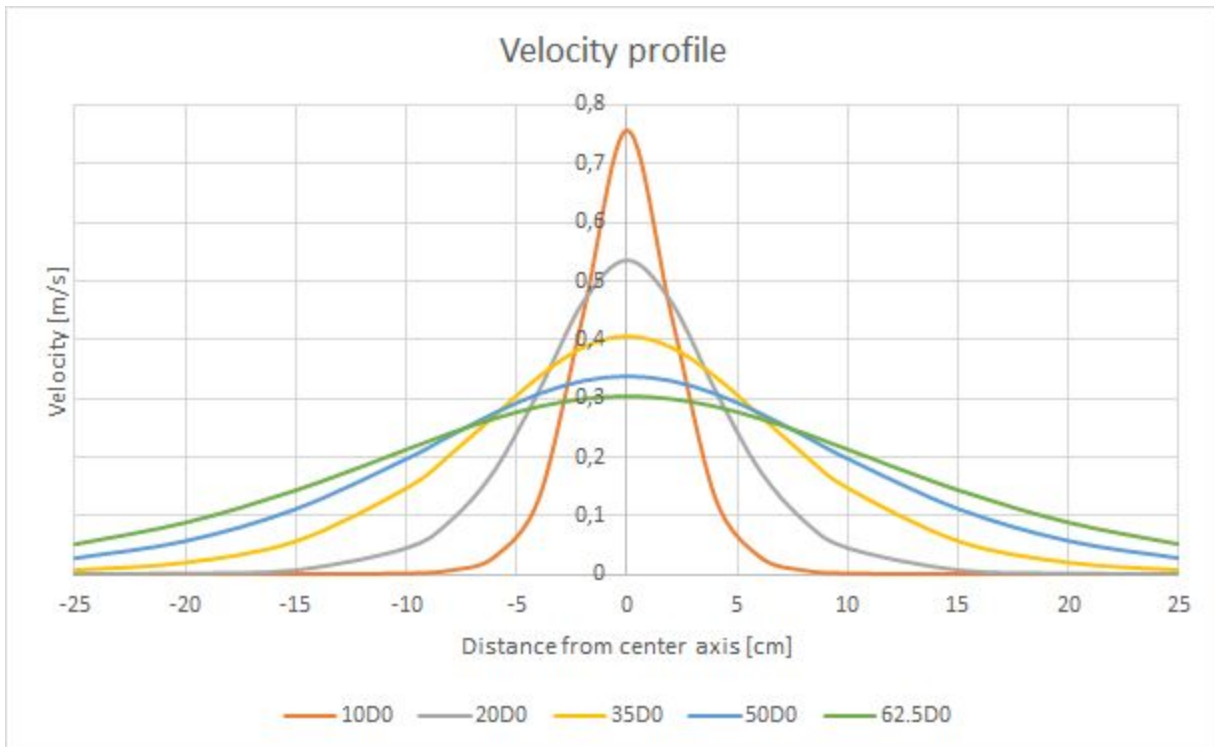

Figure 3.2 - The Schlichting velocity profile, plot of eqn. 5 with h_0=2 cm and U_0=1 m/s

The developed region is defined for a plane jet in Awbi to be from 5-100D_0 , but the exact region is not defined as it vary with the nozzle configuration. In an article by Namer et al. [18] the potential core last to about 4D_0 where self-similarity is achieved at about 40D_0. The asymptotic growth of the jet continue anywhere from 25D_0 until 200D_0. With new experimental setups, the actual length of zones need to be found experimentally while theory supply some general expectations.

In the terminal region the velocity of the jet rapidly diffuse and the jet become indistinguishable from the surrounding room air [16]. Depending on the initial velocity of the jet and the distance to opposing surface, the terminal zone might become an impinging zone. If the distance is short enough and the speed is high enough the impinging zone comprise about 15% of the total jet height [14].

3.2 Downward perforated plate ATD

The flow from a perforated plate is considered complicated, since it essentially is flow from thousands of different holes which can have a huge range of configurations [10]. This includes the shape of the holes, the spacing between them, the degree of opening area compared to the total area, the thickness of the plate, the angle of the orifice and flow properties. Awbi [16] presents a model to the velocity decay from perforated plates in his book, but the model is highly general and is only specified for plates with a perforation, or "free area" as he calles it, up to 20%. The free area is the same as the area of the sum of openings. There is not made any comments as to the applicability of the model for perforations above 20% and it can be argued that the model could work for a higher degree of perforation if it is made some adjustments to the k-factor.

The equation for the velocity decay in the developed zone is defined as

$$\frac{U_c}{U_0} = K_v/(x/\sqrt{A_0}) \qquad (6)$$

U_0 in eqn. 6 for a perforated plate is the same as U_c in eqn. 8 or 9. K_v is equal to 4 for perforated plates with perforation of 20% and outlet velocities down to 2.5m/s which is the closest to the plate used in this thesis, at 33%. A_0 is the effective area, and is defined as

$$A_0 = C_d A \qquad (7)$$

A is the free area, which is the same as the degree of perforation times the gross area of the perforated plate. C_d is the discharge coefficient which is $0.65 < C_d < 0.9$. For perforations with sharp edges C_d is equal to 0.65. With a perforated plate a constant velocity core is formed from the coalescence of individual jets, similar to the potential core of the free jet, this zone last to about 5 equivalent diameters. In this zone the velocity is equated as

$$U_c = 1.2 U_0 \sqrt{C_d R_a} \qquad (8)$$

Where R_a is the ratio of free area to gross area of the perforated plate.

If the perforations have sharp edges eqn. 8 according to Awbi [16], reduces to

$$U_c = U_0 \sqrt{R_a} \qquad (9)$$

3.3 Co-current flow

Co-current flows are similar to flows issuing into quiescent air. The main difference is that the potential core is extended and the boundary layers of the two flows gradually merge before the velocity profile is transformed into the parabolic distribution of Poiseuille flow [17]. Rajaratnam [19] sum up the relationships to calculate the length of the potential core, velocity distribution and angles of shear layers seen in figure 3.3.
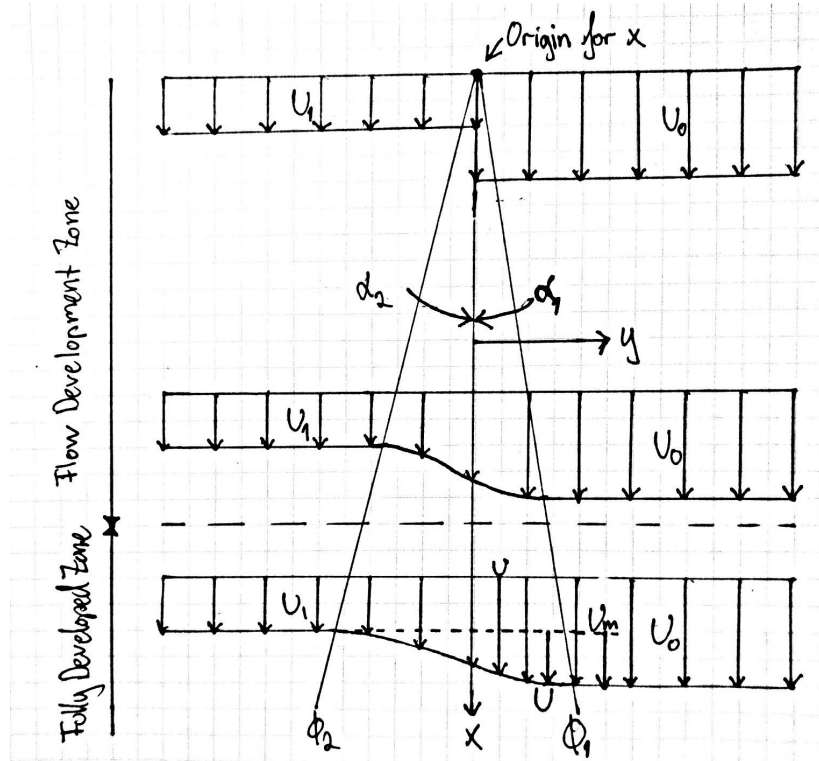

Figure 3.3 - Schematic of co-current flow

The equation for the similarity curve of co-flow presented by Rajaratnam is

$$U/U_m = exp[-0.6749\eta^2(1 + 0.027\eta^4)] \tag{10}$$

The curve show a satisfactory relation for V_r from 0.2 to 6.64. The velocity decay in the developed region is

$$U_m/\sqrt{U_0(U_0 - U_1)} = 3.41/\sqrt{x/b_0} \tag{11}$$

The variable b_0 is the same as $\frac{1}{2}h_0$ and rewriting the equation it is

$$U_m/\sqrt{U_0(U_0 - U_1)} = 2.41/\sqrt{x/h_0} \tag{12}$$

If the speed of the co-flow is 0, eqn. 12 is the same as eqn. 3, $\frac{U_c}{U_0} = K_v/\sqrt{x/h_0}$,with K_v equal to 2.41, which is approximately the same as for the Goertler solution.

9

Rajaratnam suggest that the length of the potential core can be calculated as

$$\bar{x}_0 = \frac{1}{2}h_0\frac{1}{tan(\alpha_1)}$$

(13)

Where α_1, as seen in figure 3.3, can be calculated as

$$\alpha_1 = tan^{-1}(0.087\frac{\alpha-1}{\alpha+1}\varphi_1)$$

(14)

Where φ_1 can be found graphically from figure 3.4, and

$$\alpha = V_r = \frac{U_0}{U_1}$$

(15)

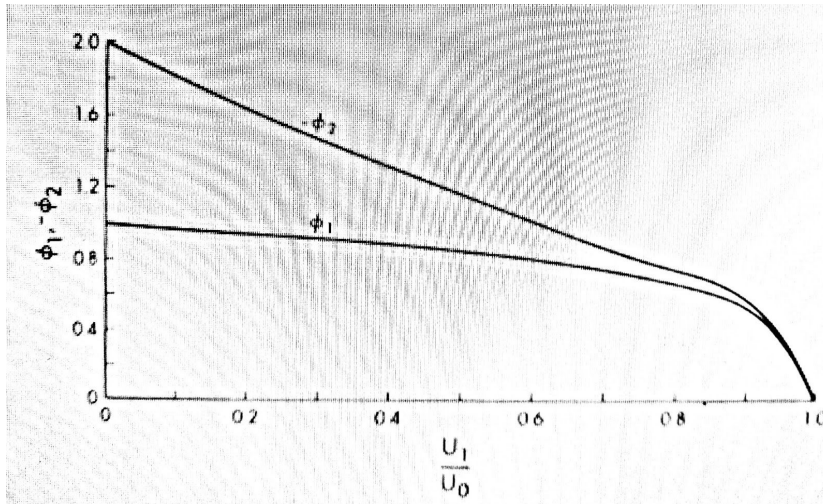Figure 3.4 - φ_1,φ_2 versus $1/\alpha$, figure copied from Rajaratnam [19]

In the book "Turbulent jets" on page 64, Rajaratnam plot the excess velocity of a plane jet in a co-flow environment to obtain a comparison of the flow to eqn. 10 with accurate comparison. The exact mechanism for the steps taken are not mentioned. The basic principle is that the excess velocity is the specific/measured velocity minus the co-flow velocity, represented in eqn. 16.

$$u_{excess} = u - u_{co-flow}$$

(16)

Regarding the development of the compound shear layers, Rajaratnam use

$$y_{1/2} = 0.115\frac{\alpha-1}{\alpha+1}x$$

(17)

Where α is equal to the velocity ratio (U_0/U_1) and x is the distance from the slot opening.

This mean the expansion of the compound shear layer decrease the higher the co-flow velocity is.

3.4 Combined downward jet

Figure 3.5 illustrate the flow configuration of the combined downward jet. Through the literature search no numerical models that describe the flow of a combined downward jet was found. This sub-chapter summarize the current literature that address the subject.

Cook et al. [5] evaluate the use of an air curtain together with a laminar airflow array for operating theatre air distribution. The experimental setup is seen in figure 3.6. In the article Cook points out that the air curtain function as a continual exhaust for the laminar airflow array (LAF), forcing the flow to expand and prevent air entrainment and helps to maintain the desired laminar velocity. The deflection of the air curtain flow is related to the velocity ratio of the flows and if the velocity ratio is too low the deflection result in a faster decaying laminar velocity and create a 'dead zone' of aging air in the centre of the LAF. PIV experimental results from the study in figure 3.7 show a constant deflection of the air curtain of about 9.5° at a V_r of about 3.3. The use of an air curtain improve effective protection area significantly, without significant increased total airflow rate, mainly because air entrainment from outside the protected zone is more or less eliminated with the use of an air curtain.
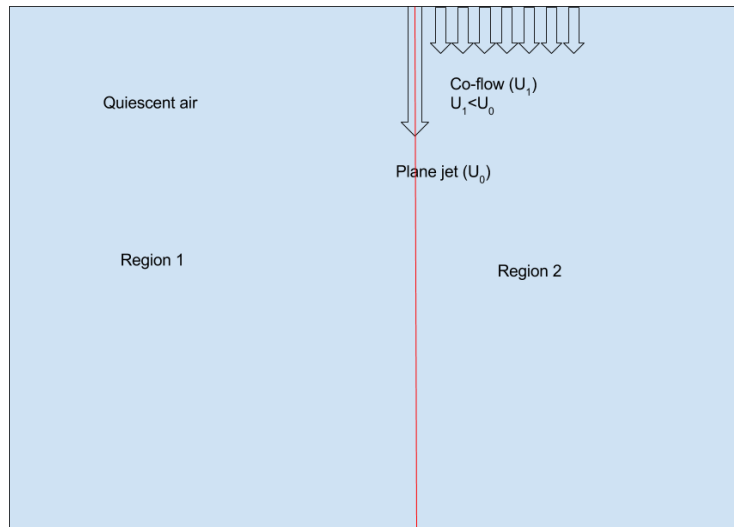

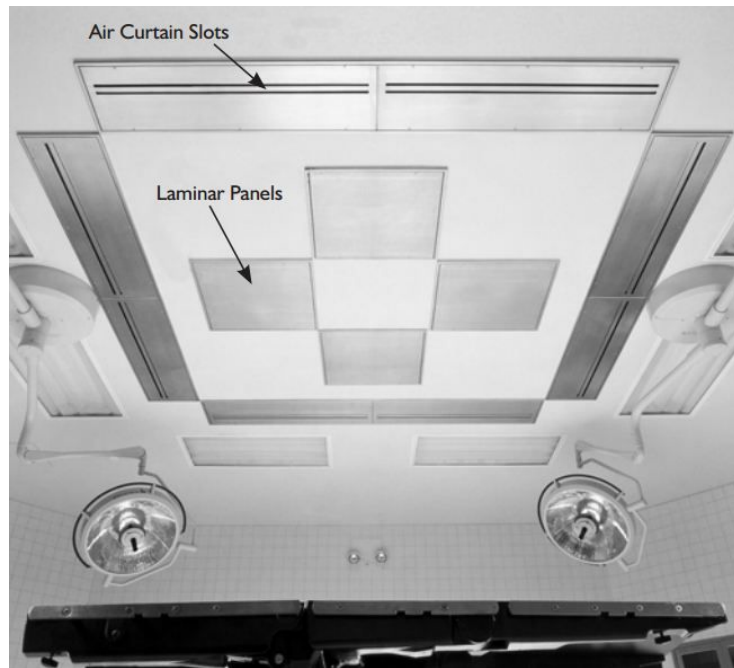Figure 3.5 - Configuration of the two flows

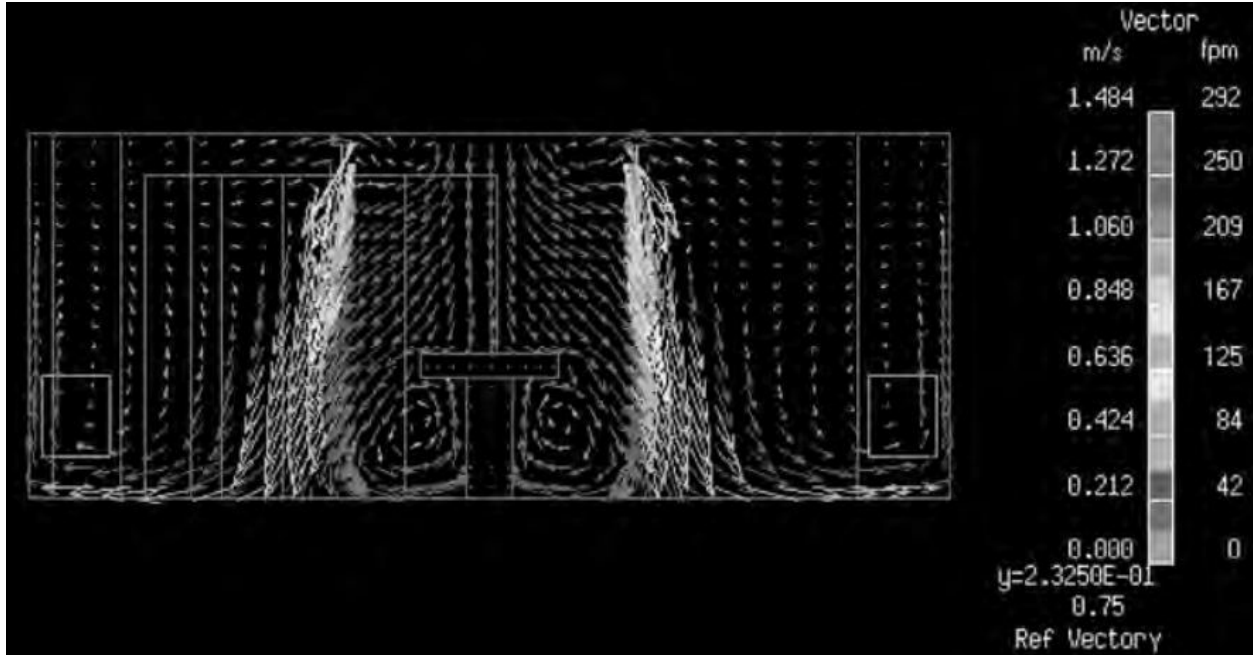

Figure 3.6 - Air curtains in OR [5]

Figure 3.7 - Velocity distribution of air curtains together with LAF in OR [5]

Since evaluating the velocity distribution of a combined jet has never been done with empirical models, the most reasonable approach is to divide the problem so it can be compared with models for co-flow and plane jet flow in quiescent air separately and create a model that unite the two approaches.

Since the excess velocity method is not described in detail, here are the main assumptions used for the method in the experiments:
It is assumed a non-ideal case where the velocity decay of the two flows are not equal, then the excess velocity is the specific/measured velocity minus the difference to the theoretical velocity, represented in eqn. 17 and illustrated in figure 3.8.

$$u_{excess} = u - \Delta u, \; where \tag{18}$$

$$\Delta u = u_{co-flow} - U_c \cdot exp[-0.6749\eta^2(1 + 0.027\eta^4)] \tag{19}$$

Where u is the measured velocity, $u_{co\text{-}flow}$ is the calculated velocity from eqn. 6 and the equation is valid for $u_{co-flow} > U_c \cdot exp[-0.6749\eta^2(1 + 0.027\eta^4)]$.

Δu is assumed equal to zero when the previous statement is not true.
Substituting eqn. 18 into eqn. 17, the excess velocity becomes

$$u_{excess} = u - \Delta u = u + U_c \cdot exp[-0.6749\eta^2(1 + 0.027\eta^4)] - u_{co-flow} \tag{20}$$

12

And the written as dimensionless velocity

$$u_{excess} = (u/U_c) + exp[-0.6749\eta^2(1+0.027\eta^4)] - (u_{co-flow}/U_c) \tag{21}$$

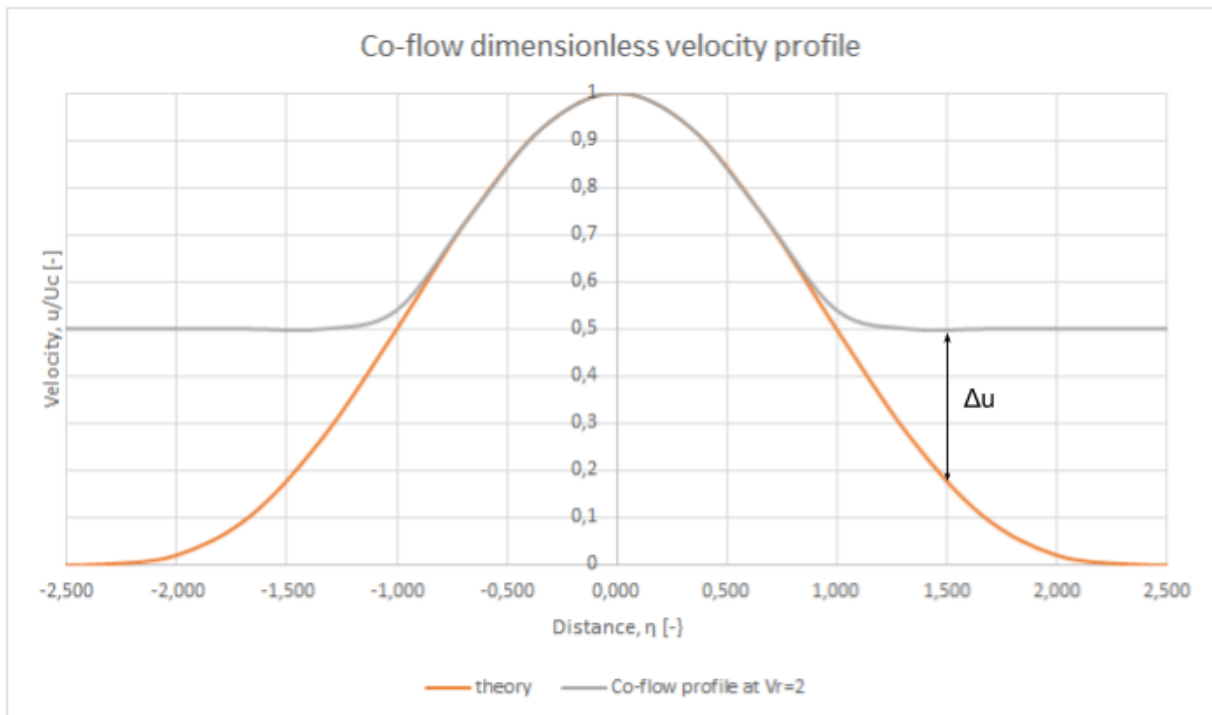Where the same assumptions as for eqn. 18 apply.

Figure 3.8 - Example of co-flow velocity profile

Chapter 4 - Experimental setup

This chapter explains the methods used in velocity distribution and visualization experiments which was conducted in the Energy and Indoor Environment Laboratory at the Department of Energy and Process Engineering at NTNU, Trondheim, Norway. The experiments took place from January 9th until January 13th 2017. The main goal of the thesis is to characterize the air distribution of a combined downward jet. Risk assessment of the experimental work can be found in appendix B.

4.1 ATD design

In this master thesis, the slot diffuser is reused from an earlier experiment by another student. The slot diffuser opening is 2.0 m long and has a width of 0.02 m. The height of the outlet slot is 0.15 m. The basic design of the slot diffuser is a 250 mm ventilation shaft which is cut in the bottom to fit the outlet slot. Inside the shaft is a perforated plate and a solid plate is placed on the perforated plate directly underneath the supply air channels, with the same shape and area as the supply channels, to even out the supply velocity distribution. The basic layout of the slot diffuser is shown in figure 4.1, and an overview of the interior build is shown in figure 4.2.
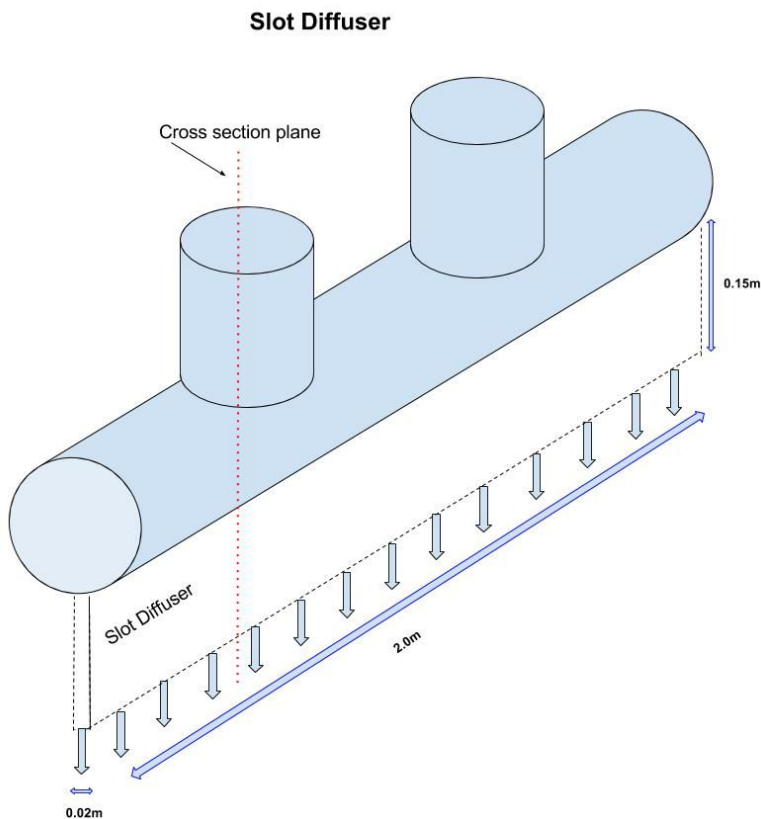

Figure 4.1 - Basic layout of the slot diffuser

Slot diffuser cross section

Supply duct

Attachment clips

Solid plate (wood)
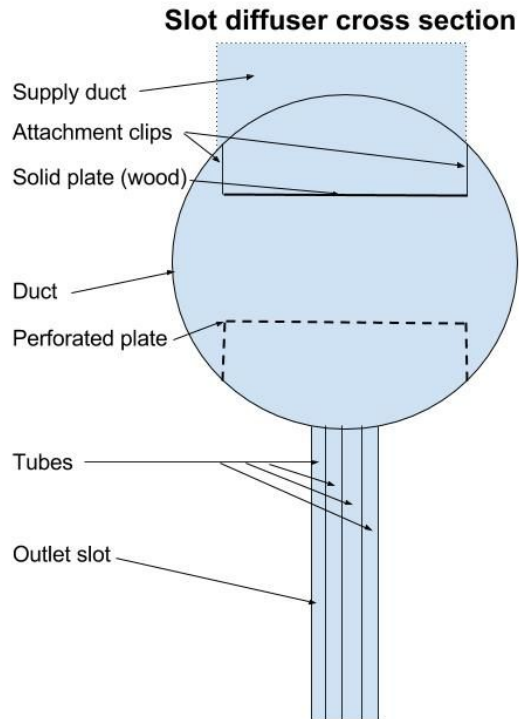
Duct

Perforated plate

Tubes

Outlet slot

Figure 4.2 - Cross section of the slot diffuser (cross section defined in figure 4.1)

The perforated plate diffuser had to be designed to fit close to the slot diffuser to achieve the co-flow situation. In effect this means the maximum height of the diffuser is 0.15 m. The main challenge of such a low diffuser height is to ensure even outlet velocity distribution. In collaboration with supervisor Guangyu Cao and technician Reidar Tellebon, the use of three layered perforated plates should increase the static pressure inside the diffuser enough to achieve satisfactory velocity distribution. The length of the diffuser is the same as for the slot diffuser, 2.0 m which is the width of the room. The diffuser is 0.8 m wide, which is wide enough that the flow cross section can be approximated as a "infinitely wide co-flow" in the range of measurements. The opening holes in the perforated plate have a diameter of 3 mm, with circular holes with sharp edges. The total opening area across the plate amount to 33% of the total area. The supply fan of the perforated plate diffuser has an outlet diameter of 250 mm, and to ensure a low air velocity into the diffuser, the supply ducts have the maximum diameter. The supply duct has a diameter of 250 mm, with a T-joint to divide the supply air into two channels and thereby effectively half the feed velocity into the diffuser. Since experiments already had been done with the slot diffuser, which showed even outlet velocities, the same distance between the feed ducts was decided, equidistant 0.5 m from each end. How the diffusers are placed with respect to each other is shown in figure 4.3 and the details of the perforated plate diffuser is shown in figure 4.4.
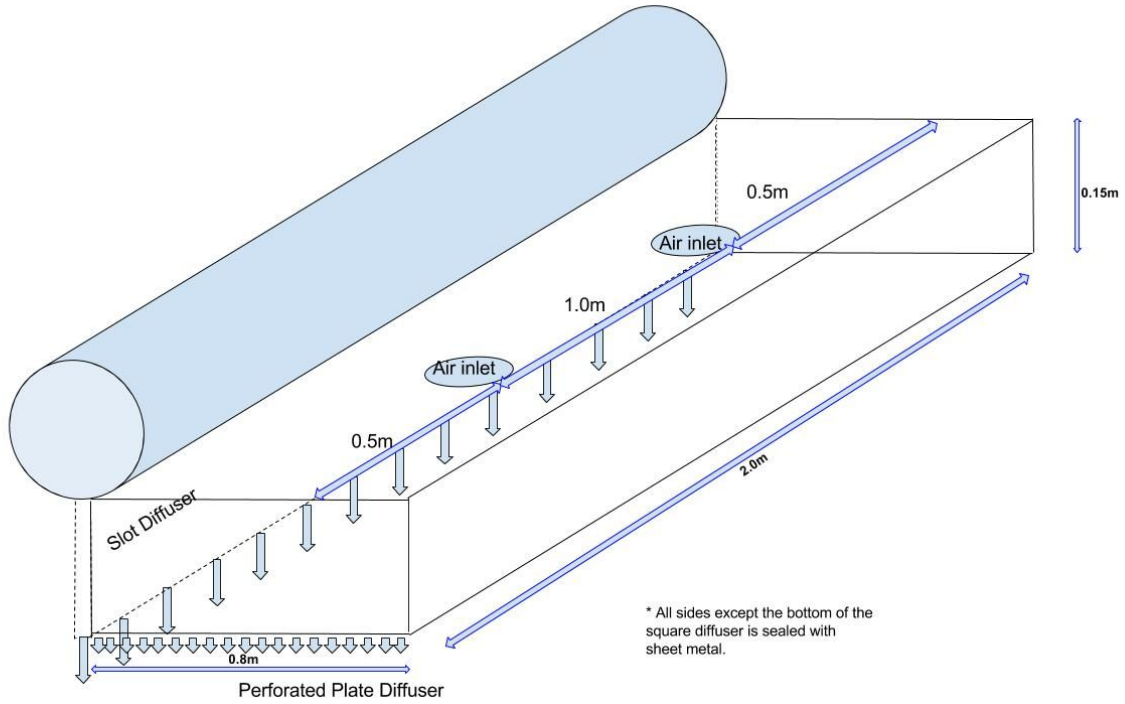
Figure 4.3 - Configuration of slot diffuser together with perforated plate diffuser
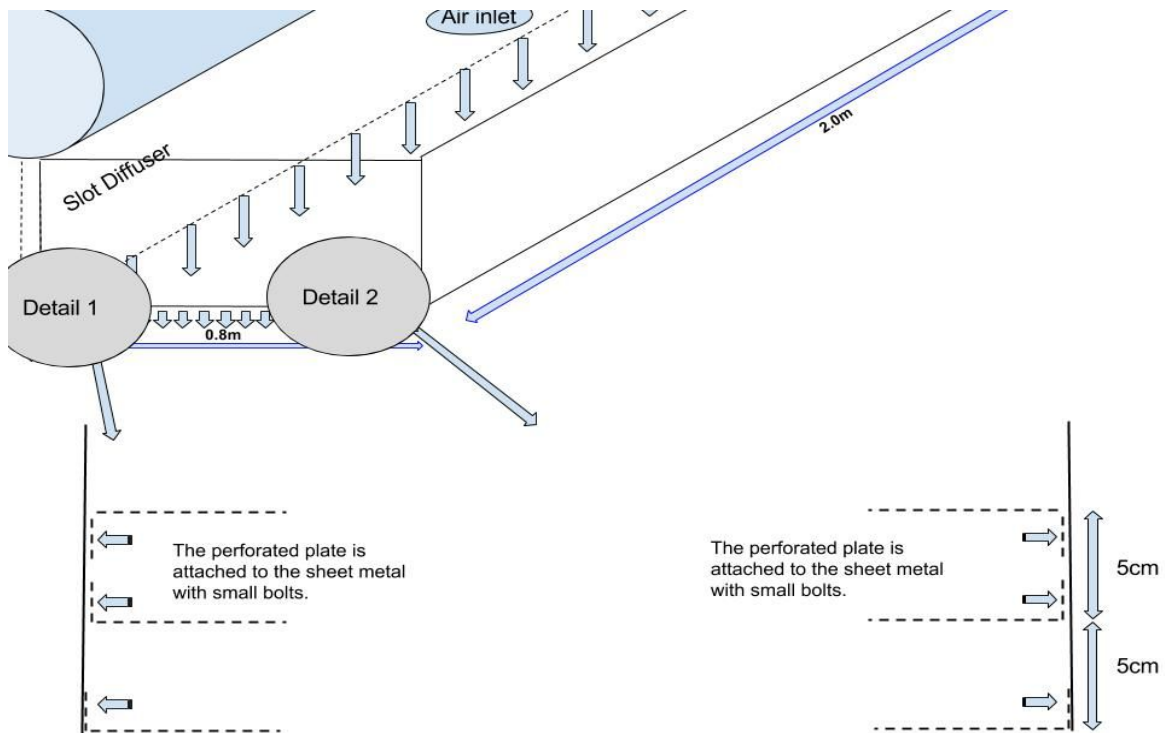
Figure 4.4 - Inside schematic of the perforated plate diffuser

4.2 Measurement locations

As mentioned in the introduction to this chapter the measurements are done at the Energy and Indoor Environment Laboratory. The laboratory has a small room in it, which is designated for controlled experiments - the climate room. Diffuser installation placement and room layout is presented in figure 4.5. The extracts are placed about 0.3 m from the ceiling and are about 1.0 m from the side walls. The extract to the right in figure 4.5 has a tube connecting to it that is leading to the floor at the left side of the diffusers, in the middle of the room about one meter from the left wall. The slot diffuser was installed before the work in this master thesis started, in which the supply ducts to the diffuser extend almost 1.0 m down from the ceiling. Without making changes to the slot diffuser, which would delay the thesis, the perforated plate diffuser was installed to accommodate the slot diffuser in it's current state. As a result the extracts are slightly higher than the supply openings of the diffusers. The room has a door on the right side in figure 4.5 and a plexiglass window on the wall with the extracts which make visualization experiments more practical.
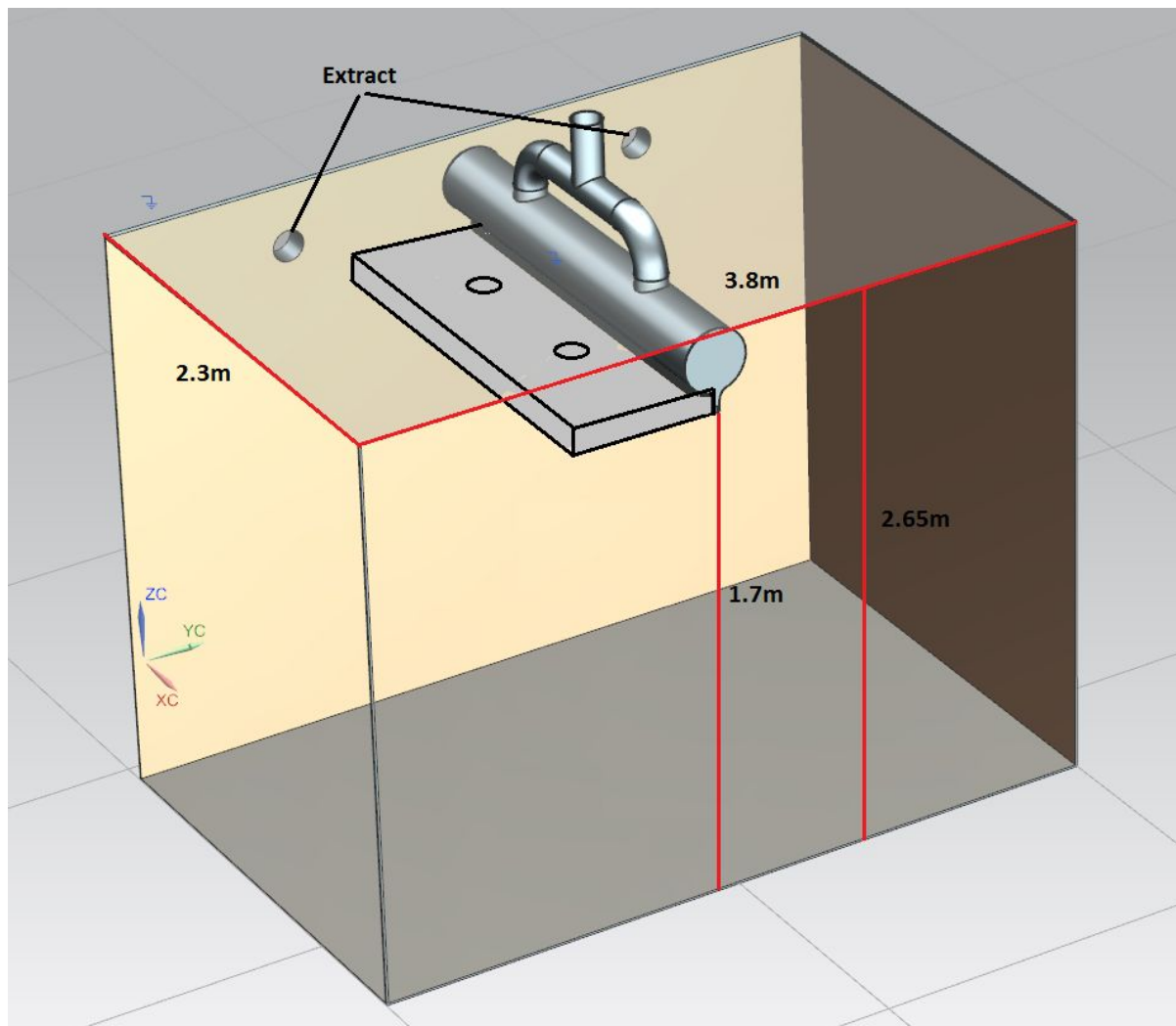
Figure 4.5 - Climate room layout with diffusers, Energy and Indoor Environment Laboratory

The initial velocities of the diffusers are measured in a grid represented in figure 4.6. A handheld anemometer is used when measuring initial velocities. Specifications of instrumentation used in the experiments are described in chapter 4.4 and full details are found in appendix A. The intercept between the red lines in the figure indicate a measurement point. The vertical and horizontal coordinates in the figure are named so each measurement point can be easily identified. The points are specified as three measurement series, S1 through S3 for the perforated plate and one series, "slot" for the slot diffuser in the vertical direction and P1 through P9 in the horizontal direction. The experiment studies four different velocity ratios for the diffusers as well as measurements of each diffuser with the other turned off. Initial velocities are measured at the start of each experiment.
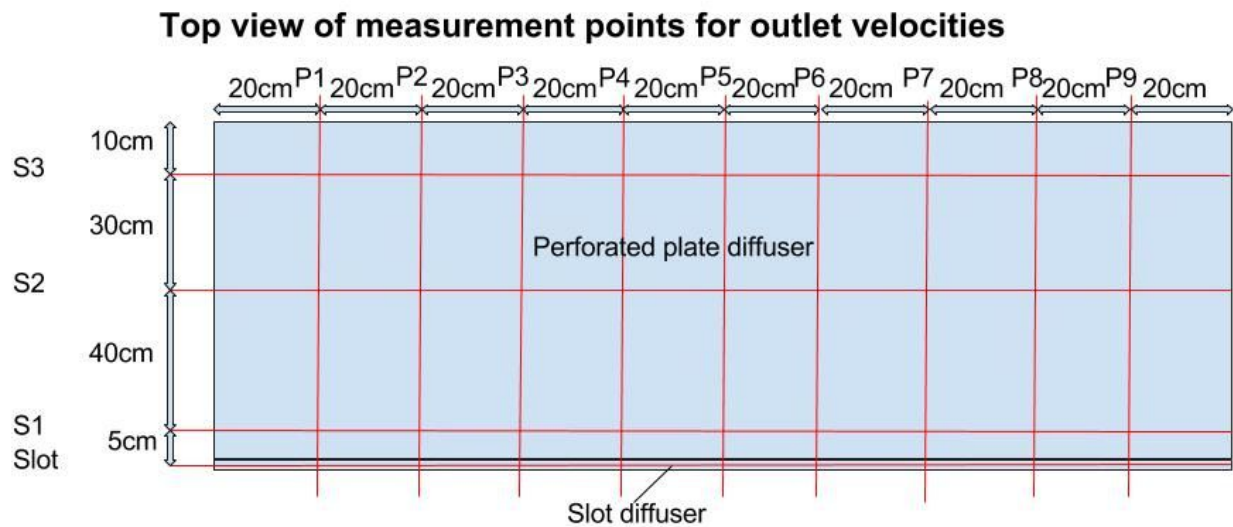
Figure 4.6 - Top view of initial outlet velocity measurement points

The velocity distribution experiments are done at one cross section of the diffusers. The cross section plane is in the y-direction in figure 4.5, at x≈1.2 m. This is the same location as a vertical line between P4 and P5 in figure 4.6. The decision to use one cross section, which is located at the same place in each experiment case, is because initial velocity measurements revealed it is the zone with the most stable velocities and that each case has a detailed velocity measurement grid. Using more than one cross section will increase the number of measurement points to an unreasonable level.

There are five anemometer probes available for the experiments. They are set up in a horizontal orientation to each other, equidistant at 4 cm. The probe configuration used in the cross section plane is provided in figure 4.7. In the figure the distance to each measurement height is (horizontal dotted lines) taken as the height from the diffuser outlets. Being downward facing diffusers the measurement heights increase the further down to the floor we go. The measurement height are selected based on previous experiments in the literature that use the same heights, this is to have a good source of comparison. The number of probe positions used at each measurement height is determined during the experiments, since the deflection of the flow is unknown. When measuring the slot diffuser while the perforated plate diffuser is turned off the number of measurement points is determined by the calculated width of the flow according to the spread angle.

Figure 4.7 - Cross section of the probe configuration used in the experiments

4.4 Preparation of the laboratory measurements

To ensure accurate measurements during experiments the measuring equipment needed to be calibrated beforehand. In the Energy and Indoor Envir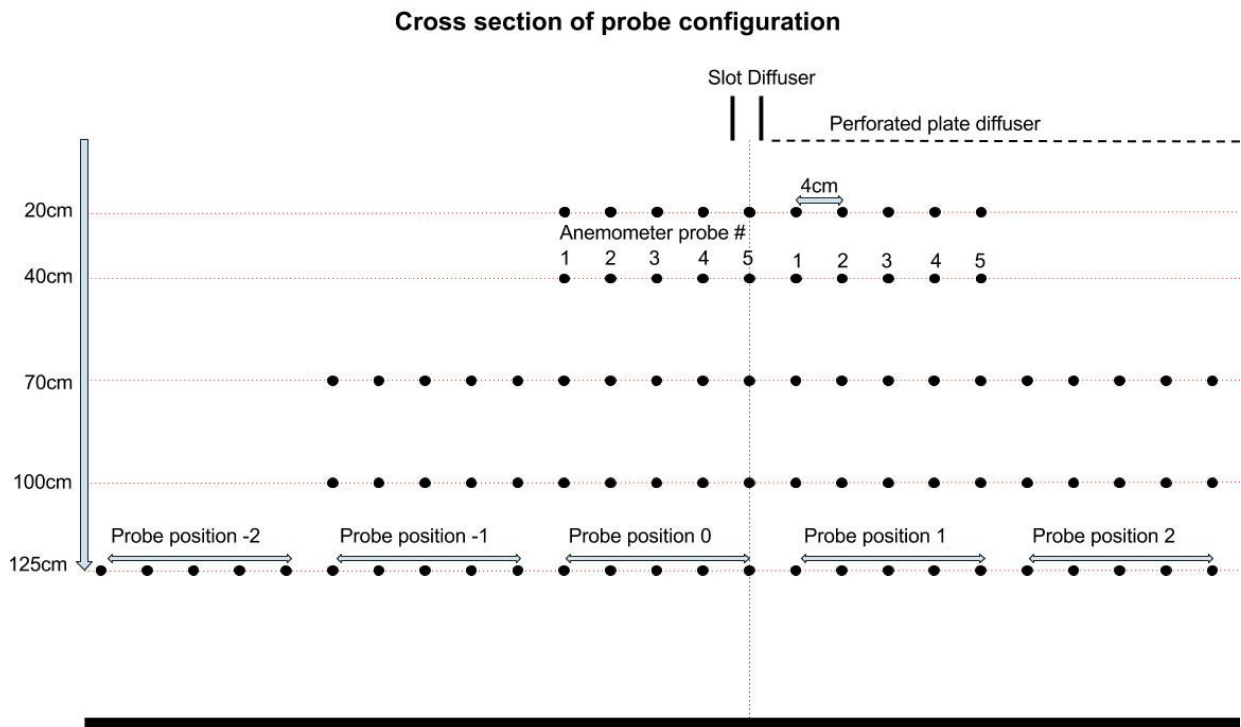onment laboratory there is a wind tunnel used to calibrate equipment. The tunnel's latest calibration is from 2012 and therefore needed to be calibrated first. During calibration of the tunnel it was apparent it was close to failure, with varying fan speeds. A new system was needed and a laminar air pressure chamber was used in which pressure difference between the inside of the chamber and outside was correlated to a pressure curve with known velocities for any given pressure. Just before commencing the experiments a new air distribution measuring system arrived, which is professionally calibrated. The new system was chosen due to its probable superior calibration.

The air distribution measuring system used is named "AirDistSys5000", delivered by Sensor-electronic. The system consist of a pressure sensor that corrects anemometer readings according to the barometric pressure, five omnidirectional anemometer probes, a wireless transmitter that transmits the readings to a USB interface that is connected to a computer and a power supply. On the computer Sensor-electronic provide software to read and log recorded data. Figure 4.8 show the components in the setup and the configuration they are used in the experiments.

The range and accuracy of sensors used in the experiments is found in table 4.1, full description of technical data of instrumentation is found in appendix A.

SensoAnemo5100LSF Transducer - Anemometer probes	
Velocity range	0.05m/s… 5.0m/s
Velocity accuracy	±0.02 m/s ±1.5% of readings
Temperature range	-10…+50 °C
Temperature accuracy	0.2 °C
TSI 962 Thermoanemometer (handheld anemometer)	
Velocity range	0m/s… 50m/s
Velocity accuracy	±3% of reading or ±0.015 m/s, whichever is greater
SensoBar 5301 Transduces - Pressure sensor	
Pressure range	500…1500 hPa
Pressure accuracy	±3 hPa

Table 4.1 - Range and accuracy of sensors
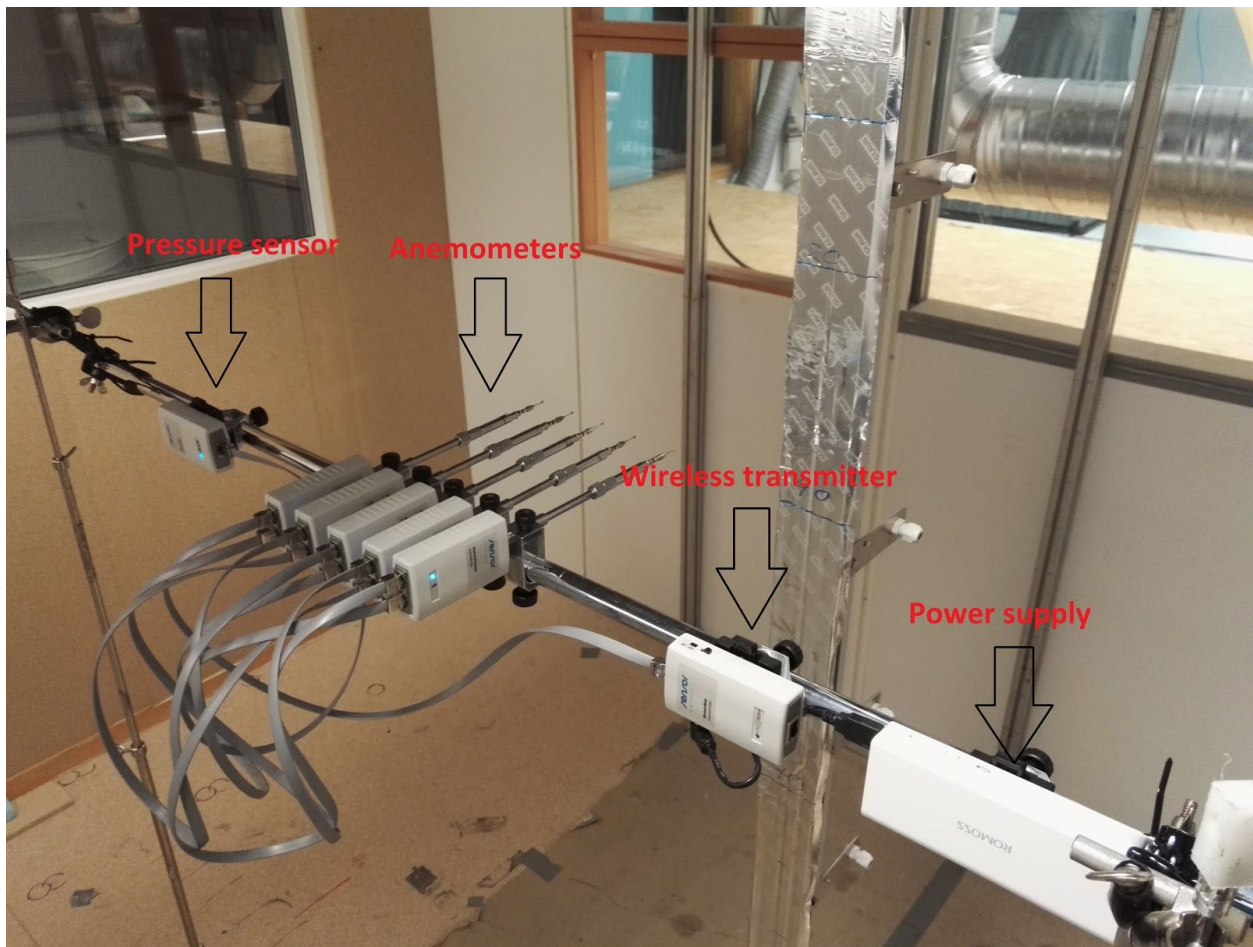
Figure 4.8 - Air distribution measurement system in its experiment setup

The handheld anemometer used when measuring initial velocities measure each point until the instrument reads a stable velocity, which is about 10 seconds per point. The anemometer probes measured at each probe position for three minutes continually before being moved to a new measurement point. Data from the probes is recorded on the computer every 2 seconds, which record temperature, velocity, pressure, turbulence intensity and standard deviation calculated by the probes. The sent data is calculated as an average value over the time between measurements.

The extract fans are axial fans with maximum air flow according to technical specifications written on the fans, 872 m^3/h per fan. After initial testing it was found that the extract on the right side of the room, according to figure 4.5 created a short circuit flow from the slot diffuser. A tube was therefore connected to the fan to extend the extract down to the floor on the left side, as described in chapter 4.2. The perforated plate diffuser is supplied by a fan with a maximum capacity of 3720 m^3/h. To adjust the airflow to the diffuser a valve needs to be manually adjusted, and comprehensive testing needed to be done to find the exact opening area of the valve to achieve the desired airflow. When the correct area was found, it was marked on the

valve so that it would be easy to adjust to the correct airflow between experiments. The slot diffuser is supplied by a central ventilation system, and the supply airflow is controlled by adjusting the main airflow at a control unit to the central ventilation system as well as electronic valves inside the laboratory. The optimal airflow and valve openings was found through testing and noted for future reference. The balance between supply and extract air was found by calculating the airflow through each diffuser based on average measured velocities from the supply and extract air.

4.5 Measurement conditions

Before experimenting with the velocity distribution from the slot diffuser and perforated plate diffuser at different velocity ratios, the diffusers are tested separately. Table 4.2 has the basic experimental properties with the diffusers tested separately. U_0 denote the initial velocity from the slot diffuser and U_1 denote the initial velocity from the perforated plate diffuser.

	U_0 [m/s]	U_1 [m/s]	Volume flow [m^3/h]
Test 1	1.5		216
Test 2	0	0.2	380.16
Test 3	0	0.5	950.4
Test 4	0	0.75	1425.6
Test 5	0	1.0	1900.8

Table 4.2 - Basic experimental properties of diffusers separately

The purpose of the tests are to establish a foundation which can be used to comparison the velocity ratio experiments with. Another reason to have the tests are to establish a correlation with known literature to validate the theoretical foundation.

There are four different velocity ratios used in the experiments, 1.5, 2.5, 3.0 and 7.5. The velocity ratio is defined in eqn. 15 as the slot velocity divided by the co-flow velocity. The velocity ratios are selected based on the range of previous experiments on co-flow, which range up to velocity ratios of about 7. Table 4.3 contain the basic properties of the diffusers in the co-flow experiments.

Velocity ratio	U_0 [m/s]	U_1 [m/s]	Re slot	Total volume flow [m^3/h]
V_r=1.5	0.6	0.4	787	846.72
V_r=2.5	1	0.4	1312	904.32
V_r=3	1.5	0.5	1968	1166.4
V_r=7.5	1.5	0.2	1968	596.16

Table 4.3 - Experiment properties of the combined downward jet

During the experiments the door to the room is closed at all time to prohibit any outside disturbance and measurements of extract flow is measured to ensure balanced ventilation. Some of the extract air capacity was lost due to the increased pressure loss in the extension tube. The velocities from the combined jet were set lower in order to balance supply and extract air. In order to maintain balanced ventilation the total volume flow had to be reduced from its original design, and that is the reason the initial test velocities are not all the same as for the velocity ratio experiments. Although the velocities are not the same, the velocity distribution models can still be validated, and the different velocities are of no consequence to the experiment results.

Smoke visualization tests are done when the room is cleared of all technical equipment to avoid damage. The purpose of the smoke visualization tests are to reveal the flow pattern and velocity distribution in an apparent way, since the anemometer probes only record the velocity magnitude and not the direction. The smoke test also function as an confirmation technique to the results from the anemometers where careful examination of the video can reveal deflection angles, spread and velocities. The smoke test can also shed light on the stability of the flow and entrainment vortices which the anemometers cannot. A black fabric is placed on the opposite wall of the camera to achieve the highest contrast to the white smoke and the fabric is marked at specific locations so it is possible to evaluate distance from the video. Since the static pressure in the supply channel is too high for the smoke from the smoke machine to enter, the smoke is released inside the room near or underneath the diffusers. The central ventilation system outside the test room is set to maximum extract during smoke test to clear the smoke leaving the test room as quickly as possible.

Error estimation is carried out for each experiment. In the results chapter the errors are presented as error bars in selected figures. The errors are calculated as instrumentation percentage error of measured value plus instrumentation fixed error plus standard error. Standard error is calculated as standard deviation divided by the square root of number of measurements. Since the measurements are done over a three minute period with values being recorded every two seconds, the number of data points are sufficient enough that it seems appropriate to use standard error rather than standard deviation. With instrumentation error added on top of standard error, the overall error estimate is more than generous. Initial velocity measurements using the handheld anemometer use only instrumentation error, since the results are recorded analog.

The main points in this chapter is to give a clear picture of the room geometry, placement of measuring equipment during experiments, how the equipment is set up and which experiments are done. The next chapter present the findings from the experiments and they are presented in the same order as they are presented in this chapter, with initial measurements first, then diffuser tests and finally velocity ratio experiments.

Chapter 5 - Results

In this chapter results from the experiments are presented. First in chapter 5.1 results about the downward plane jet are presented, then in chapter 5.2 results from the perforated plate diffuser are presented and finally in chapters 5.3-5.7 the velocity ratio experiments are presented. The velocity ratio experiments are the main area of interest in this dissertation. Results about the downward plane jet and perforated plate diffuser are meant to establish a foundation which the velocity ratio experiments later can be compared with. In each sub-chapter the initial outlet conditions are presented first, then velocity decay, velocity profile and at last dimensionless velocity profiles.

5.1 The downward plane jet

The downward plane jet is only tested at an outlet velocity of 1.5 m/s. Since 1.5 m/s is the highest velocity of the plane jet during all of the experiments it is the velocity deemed to yield the most accurate comparison to theory. Since it is the highest momentum of the jet, it is least disturbed by outside disturbances such as random room air movement. Outlet velocities are presented in figure 5.1. The measurement points are explained in figure 4.6 and the measurement plane in which further measurements are done is between P4 and P5. The average outlet velocity presented in figure 5.1 is 1.54 m/s. The supply temperature is equal to the average room temperature at 22 $^{\circ}$C and the average turbulence intensity is measured 20 cm from the slot at 4.8%.
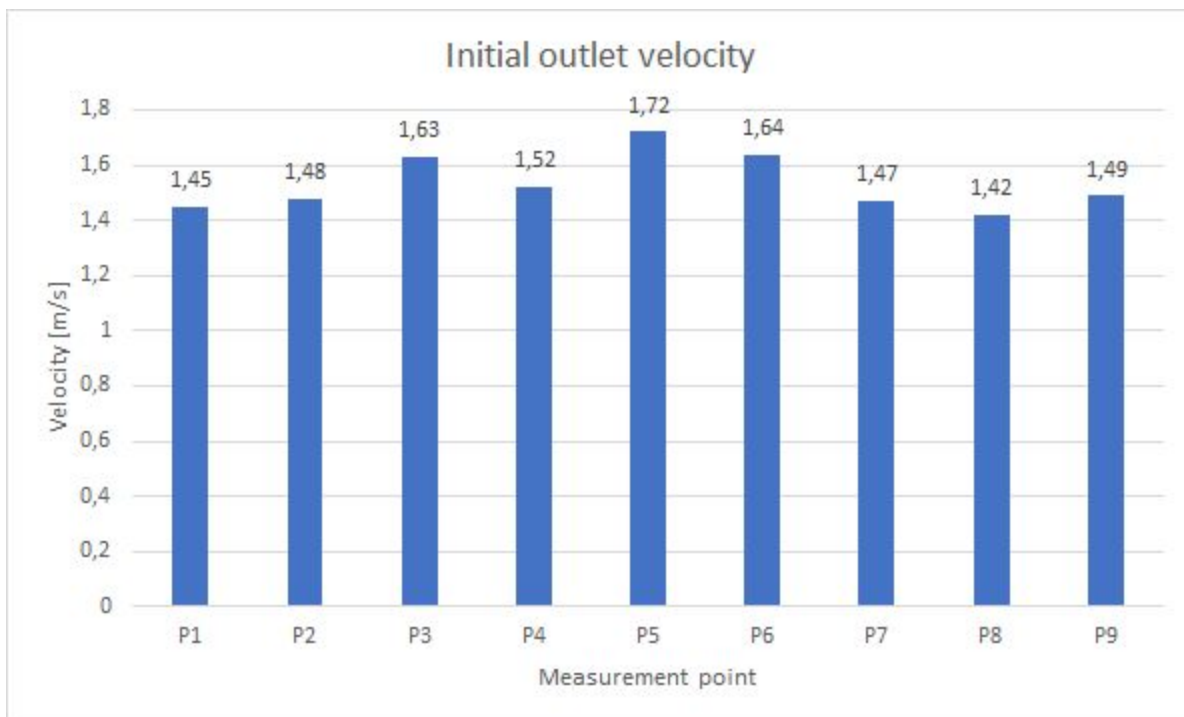
Figure 5.1 - Initial outlet velocity of the downward plane jet

In figure 5.2 the measured maximum centerline velocity is compared with the theoretical models. The distance from the slot opening is given as number of opening diameters, D_0. D_0 is equal to x/h_0 where h_0 is the height of the slot. The different models used for the developing region and the developed region do not overlap. One explanation is that they are used in different regions with have different flow development and are not meant to create continuity with each other. The Schlichting model for the developing region use σ_1=13.5 as is the recommended value according to Schlichting. The models for the developed region use C_1 and K_v equal to 2.47 from respectively Schlichting and Awbi. Eqn. 5 is an equation for velocity distribution, however if y=0 in the equation, it can be used to find the centerline maximum velocity. It is found that equation 5 yields the exact same curve slope as eqn. 2 and 3, with an equivalent k_v-factor of 2.4. The average k_v-factor from measured velocities in the developed region remained stable at around 2.5.
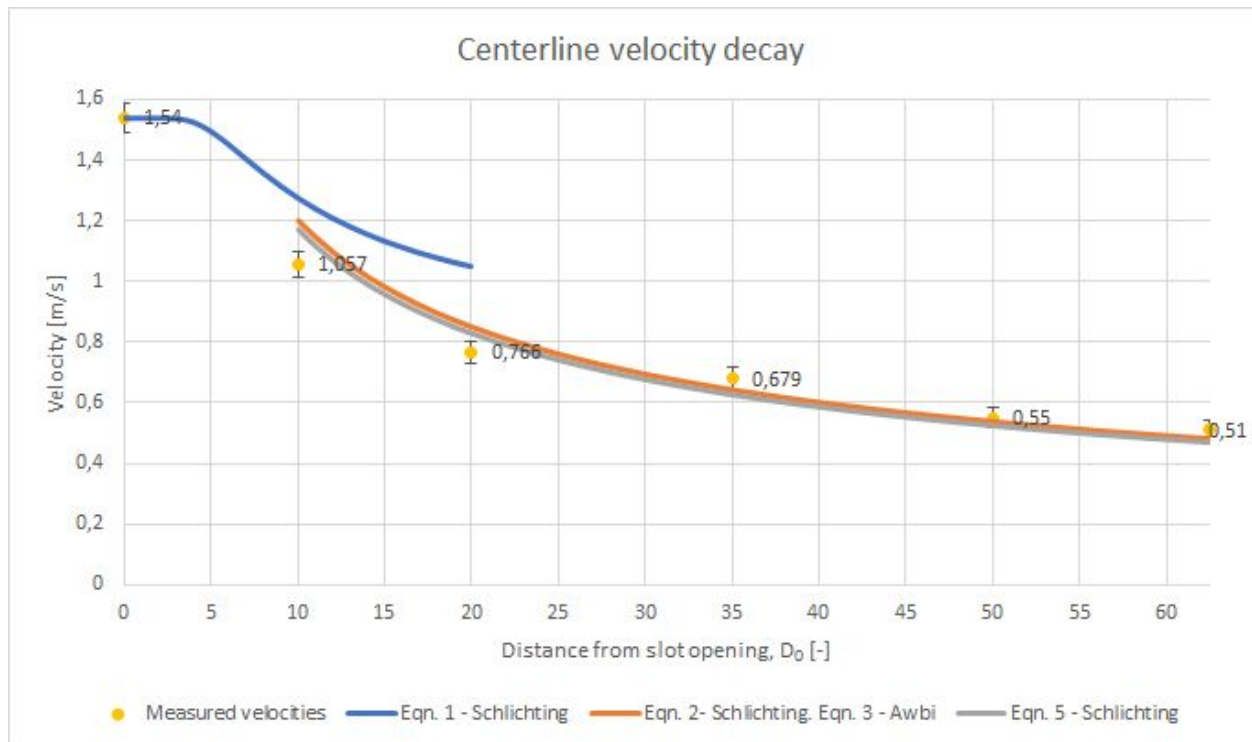
Figure 5.2 - Velocity decay in the centerline of the downward plane jet with error bars

Figure 5.3 show the velocity profile of the flow at the five measurement heights, from $10 \geq D_0 \leq 62.5$. The figure is a "real" view of the velocity profile without correcting for deflection of the flow. The deflection at $20D_0$ is about 1 cm to the right, at $35D_0$ it is about 4 cm, at $50D_0$ it is 10 cm and at $62.5D_0$ it is 4 cm from the center axis. Slight misdirection of the slot itself, the tubes inside the slot and the mounting of the entire diffuser can affect the initial outlet angle which need to be considered. Slight variations in deflection of the jet centerline from the center

axis due to room air movement is also to be expected. Perhaps the main explanation of the deflection is the placement of extracts, since they are designed for flow from both the slot and perforated plate diffusers simultaneously have a focused extract at the right side in figures which is at the side of the slot which has the perforated plate diffuser in parallel.
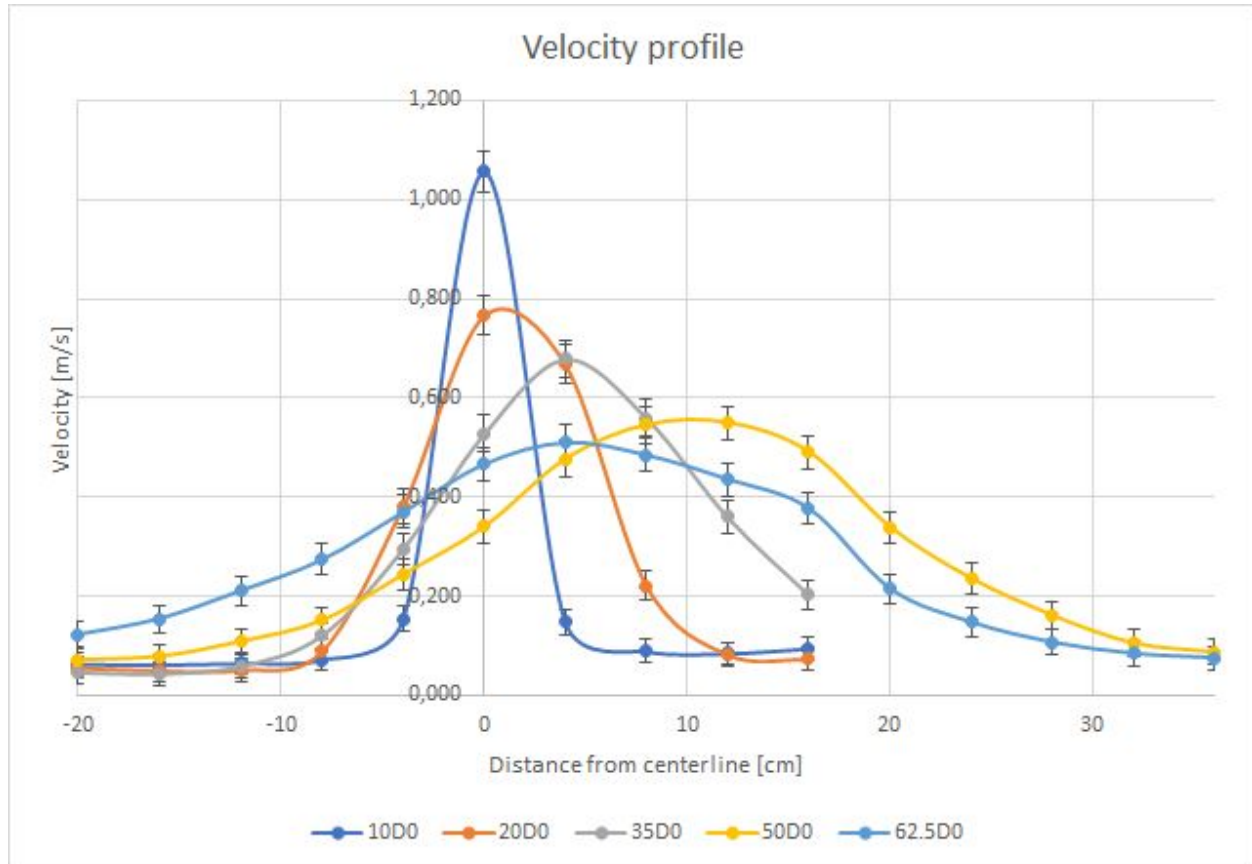
Figure 5.3 - Velocity profile of the downward plane jet with error bars

Figure 5.4 show the dimensionless velocity profile of the flow from the slot. The measured velocities at their respective heights are compared with the Gaussian error curve from equation 4 which is the generally accepted model for the flow profile from a plane jet. The difference from the Gaussian error curve in the measurements generally increase with the dimensionless distance, η. The velocity measurements never reach zero, as there is slight room air disturbance and some effects from entrainment air velocities. The distance $y_{1/2}$ is calculated at each measurement height graphically from plots of the measurements as the distance from the point of maximum velocity to the point where the velocity is half of the maximum velocity, illustrated in figure 3.1. In the theoretical models $y_{1/2}$ develops at a rate of 0.1 times the distance from the slot opening, however $y_{1/2}$ might differ from the theoretical models, and need to be confirmed by measurements. In this case $y_{1/2}$ developed as 0.119x, 19% higher than in the theoretical model of Awbi. At measurement distances close to the slot opening there is a chance that the actual jet maximum velocity is between measuring probes, due to the jet width being narrow, however this risk minimizes with increasing distance distance from the slot opening as the width of the jet increase.
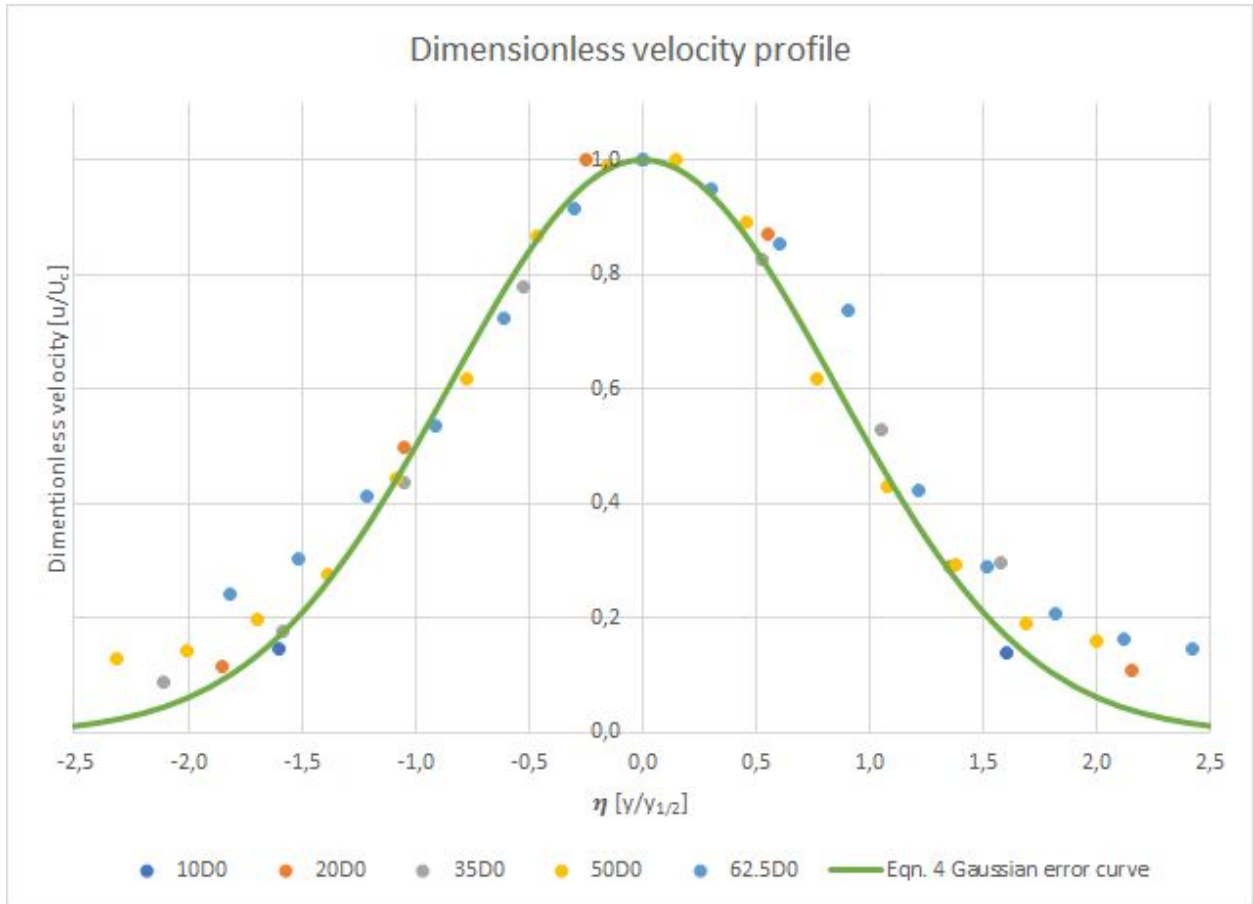
Figure 5.4 - Dimensionless velocity profile of the downward plane jet

5.2 The perforated plate diffuser

Stabilizing the evenness of the outlet flow from the perforated plate diffuser proved a challenge. Although three perforated plates are used inside the diffuser in order to even the flow, the results from the tests show great variation in outlet velocities. Table 5.1-5.4 show measured outlet velocities. The location of measurement points on the diffuser is explained in figure 4.6. Measuring series 2 show the lowest average velocity of all the series for all target velocities and is also the series with the biggest variation between measuring points. Fortunately the most extreme velocities are recorded toward the ends of the diffuser, at P1 and P9, which are the furthest away from the cross section used in room measurements.

Measured outlet velocities [m/s]									
	P1	P2	P3	P4	P5	P6	P7	P8	P9	Average velocity [m/s]
Series 1	0.21	0.2	0.2	0.23	0.27	0.3	0.23	0.22	0.28	0.19
Series 2	0.06	0.19	0.11	0.15	0.27	0.15	0.17	0.2	0.19	0.17
Series 3	0.23	0.14	0.21	0.19	0.19	0.21	0.13	0.16	0.25	0.24

Table 5.1 - Measured outlet velocities at 0.2 m/s average velocity

Room temperature when measuring 0.2 m/s average outlet velocity is 22℃ and the average turbulence intensity 20 cm from the diffuser outlet in the room measurement plane is 8.4%.

Measured outlet velocities [m/s]									
	P1	P2	P3	P4	P5	P6	P7	P8	P9	Average velocity [m/s]
Series 1	0.68	0.42	0.56	0.54	0.55	0.8	0.45	0.65	0.95	0.62
Series 2	0.2	0.43	0.19	0.45	0.59	0.14	0.24	0.41	0.31	0.33
Series 3	0.52	0.4	0.4	0.61	0.52	0.4	0.23	0.3	0.83	0.47

Table 5.2 - Measured outlet velocities at 0.47 m/s average velocity

Room temperature when measuring 0.5 m/s average outlet velocity is 23.7℃ and the average turbulence intensity 20 cm from the diffuser outlet in the room measurement plane is 10.8%.

Measured outlet velocities [m/s]									
	P1	P2	P3	P4	P5	P6	P7	P8	P9	Average velocity [m/s]
Series 1	0.78	0.43	0.6	0.75	0.94	0.99	0.8	0.85	1.45	0.84
Series 2	0.15	0.45	0.2	0.5	0.76	0.2	0.24	0.59	0.39	0.39
Series 3	0.82	0.44	0.65	0.83	0.81	0.54	0.34	0.4	1.1	0.66

Table 5.3 - Measured outlet velocities at 0.63 m/s average velocity

Room temperature when measuring 0.75 m/s average outlet velocity is 24℃ and the average turbulence intensity 20 cm from the diffuser outlet in the room measurement plane is 11.3%

Measured outlet velocities [m/s]										Average velocity [m/s]
	P1	P2	P3	P4	P5	P6	P7	P8	P9	
Series 1	1.51	0.71	0.92	1.06	1.55	0.94	1.33	1.31	2.09	1.27
Series 2	0.19	0.65	0.3	0.72	1.13	0.21	0.35	0.75	0.5	0.53
Series 3	1.47	0.79	0.9	0.94	1.13	0.65	0.4	0.74	1.59	0.96

Table 5.4 - Measured outlet velocities at 0.92 m/s average velocity

Room temperature when measuring 1.0 m/s average outlet velocity is 24.7°C and the average turbulence intensity 20 cm from the diffuser outlet in the room measurement plane is 10.4%

In chapter 3.2 there is presented a method to estimate the velocity issuing from a perforated plate. Solving equation 6 for U_c predict the velocity at any distance from the diffuser in the developed zone. Since the solution by Awbi only specify the k-factor in the equation for perforations less than what is used in these experiments and at higher velocities, the actual k-factor for this specific diffuser is found experimentally. Following are the steps taken to calculate the k-factor.

U_0 in eqn. 6 is equal to U_c in eqn. 8 $= 1.2U_o\sqrt{C_dR_a}$, where U_0 is the average measured outlet velocity from the diffuser, C_d is equal to 0.65 since the holes in the plate have sharp edges and R_a is equal to 0.33 which is the degree of perforation in the plate. A_0 in eqn. 6 is equal to the discharge coefficient, C_d times free area, A where C_d is equal to 0.65 and the free area is total opening area which is equal to gross area times the perforation degree

$\Rightarrow A_0 = C_dA = 0.65 \cdot (1.6m^2 \cdot 0.33) = 0.3432m^2$. Eqn. 6 solving for K_v then boils down to

$\Rightarrow K_v = U_c(x/\sqrt{A_0})/U_0 = U_c(x/\sqrt{0.3432m^2})/U_0$. Using the average measured outlet velocities the results from eqn. 8 is presented in table 5.5.

Measured outlet velocity [m/s]	Calculated velocity core speed, U_c from equation 8 [m/s]
0.2	0.11
0.47	0.26
0.63	0.35
0.92	0.51

Table 5.5 - Calculated velocity core speed from equation 8

Using the calculated velocity core speed from equation 8 as U_0 in equation 6 and solving equation 6 for K_v the results are plotted in figure 5.5.
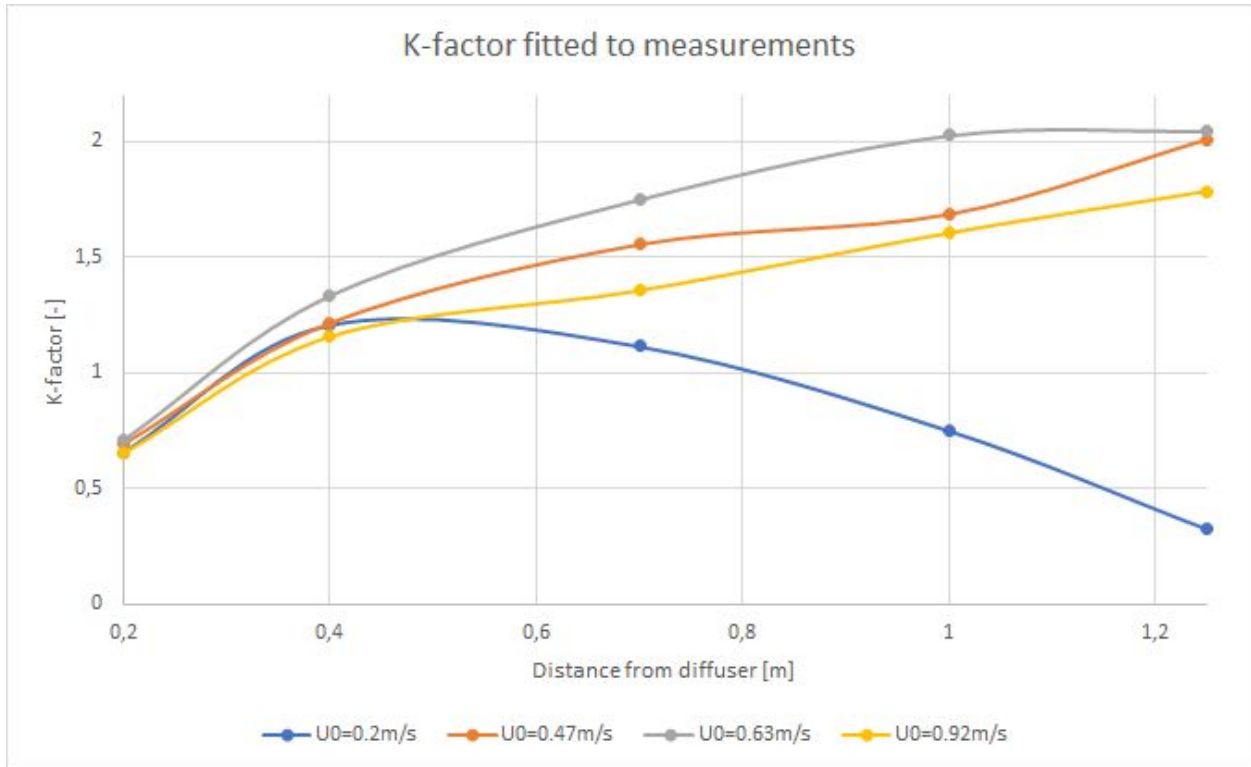
Figure 5.5 - Calculated K-factor from equation 8 with measured velocities

In figure 5.5 there is good agreement between plots for outlet velocities above 0.2 m/s, while all the plots agree at a distance between 0.2 m and 0.4 m. The main reason for the curve belonging to the outlet velocity of 0.2 m/s differs from the other curves is that the outlet velocity is so low that it quickly transitions to the terminal region. As can be seen in figure 5.6 the measured velocity after about 0.7 m is about the same as can be expected by random room air movement. Disregarding the development of the curve with the outlet velocity of 0.2 m/s all of the curves enter a linear development of the k-factor from 0.4 m. The average development of K_v can be approximated as $K_v \approx 0.824x + 0.87,\ x \in\ < 0.4m..\ 1.25m$. The flow is assumed to be in the developing region before 0.4 m since there only is a relative flat velocity in the region as seen in figure 5.6 and that K_v changes rapidly in the region as seen in figure 5.5. With a linear increase of K_v in the developed region the average K_v value for the three outlet velocities above 0.2m/s is in average K_v=1.44.

Figure 5.7 show the velocity distribution from the perforated plate diffuser across half the width of the diffuser where the x-axis in the figure represent the distance from the slot diffuser. Only the velocity distribution at 0.47 m/s outlet velocity is included in the results as the shape of the distribution is similar for all outlet velocities. As expected from the initial outlet velocity measurements in table 5.2 the velocity decreases toward the middle of the diffuser.
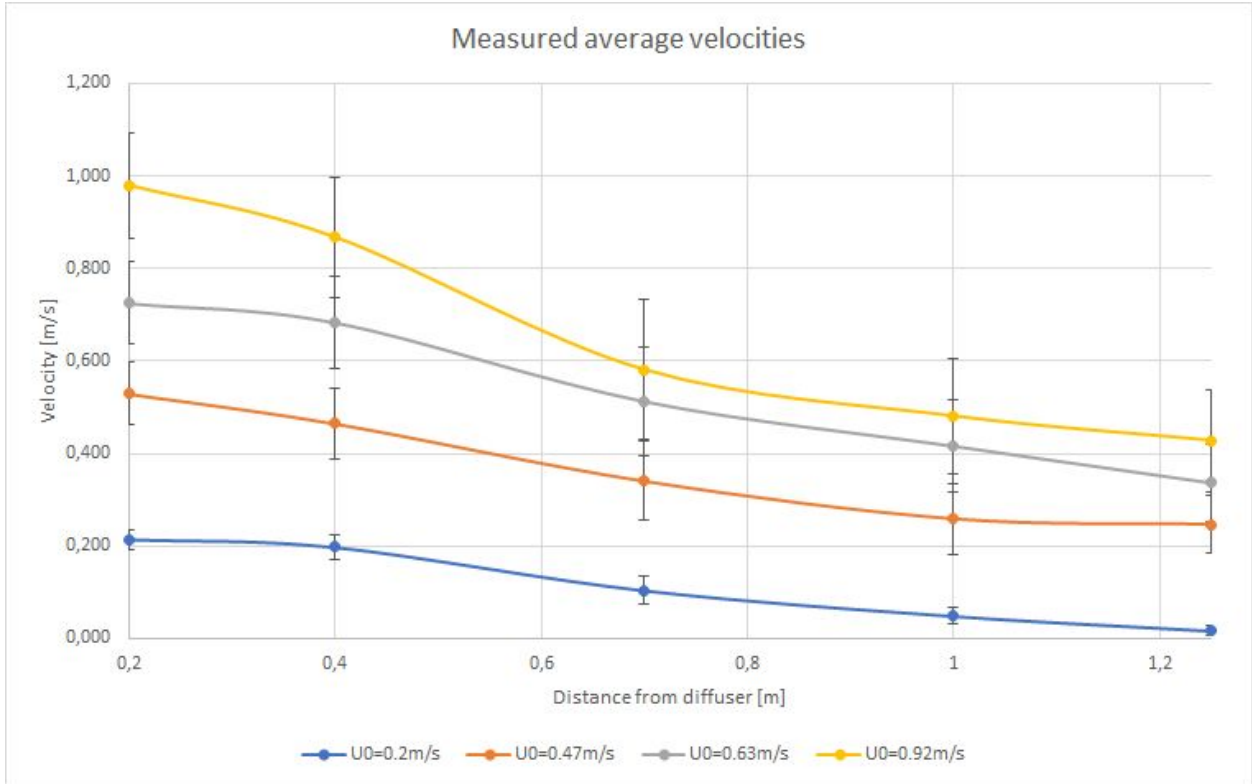
Figure 5.6 - Average measured velocities from the perforated plate diffuser with error bars
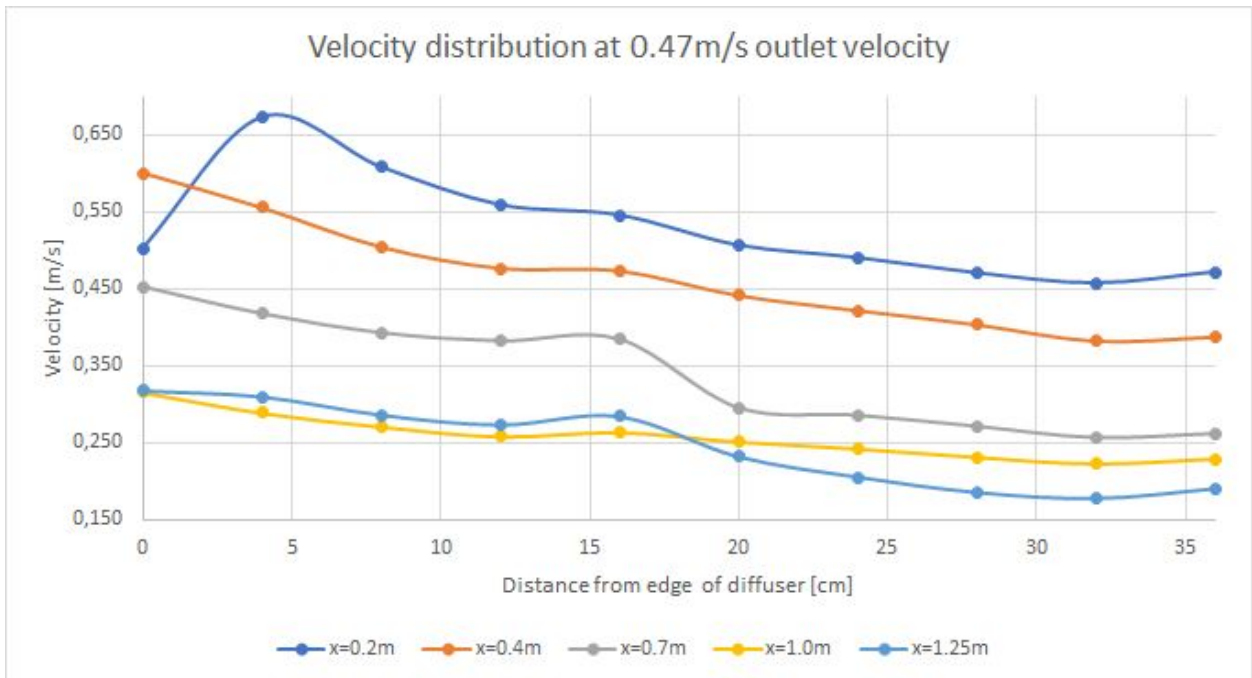
Figure 5.7 - Velocity distribution across half the diffuser at 0.47 m/s outlet velocity

5.3 Velocity ratio of 1.5

In this subchapter the velocity ratio of 1.5 is examined. The initial outlet velocities have a similar distribution as those presented in subchapter 5.1 and 5.2 and thus only average outlet velocities are mentioned. Tables with the specific outlet velocities are found in appendix C. The results are presented with initial conditions first then evaluation of the centerline velocity decay, velocity profile and at last dimensionless velocity profiles with and without the excess velocity method.

The measured velocity ratio is 1.54 as average outlet velocities are U_0=0.63 m/s and U_1=0.41 m/s. The room temperature during measurements is 24.2°C and the turbulence intensity is 7% and 15% in average at 20 cm from the slot and perforated plate diffuser respectively.

The maximum velocity decay of the plane jet, illustrated in figure 5.8, maintained a velocity well above the theoretical models. With this velocity ratio, the co-flow seem to have a significant impact on the velocity decay of the plane jet, with calculated k-factors from measurements well above 2.47, the theoretical value validated by the stand alone experiment in chapter 5.1.
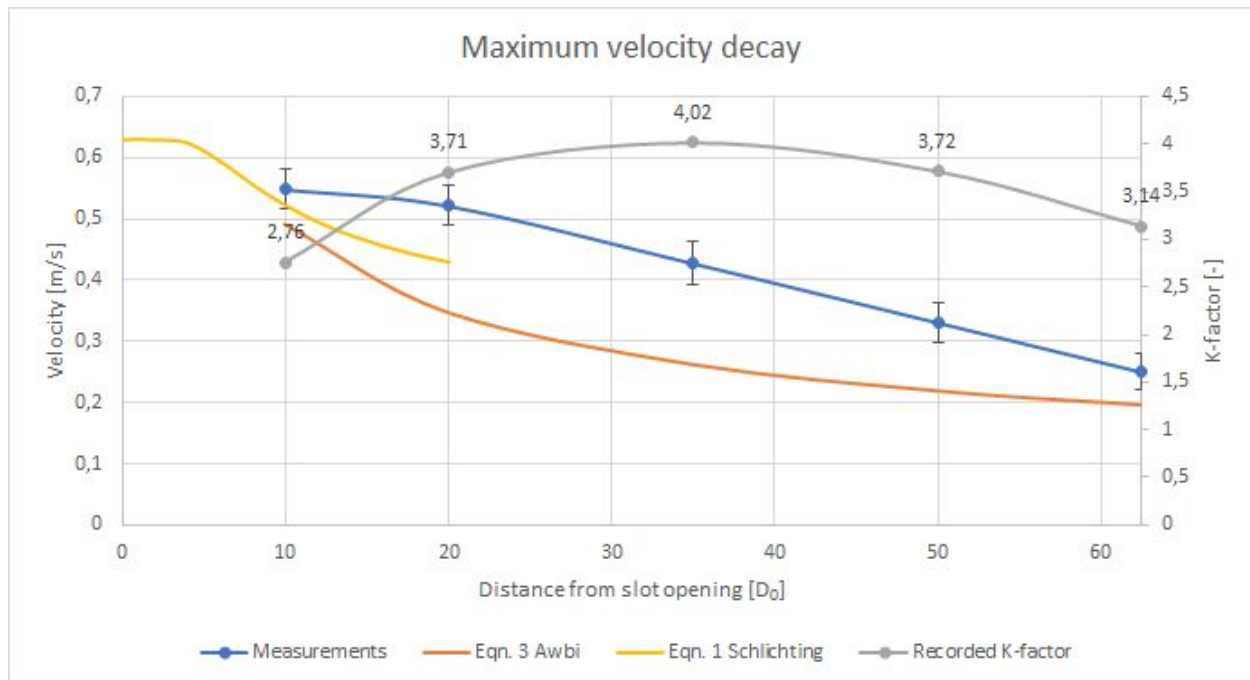
Figure 5.8 - Decay of maximum velocity with resulting K-factor from measurements

Figure 5.9 show the velocity distribution of the flow from the diffusers. At distances 10-35D_0 from the diffusers the profiles show similarity to the Gaussian error curve, while further down the profiles remain relatively flat and with significant random variations between measurement points. One of the issues than could explain this behavior is that the maximum velocity centre of the flow do not remain constant at a specific distance from the centre axis. The reasons to this could be many, of whom random air movement and slight variations in both supply and extract velocities can be significant, especially because of the low outlet velocity and the further decay of the maximum velocity at those distances. From the figure the deflection of the maximum velocity is insignificant at 10D_0, 2 cm at 20D_0, 15 cm at 35D_0, 20 cm at 50D_0 and about 45 cm at 62.5D_0. As in chapter 5.1, random room air movement and influence from extracts can influence results, however with co-flow the deflection is the other way of that in chapter 5.1 and indeed deflection is an expected result from co-flow theory. However a problem that comes with flow deflection in experiments is that it affect the perceived distance between measurement probes. This problem is addressed in greater detail in chapter 6. With the outlet velocities used at this velocity ratio the measurements from 50D_0 and 62.5D_0 should be considered with great caution, as they might well be in the terminal region.

Figure 5.9 Velocity profile with error bars

Figure 5.10 show the dimensionless velocity profile without using the excess velocity method. Eqn. 10 which is used as the theoretical profile is slightly more narrow than the Gaussian error curve in eqn. 4 which is used for plane jets without co-flow. The reason for the higher than theoretical velocity on the ri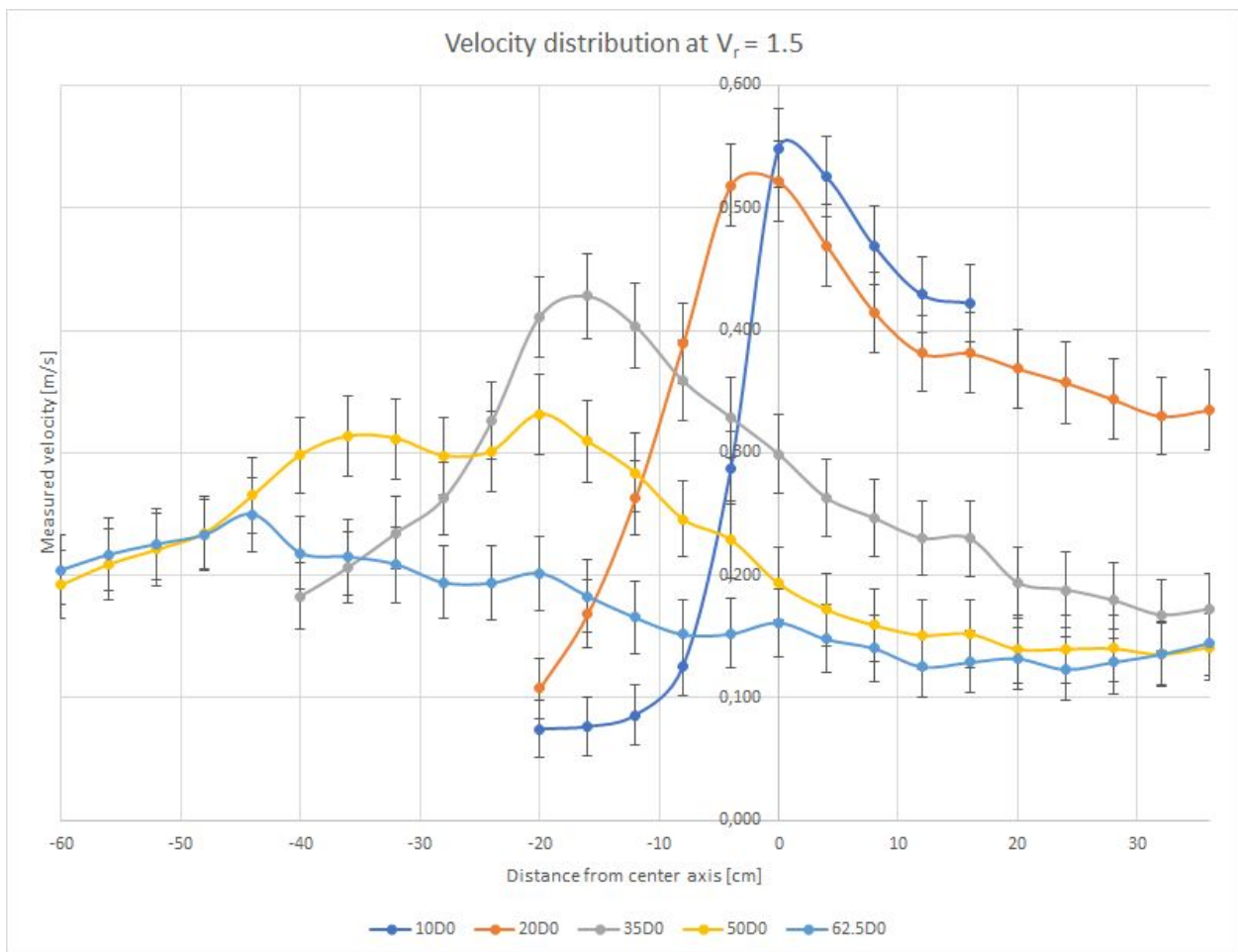ght side in the figure is due to the co-flow. Measuring $y_{1/2}$ show a general development as 0.25x, which is 2.5 times the theoretical expansion rate. At 50-62.5D_0 the expansion rate is even higher up to 0.42x at 50D_0. The rapid expansion rate from 50D_0 suggest rapid diffusion and that from this distance the flow is indeed in the terminal region. The two points are not included in the calculation of the expansion rate since they likely are not in the developed zone. The expansion rate in theory is supposed to decrease the closer the co-flow is to the plane jet flow, however this is not the case in this experiment since co-flow only exist on one side of the plane jet. It should be noted that the order in which the co-flow curves on the right are in compared with their distance to the diffusers not necessarily are logical. The co-flow has a different decay rate to that of the plane jet which is the relative velocity it is being compared with.

Figure 5.11 show the dimensionless velocity profile using the excess velocity method on the co-flow which is to the right in the figure. Using the excess velocity method the flow coincide with the theoretical curve, being generally slightly above the curve up to about 35D_0, while slightly below at greater distances. As explained in chapter 3.4 the excess velocity method subtract the Δu between the value of the velocity profile curve (eqn. 10) and the calculated dimensionless co-flow velocity, when the dimensionless co-flow velocity is higher than the value of the velocity profile curve at that point. Although not apparent in figure 5.10, in figure 5.11 it is more obvious that the plots are slightly affected by the non-flat velocity profile of the co-flow which is seen in figure 5.7. Since the excess velocity method only subtract the average co-flow velocity it subtracts a little less than the real velocity close to η=0 and a bit too much toward the end points further out since the velocities there are respectively higher and lower than the average. Because of this the points furthest away from η=0 can have negative velocities equal to the amount below the average velocity that point is.

Figure 5.10 - Dimensionless velocity profile without excess velocity method

5.11 - Dimensionless velocity profile using excess velocity method

5.4 Velocity ratio of 2.5

In this subchapter the velocity ratio of 2.5 is examined. The results for this velocity ratio are presented in the same manner as in subchapter 5.3.

The measured velocity ratio is 2.41 as average outlet velocities are U_0=0.99 m/s and U_1=0.41 m/s. The room temperature during measurements is 24°C and the turbulence intensity is 8.7% and 10.4% in average at 20 cm from the slot and perforated plate diffuser respectively.

The maximum velocity decay of the plane jet, illustrated in figure 5.12, maintained a velocity close to the theoretical models. At this velocity ratio, the co-flow seem to have a minor impact on the velocity decay of the plane jet, with calculated k-factors from measurements averaging slightly above 2.47. The biggest impact seem to be at the three middle points, which are after the developing zone and likely before the terminal zone.
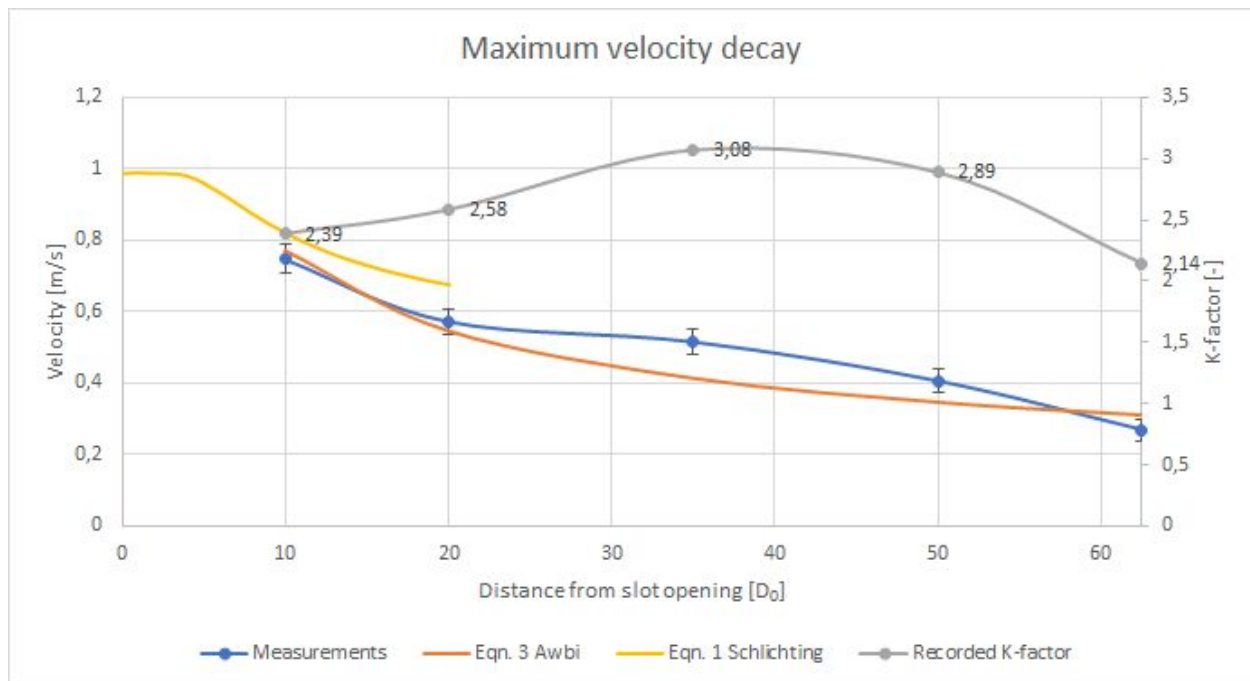
Figure 5.12 - Decay of maximum velocity with resulting K-factor from measurements

Figure 5.13 show the velocity distribution of the flow from the diffusers. At distances 10-50D_0 from the diffusers the profiles show similarity to the Gaussian error curve, with a relatively broad flat profile around the maximum velocity at 50D_0. At 62.5D_0 the profile remain flat which might indicate it is in the terminal region. As in chapter 5.3 an explanation of the flat profile around the maximum velocity at 50D_0 might issue from a wandering maximum velocity centerline at the furthest measurement distances. From the figure the deflection of the maximum velocity is insignificant at 10D_0, 4 cm at 20D_0, 15 cm at 35D_0, 30 cm at 50D_0 and about 40 cm at 62.5D_0. The reasoning for the deflection remain the same as in chapter 5.3 which is that it is expected according to theory, only the magnitude of the deflection is a subject to discussion.

Figure 5.13 - Velocity profile with error bars

Figure 5.14 show the dimensionless velocity profile without using the excess velocity method. The explanation to the theoretical curve used and why the velocity remain high at the right side in the figure are found in chapter 5.3. Measuring $y_{1/2}$ show a general development as 0.182x at this velocity ratio, which about 2 times the theoretical expansion rate. At $62.5D_0$ the expansion rate balloon to 0.64x which is evidence of rapid diffusion and grounds to claim the flow is in the terminal zone and thus the point is not included in the calculated expansion rate. As in chapter 5.3 the inflation of the expansion rate is not mentioned in theory which address co-flow on one side of a plane jet, although the literature on this subject is lacking.

Figure 5.15 show the dimensionless velocity profile using the excess velocity method on the co-flow which is to the right in the figure. Using the excess velocity method the flow coincide with the theoretical curve satisfactory up to $35D_0$, while at greater distances they remain the same as in figure 5.14 because the co-flow velocity is lower than the velocity profile curve value at those points. The excess velocity method is explained in chapter 3.4. As in chapter 5.3 the excess velocity has a slightly simplified view of the velocity distribution using only the average velocity. The excess velocities are calculated based on the measured k-factors at an outlet velocity from the perforated plate diffuser of 0.47 m/s, which is a slightly higher velocity than that which is used in this particular experiment.
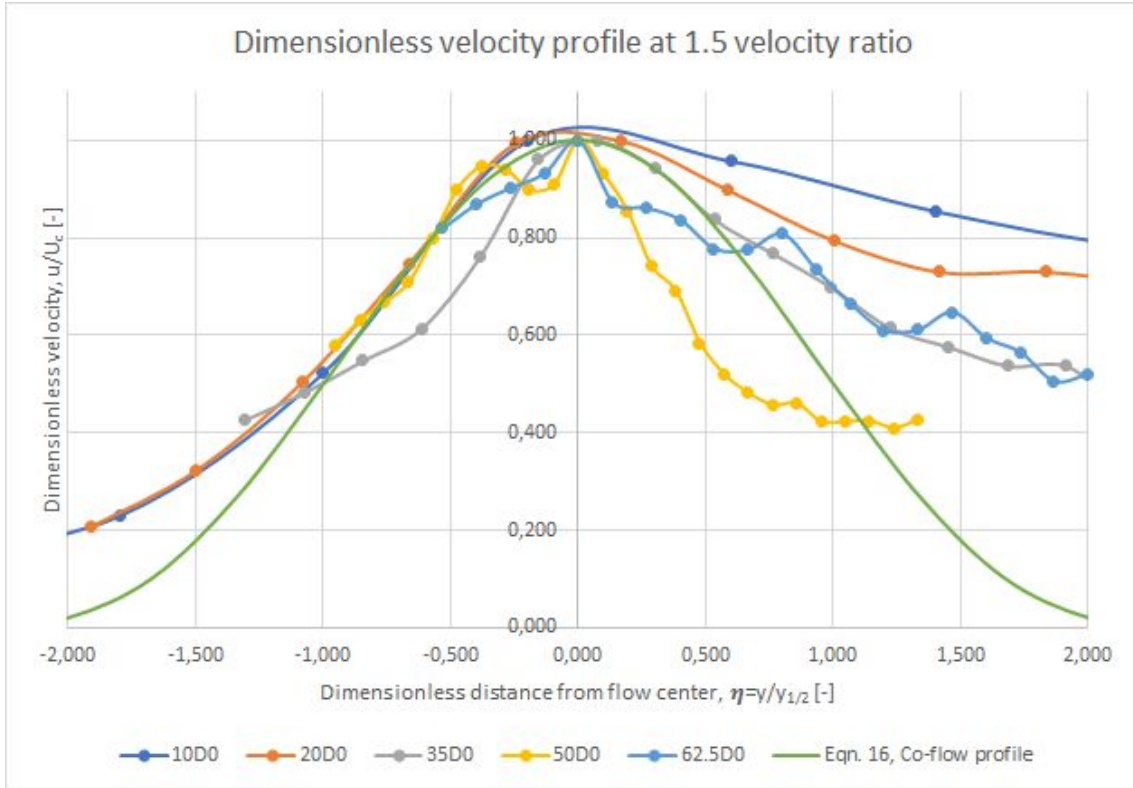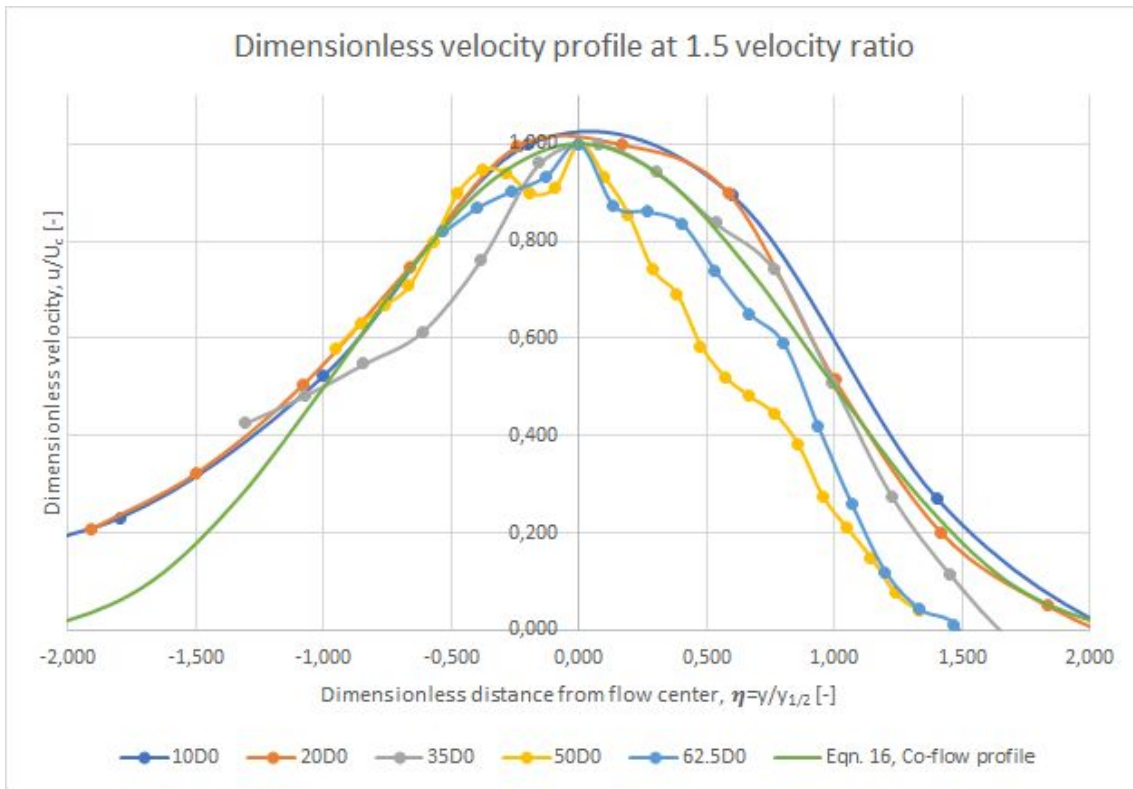
5.14 - Dimensionless velocity profile without excess velocity method
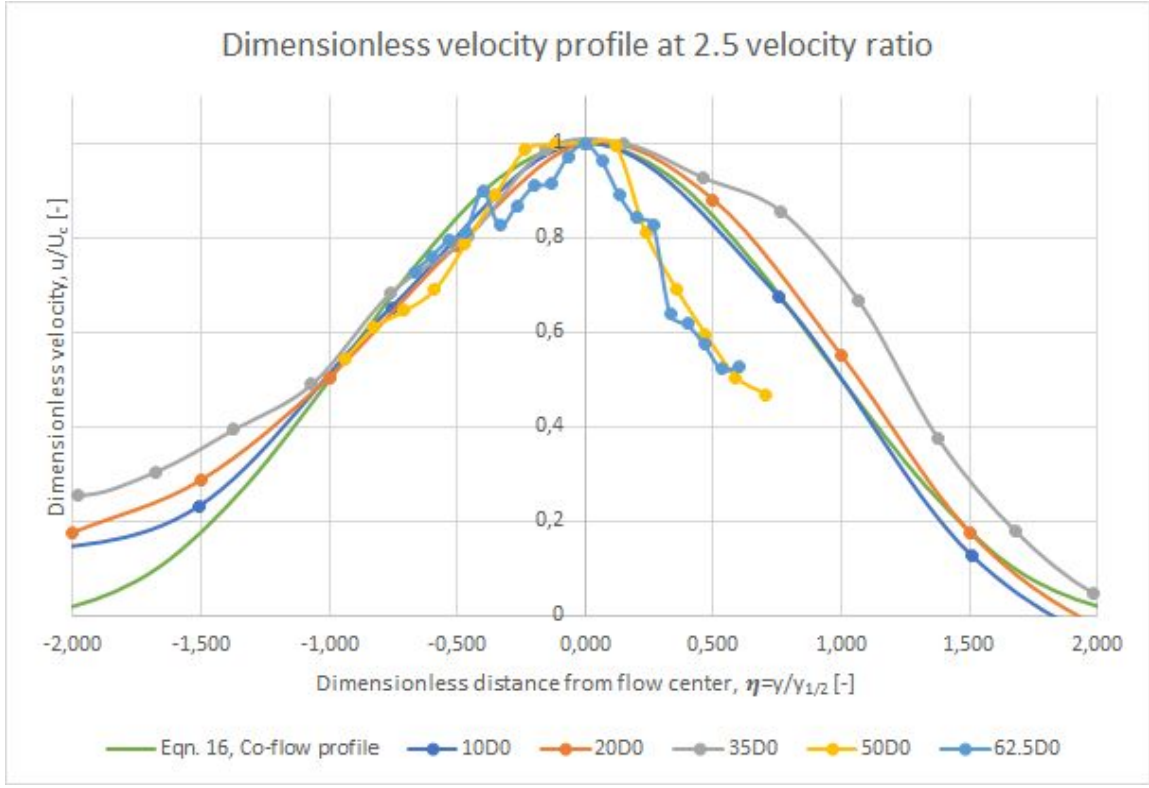
5.15 - Dimensionless velocity profile using excess velocity method

5.5 Velocity ratio of 3.0

In this subchapter the velocity ratio of 3.0 is examined. The results for this velocity ratio are presented in the same manner as in subchapter 5.3 and 5.4.

The measured velocity ratio is 3.39 as average outlet velocities are U_0=1.49 m/s and U_1=0.44 m/s. The room temperature during measurements is 24.2°C and the turbulence intensity is 7% and 14% in average at 20 cm from the slot and perforated plate diffuser respectively.

The maximum velocity decay of the plane jet, illustrated in figure 5.16, maintained a velocity close to the theoretical models. At this velocity ratio, the co-flow seem to have a minor impact on the velocity decay of the plane jet, with calculated k-factors from measurements averaging slightly above 2.47. All points, except the first at $10D_0$ are above 2.47.
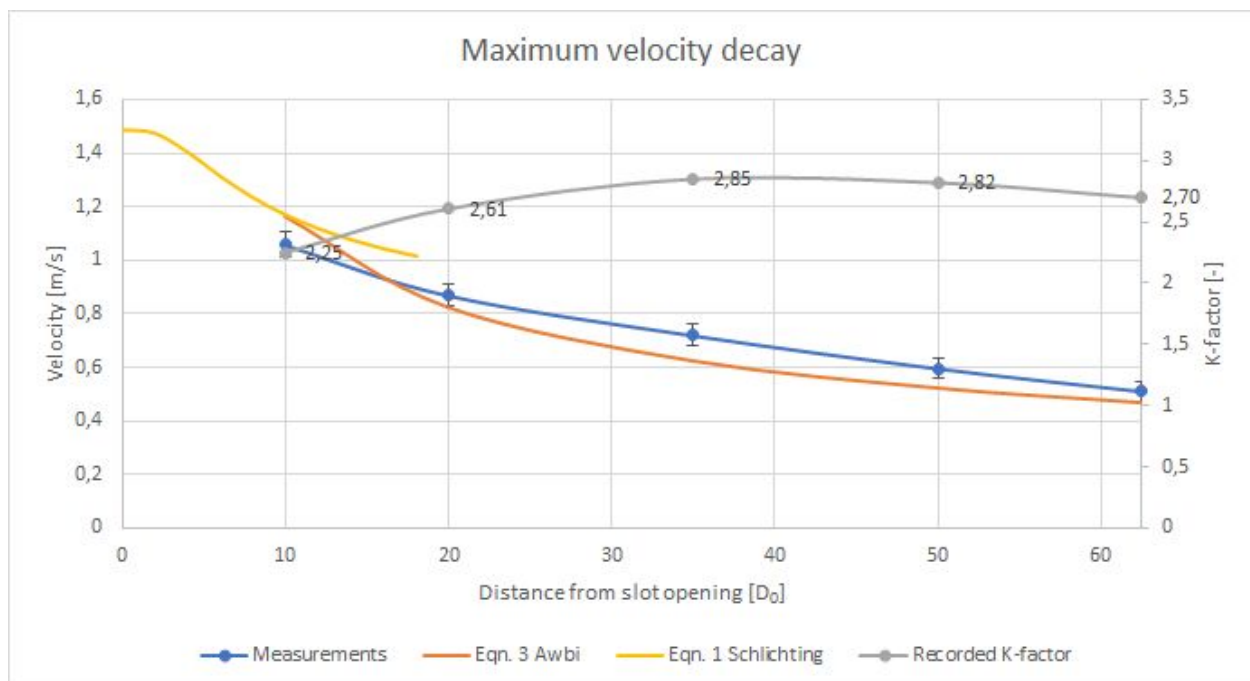
5.16 - Decay of maximum velocity with resulting K-factor from measurements

Figure 5.17 show the velocity distribution of the flow from the diffusers. The profiles show similarity to those in chapter 5.4, however with an improved profile at $50D_0$ compared with lower velocity ratios. At $62.5D_0$ the profile is not as flat as at lower velocity ratios, however it has a relatively flat profile. From the figure the deflection of the maximum velocity is insignificant at $10D_0$, 4 cm at $20D_0$, 15 cm at $35D_0$, 25 cm at $50D_0$ and about 40 cm at $62.5D_0$. The deflection is similar to that with 2.5 velocity ratio, however with slightly less deflection at $50D_0$. At higher velocity ratios the momentum of the jet is higher than that of the co-flow which might be an explanation to the slightly lesser deflection.
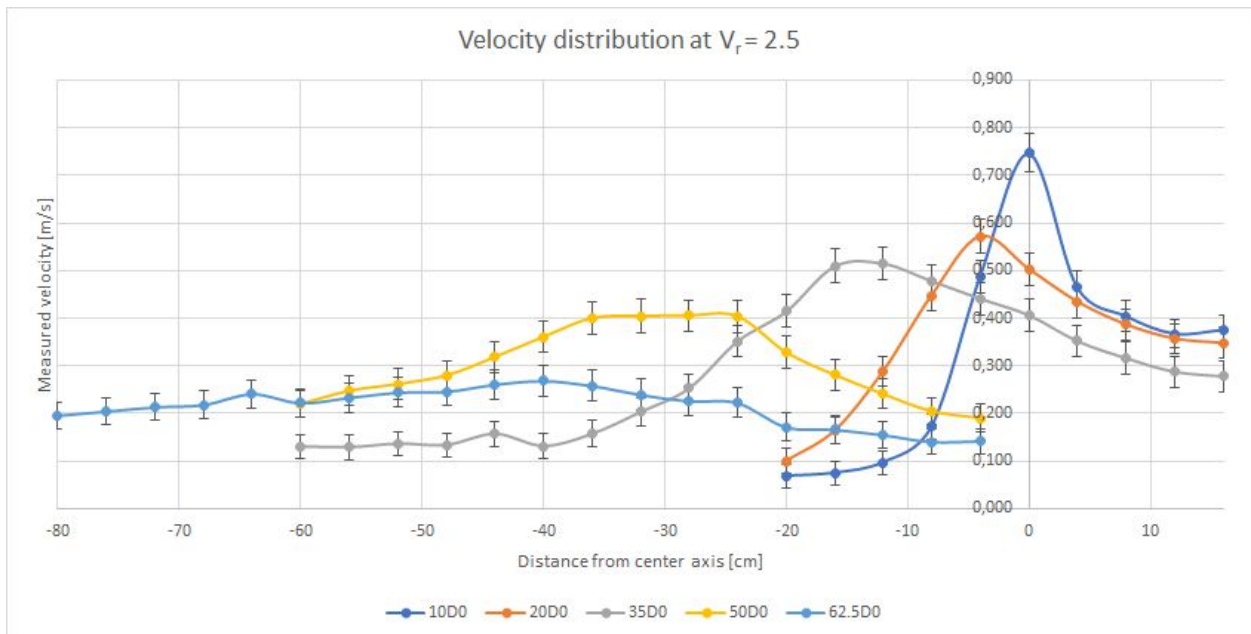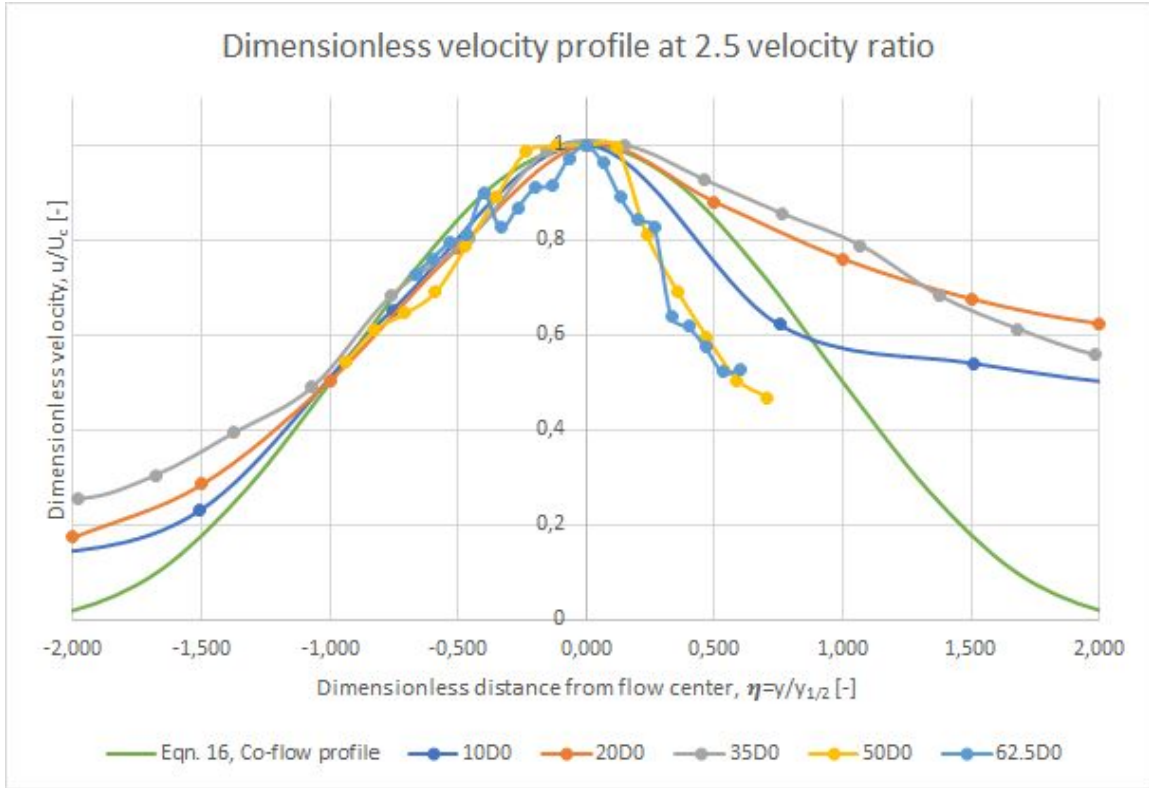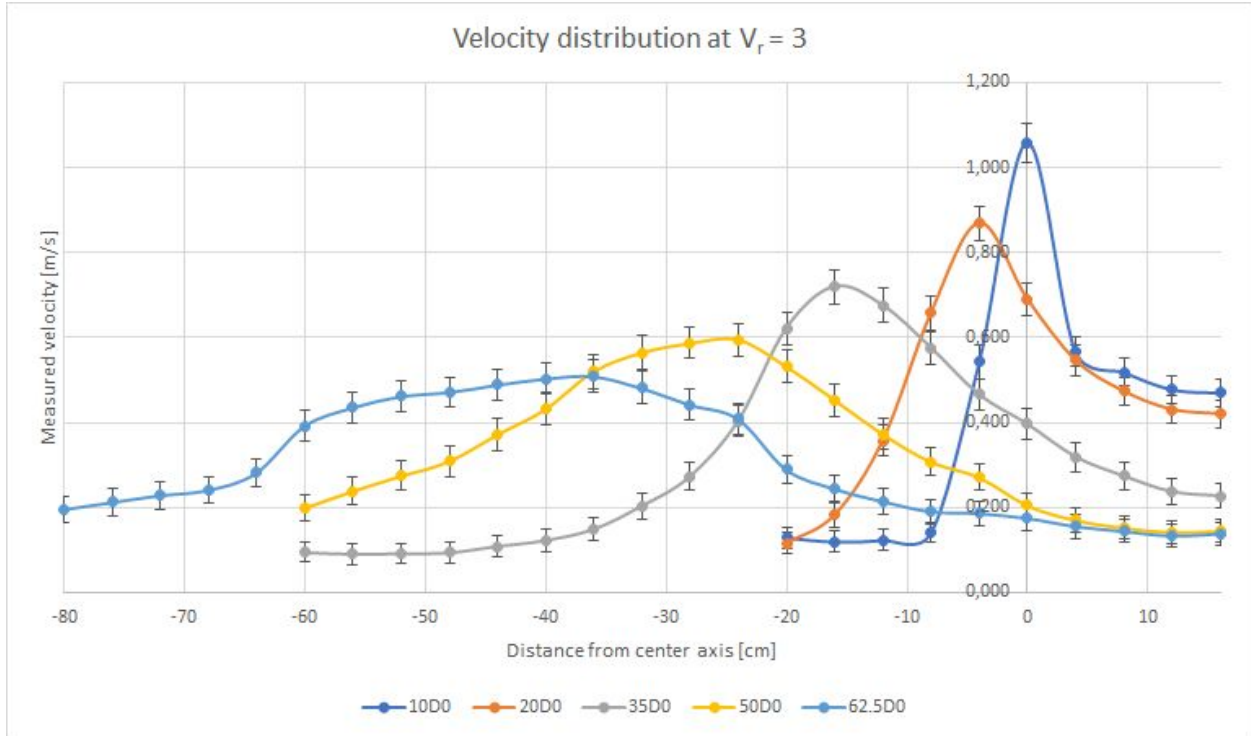
5.17 - Velocity profile with error bars

Figure 5.18 show the dimensionless velocity profile without using the excess velocity method. The explanation to the theoretical curve used and why the velocity remain high at the right side in the figure are found in chapter 5.3. Measuring $y_{1/2}$ show a general development as 0.195x at this velocity ratio, which about 2 times the theoretical expansion rate. The expansion rate remain reasonable throughout all measurement distances, however with an increase from 0.17x average at distances below $50D_0$ to 0.24x average at $50D_0$ and onward. The increase from $50D_0$ is not as extreme as with lower velocity ratios and the points are included since it is not obvious that they are in the terminal zone.

Figure 5.19 show the dimensionless velocity profile using the excess velocity method on the co-flow which is to the right in the figure. Using the excess velocity method the flow coincide with the theoretical less than with the lower velocity ratios. While the lower velocity ratios have the same co-flow velocity they might have more correct k-factors used in their equations than that in this experiment. All three velocity ratios at 3.0 or below use the same k-factors for the co-flow, since the closest experimental results for their k-factors used an outlet velocity of 0.47 m/s. Similarly to the lower velocity ratios, the distances from $50D_0$ show the greatest variation from the theoretical curve.
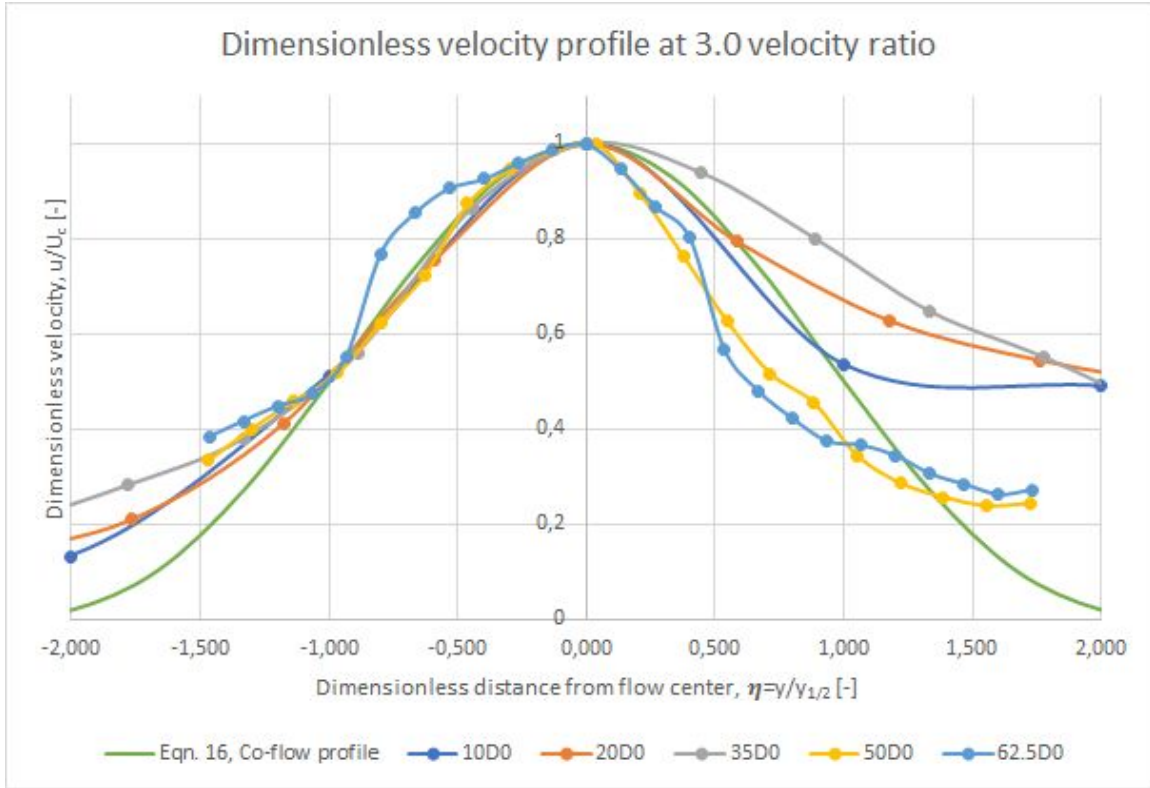
5.18 - Dimensionless velocity profile without using excess velocity method
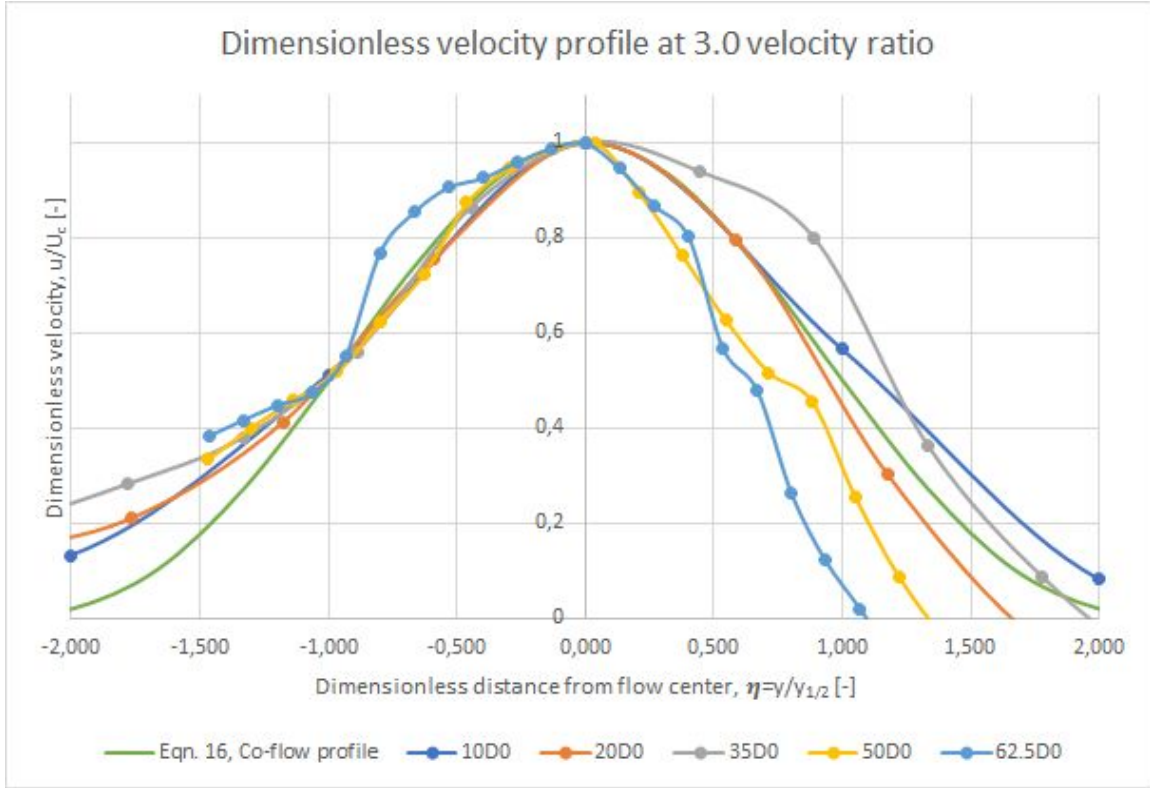
5.19 - Dimensionless velocity profile using excess velocity method

5.6 Velocity ratio of 7.5

In this subchapter the velocity ratio of 7.5 is examined. The results for this velocity ratio are presented in the same manner as in subchapter 5.3, 5.4 and 5.5.

The measured velocity ratio is 7.24 as average outlet velocities are U_0=1.52 m/s and U_1=0.21 m/s. The room temperature during measurements is 24.9°C and the turbulence intensity is 4% and 10.6% in average at 20 cm from the slot and perforated plate diffuser respectively.

The maximum velocity decay of the plane jet, illustrated in figure 5.20, maintained a velocity close to the theoretical models. At this velocity ratio, the co-flow seem to have a minor impact on the velocity decay of the plane jet, with calculated k-factors from measurements averaging slightly below 2.47, excepting the point at $10D_0$. All points, except the first at $10D_0$ are below 2.47.
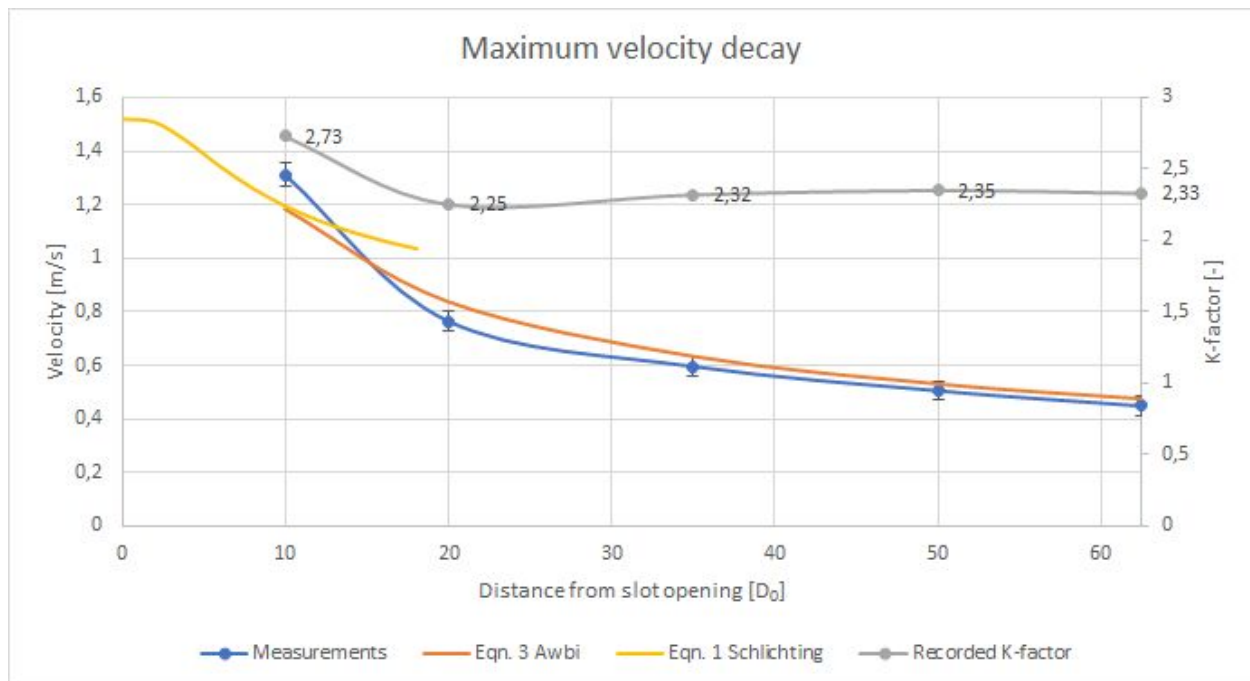
5.20 - Decay of maximum velocity with resulting K-factor from measurements

Figure 5.21 show the velocity distribution of the flow from the diffusers. The profiles show a better similarity to what is seen in literature than with lower velocity ratios. At $62.5D_0$ it is grounds to call the profile "wide" instead of flat. From the figure the deflection of the maximum velocity is insignificant at $10D_0$, 2 cm at $20D_0$, 8 cm at $35D_0$, 12 cm at $50D_0$ and about 18 cm at $62.5D_0$. The deflection is about or less than half when comparing to the lower velocity ratios. As in chapter 5.5 the explanation to the decrease in deflection can be that the momentum of the jet is higher than that of the co-flow at lower velocity ratios.
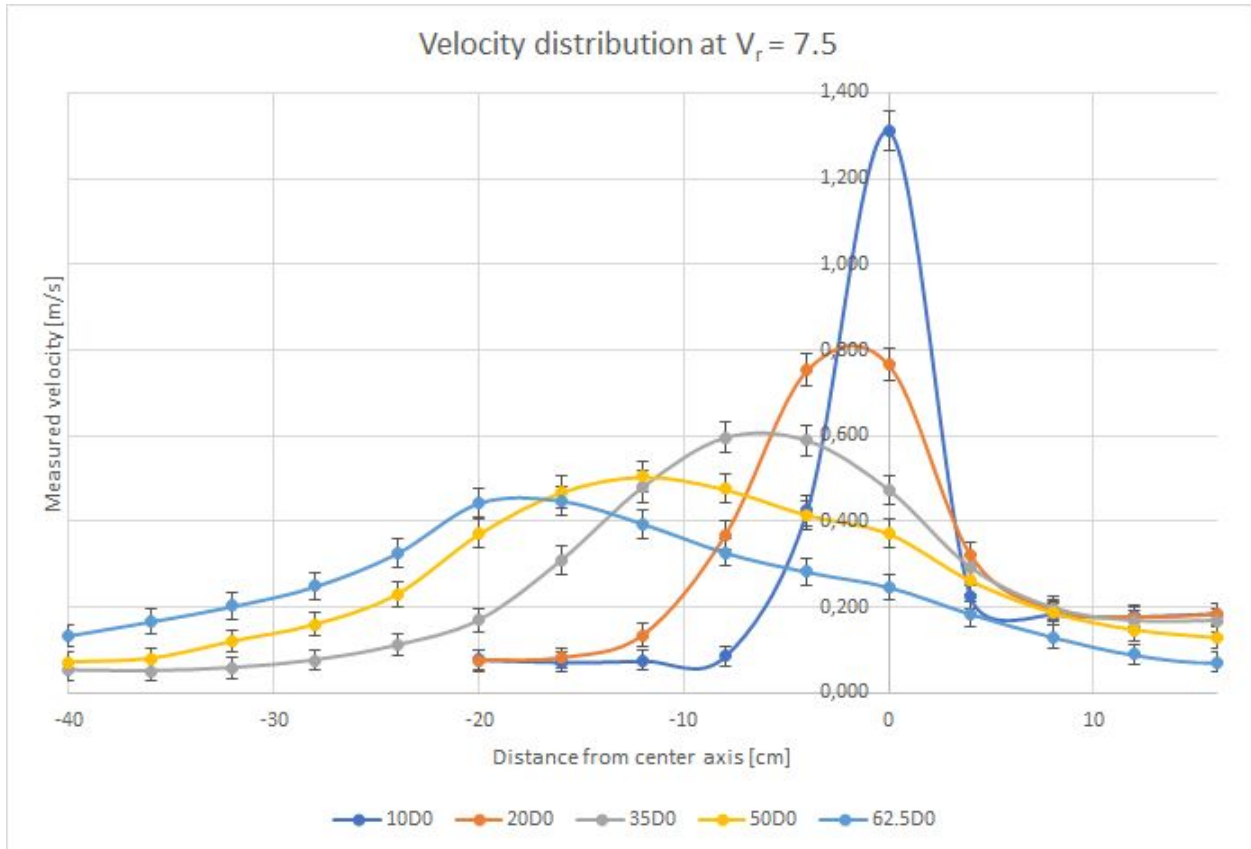
5.21 - Velocity profile with error bars

Figure 5.22 show the dimensionless velocity profile without using the excess velocity method. The explanation to the theoretical curve used and why the velocity remain high at the right side in the figure are found in chapter 5.3. Measuring $y_{1/2}$ show a general development as 0.125x at this velocity ratio, which about 25% higher than the theoretical expansion rate, but only slightly higher to the expansion rate found when testing the slot alone. The expansion rate remain reasonably even throughout all measurement distances, with a slight decrease the greater the distance.

Figure 5.23 show the dimensionless velocity profile using the excess velocity method on the co-flow which is to the right in the figure. Using the excess velocity method does not change the profile much compared to not using the method. The main explanation is that the co-flow velocity is low compared with the plane jet flow and thus has little impact. However the relationship from the lower velocity ratios remain, the further the distance the less the modified curve coincide with the theoretical curve. Since the k-factors for the co-flow only are evaluated when using the perforated plate diffuser alone, the impact from the plane jet flow on the co-flow is not taken into consideration when evaluating k-factors. Since the model is less accurate at further distances where the plane jet flow is wider it is logical it might have a bigger impact than closer to the diffuser outlets.
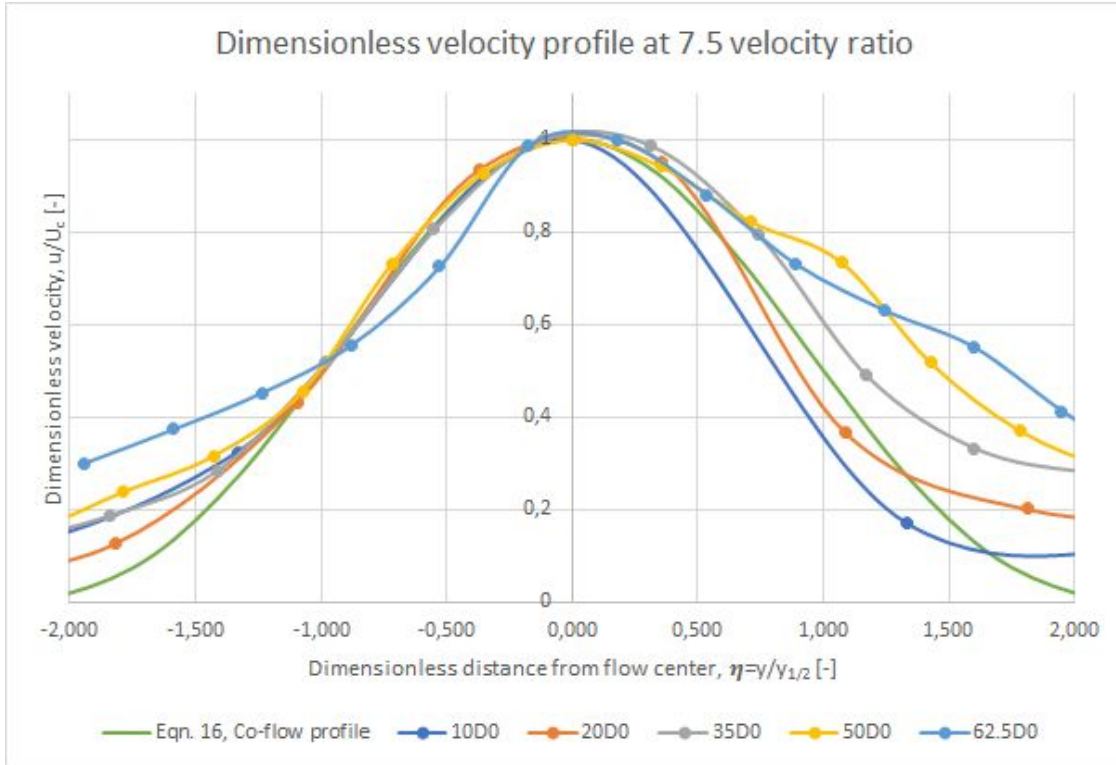
5.22 - Dimensionless velocity profile without using excess velocity method
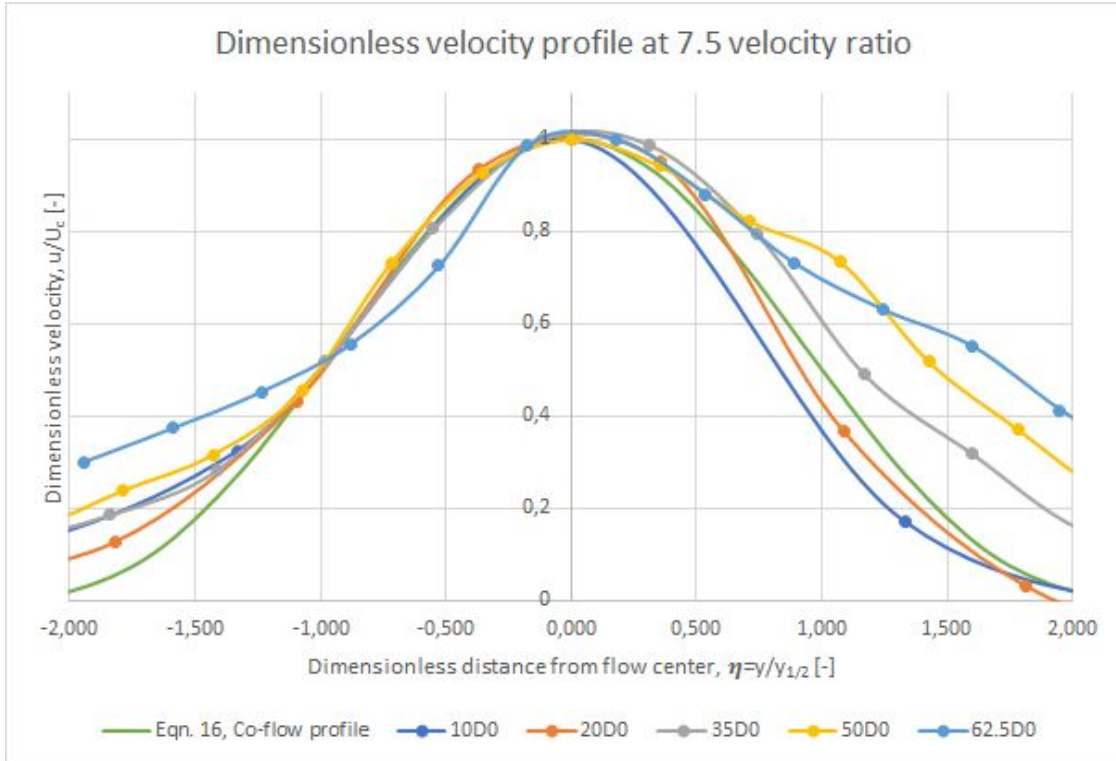
5.23 - Dimensionless velocity profile using excess velocity method

5.7 Visualization

The smoke test is conducted at three velocity ratios, V_r equal to 1.5, 3.0 and 7.5. The case with a velocity ratio of 2.5 is deemed redundant as the velocities are too similar to the 3.0 case. The pictures below show the flow pattern from the slot diffuser since that is what disrupt the smoke. The smoke had to be released under the perforated plate diffuser due to the pressure in the supplying duct to the slot diffuser being too high for the smoke to enter. The pictures are taken through the plexiglass window at the wall with the extracts as seen in figure 4.5.

Figure 5.24 - Visualization of flow at V_r=1.5

Figure 5.24 show a deflection of about 30 cm at a distance from the slot of 100 cm which is equal to 50D_0. During the test the deflection varied between 20 cm and more than 40 cm at times. The figures are a representation of the average values. The anemometers show a deflection of 25 cm at this distance, which is slightly less, however the exact conditions during

separate experiments are hard to replicate perfectly. In the photo the smoke machine had been on for a short period.
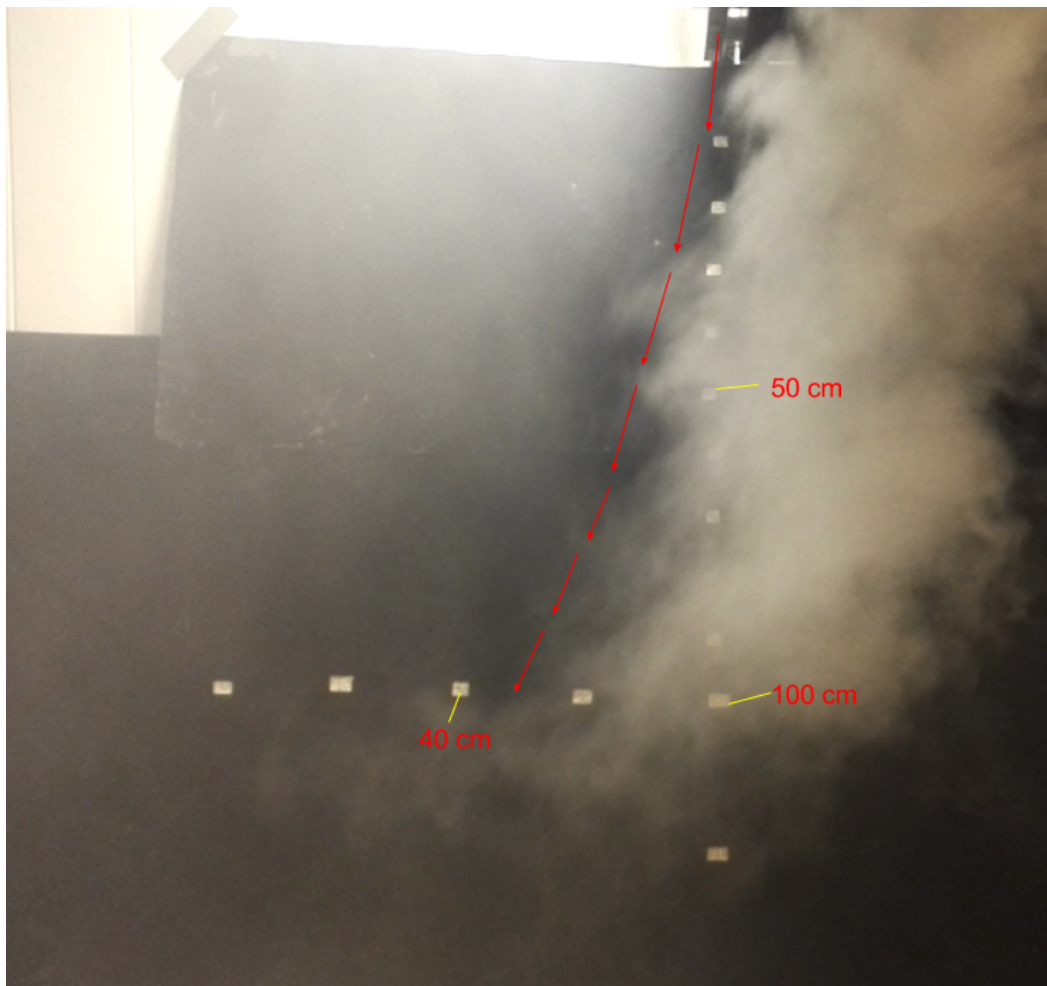
Figure 5.25 - Visualization of flow at V_r=3.0

Figure 5.25 show a similar deflection as in figure 5.24 at about 30 cm. At a velocity ratio of 3.0 the anemometers recorded the same deflection as with a velocity ratio of 1.5 which is 25 cm. This point to the anemometers reading the correct values since the deflection remain the same. In the photo the smoke had been on for some time and smoke partially had spewed throughout the room, however the most of the smoke was still under the perforated plate diffuser.

Figure 5.26 - Visualization of flow at V_r=7.5

Figure 5.26 show a deflection at about 15 cm, although the smoke test is not accurate enough to identify the deflection down to the cm. The anemometers show a similar result at 12 cm. In the photo the smoke had been on for some time and changes in velocities before this photo was taken managed to spread the smoke evenly throughout the room which help reveal the flow pattern of the plane jet better. There is video of the smoke test which can be used to identify further details as the development of the boundary layer and reveal vortexes from the entrainment air, however no photos of those scenarios are clear enough to be presented.

Chapter 6 - Discussion and comparison

The goal of this thesis is to characterize the air distribution of a combined downward jet. The characteristics considered are initial flow conditions, velocity decay, velocity distribution and flow expansion. The tasks are to conduct a literature review of air distribution methods for protected occupied zone ventilation and to obtain a model for the velocity distribution of the combined downward jet.

In this chapter the main findings are discussed and compared with literature. The results from the experiments are compared with each other where appropriate. Chapter 6.1 analyze the downward plane jet, without a co-flow. Chapter 6.2 analyze the perforated plate diffuser, which is the diffuser responsible for the co-flow and chapter 6.3 analyze the combined downward jet from the velocity ratio experiments.

Each sub-chapter analyze the main characteristics in the same order as they are presented in the first paragraph.

6.1 The downward plane jet

The outlet velocity from the plane jet is distributed as should be expected from experimental work. There is some variation between measurement points, however it remained satisfactory close to the average of 1.54 m/s as seen in figure 5.1.

The measured centerline velocity decay perform close with the theoretical models. The average k-factor from measurements is 2.50. The theoretical velocity decay models represented by eqn. 2, 3 and 5 by Schlichting and Awbi use either the Goertler, Tollmien or Rajaratnam solutions of 2.4, 2.47 or 2.67. The differences between the equations and the k-factors they use remain relatively marginal, and the measured average of 2.50 remain well within the bounds of these solutions. Eqn. 1 by Schlichting for the velocity decay in the developing region remain unconcluded since the number of measurement points in this region are few, although it seems the recommended value for σ_1 is too high, since the curve does not intersect with the equations for the developed zone.

The velocity profile based on measurements agreed with the theoretical curves when comparing to the experiments of Tollmien, however with some disturbance in the curve at $62.5D_0$. There is evidence of some deflection but in experiments using only the plane jet the volumetric flow is so small that it is difficult to adjust the extract properly. Measuring the expansion of the boundary layer is difficult in experiments, since the anemometers also measure entrainment velocities and random room air movement. Measuring the expansion of the half-velocity is a much more accurate method to evaluate the expansion of the jet. The measured development of $y_{1/2}$ is 0.119x which is significantly higher than what is used in the theoretical models of 0.1x. A more rapid development of $y_{1/2}$ should in fact increase the velocity decay since the available

momentum of the jet is spread across a larger area than in theory. Since there is no evidence of faster velocity decay the effect of the increased spread is the least not significant. There are significant sources of error with the measuring probes being too far apart and imperfections in the slot opening that might increase the development. The dimensionless velocity profile is a good tool to use when comparing the measurements to the theory since all measurements should have the same profile if they fit the theory, and figure 5.4 agrees with theory as close as should be expected with the experimental setup.

6.2 The perforated plate diffuser

The initial outlet velocities from the perforated plate diffuser is not even. The tested velocities are 0.2, 0.47, 0.63 and 0.92 m/s. The design has room for improvement, however the lower the outlet velocity is, the more even the flow is. From the range of velocities tested only the lowest velocities are used in the combined downward jet experiments.

The calculated velocity decay use eqn. 6 based on a calculated velocity core speed. In the measurements the recorded velocities remain well above those of the velocity core far from the outlet. Since the equations by Awbi for perforated plate diffusers are defined for perorations less than what is used in this experiment and at higher outlet velocities the measured k-factors cannot be compared with theory. The measured k-factors agree with each other at the three velocities tested that are above 0.2 m/s outlet velocity. They do not remain constant, but has a general linear increase. At 0.2 m/s outlet velocity the measured k-factor had a generally linear decrease from about 0.5 m from the diffuser opening. The most prevalent explanation is that the flow behaves differently at such a low outlet velocity and that it must be in the terminal region. The measured k-factors from the experiment are used further on in the excess velocity calculations, since they do not differ much at outlet velocities above 0.2 m/s.

The velocity distributions from the tests agree with what is expected based on the measurements of the outlet velocities. The profiles are not flat as they ideally should be, but gradually decline toward the center of the diffuser which has the lowest average velocity across the diffuser. The impact from the skewed velocity profiles are that they disturb further calculations on the combined downward jet which base on a good understanding of the co-flow.

6.3 The combined downward jet

The initial conditions of the flow from the combined downward jet has similar velocity distributions at the outlets as in the tests of the diffusers alone. The velocity ratios tested are U_0/U_1 equal to 1.54, 2.41, 3.39 and 7.24. The two diffusers has no significant impact on each other before their flows interact. This is good news that suggest it might not be a huge mistake to use data from the measurements on the diffusers alone further in calculations on the combined downward jet.

The impact of the co-flow on velocity decay of the plane jet suggest that the theoretical claim that the velocity decay decrease as the velocity of the co-flow increase. The decrease in velocity decay is explained in theory as an effect of increasing length of the potential core and by that effect delaying the onset of the axisymmetric decay. The results support this claim as average measured k-factors using the plane jet velocity decay equations are above 3 at V_r=1.54, slightly less than 3 at V_r=2.41, about 2.7 at V_r=3.39 and about 2.35 at V_r=7.24. All the tested velocity ratios except the 7.24 velocity ratio have k-factors above the theoretical values of a plane jet. At the highest velocity ratio the behavior is similar to that of a plane jet without co-flow, which can be explained with the co-flow having a minimal impact on the plane jet.

The velocity profiles are similar to the Schlichting curves from figure 3.2 on the side of the maximum velocity without the co-flow. At the side of the co-flow the curves develop from the velocity centre as the Tollmien curves at first, until they reach the velocity of the co-flow. When the curves reach the point of co-flow velocity they are extended horizontally decreasing slowly further away from the velocity centre. The slight decrease horizontally is most likely due to the unevenness of the velocity profile of the co-flow as discussed in chapter 6.2. The horizontal extension is obvious at measurement distances up to $35D_0$ and further down the curves are less obvious since the effect is smaller due to velocity decays of the two flows. The deflection remain more or less constant at 1.54 and 2.41 velocity ratio, with a slight decrease at V_r=3.39 at the furthest distances while the deflection rapidly decrease at the highest velocity ratio, V_r=7.24. Deflection is mentioned in the theory, but not specified as a function or any other mention of its magnitude. In the experiments the deflection at $50D_0$ is confirmed with smoke tests to be about 30 cm at V_r=1.54 and V_r=2.41, decreasing to about 25 cm at V_r=3.39 and then about 12 cm at V_r=7.24. The impact of the deflection can be a welcome one since it force air to exit on one side instead of impinging on the floor spreading the air both ways.

The expansion of $y_{1/2}$ vary from 0.125x at the highest velocity ratio to about 0.19x at the two middle velocity ratios and 0.25x at the lowest velocity ratio. At the highest velocity ratio the expansion is close to the one found when testing the slot diffuser alone. The increase in expansion rates are clearly coupled with the velocity ratio, however the effect is the opposite of what should be expected according to theory. With co-flows the jet spread should be smaller than without co-flow since the potential core is extended and the velocity decay is slower. The fact that the spread increase the lower the velocity ratio while the velocity decay slows down are

contradicting. Following the preservation of momentum, the jet has to increase its momentum if both observations remain true. The most obvious explanation is that with co-flow on only one side, the plane jet gains momentum from the co-flow, however it is not clear from the conducted experiments. The dimensionless velocity profiles show a similar effect as with measured velocity profiles that the co-flow extends horizontally on the side of the co-flow. Using the excess velocity method the dimensionless profiles show good agreement to the theoretical co-flow profile up until $35D_0$. The method agree better at lower velocity ratios, since small errors in the calculation of the co-flow velocity decay are more dominant at low co-flow velocities. The method is not explained in detail in theory, and although the principle of the method is known, the assumptions used in this thesis might not be correct. In theory the flows are also theoretical and do not have imperfect profiles which the method assume. The impact of the plane jet flow on the co-flow is also not considered, however if the plane jet in-fact draw momentum from the co-flow the velocity decay of the co-flow which is based on measurements on the co-flow diffuser alone might not be accurate. Overall the excess velocity method used in this thesis is a novel approach to the combined downward jet and needs maturing and validation.

Chapter 7 - Conclusion

The goal of this thesis is to characterize the air distribution of a combined downward jet. The characteristics considered are initial flow conditions, velocity decay, velocity distribution and flow expansion. The tasks are to conduct a literature review of air distribution methods for protected occupied zone ventilation and to obtain a model for the velocity distribution of the combined downward jet.

Since traditional ventilation systems do not reduce the risk, rather increase the risk of exposure to indoor pollutants, new ventilation systems that reduce exposure are needed. Most air distribution methods rely on the air mixing effect from the whole-room air distribution system. Systems that aim to reduce exposure use a traditional air distribution system in addition to supply enough fresh air.

POV differ from the other distribution systems by the effect of creating separate zones for its occupants. Current POV systems also use a traditional distribution system in addition in order to obtain a sufficient supply of fresh air, although seemingly the secondary supply air system is placed so it avoids interaction with the air curtain. While the combined jet can be classified as a POV-system, the secondary flow intentionally interact with the flow of the air curtain.

The literature review revealed that there is little current knowledge of the specific characteristics of a combined downward jet. The literature maintain general and unspecific characterizations of the flow. The impact of the research done in this master thesis is of the utmost significance towards achieving empirical and numerical models of the flow from a combined downward jet, although the limitations in this research rely on future work to be validated and refined.

The main limitations of this research is that although a wide range of velocity ratios are tested, the configuration of the two diffusers remained the same. The width of the slot diffuser outlet need to be tested at a magnitude of nozzle widths. Although the range of velocity ratios are wide, their outlet velocities need to be tested at different initial velocities than just those in this experiment.

The air distribution of the combined downward jet is characterized in this research. There are some unwanted variations of initial velocities from the diffusers that increase the difficulty in obtaining a solid flow characterization while the research methodology reduce their significance as much as possible.

The velocity decay is affected by the combined flow with an extension of the the developing zone, which is seen in the research as the delayed onset of characteristic decay. The characteristic decay, described by theoretical equations, measures the extension of the developing zone as an increase of the k-factor. The higher the co-flow velocity is to the plane jet velocity, the longer the extension of the developing zone is. It agrees with co-flow theory,

however the magnitude of effect at different velocity ratios is not previously modelled for a combined downward jet.

The velocity distribution show a deflection of the flow that increase with the distance from the slot opening and increase the higher the co-flow velocity is to the plane jet velocity. It agrees with theory of combined downward jets, however there is little data on the magnitude of the deflection. In the experiments there is no obvious correlation of its magnitude to the velocity ratio, only a general trend. At high velocity ratios the deflection is small and at lower velocity ratios the deflection seem to plateau.

The development of $y_{1/2}$ increases with increasing co-flow velocity to the plane jet velocity. In co-flow theory, when there is co-flow on each side of the plane jet, the development of $y_{1/2}$ should decrease the lower the velocity ratio is. When there is co-flow on only one side of the plane jet, as is the case with the combined jet, the development of $y_{1/2}$ is the opposite of what is seen in co-flow theory. At a velocity ratio of 1.5 the development of $y_{1/2}$ is almost 2.5 times that of a plane jet in quiescent air which is $0.1x$. The more rapid development of $y_{1/2}$ is surprising, since the velocity decay seem to agree with co-flow theory. The sum of these effects are that the momentum of the plane jet increases with distance to the slot opening, which breaks one of the most fundamental conservation laws - conservation of momentum. The most likely explanation is that the plane jet steals momentum from the co-flow and this is one of the results that need to be investigated in future research.

The use of the excess velocity method is an attempt to create a model of the combined downward jet. The results using it show the most promise at lower velocity ratios and at the distances closest to the diffusers. Since it relies on accurate calculations of the co-flow velocity decay the model is prone to errors which are more evident at greater distances and lower velocities. The impact of the plane jet on the co-flow is also a big unknown in the equation, which assumes that because of the much greater momentum of the co-flow to the plane jet it is not affected to a significant degree. This claim needs to be validated in future work.

Chapter 8 - References

[1]   Bolashikov, Z.d., and A.k. Melikov. "Methods for Air Cleaning and Protection of Building Occupants from Airborne Pathogens." *Building and Environment* 44.7 (2009): 1378-385.

[2]   Bolashikov, Zhecho D., et al. "Exposure of health care workers and occupants to coughed airborne pathogens in a double-bed hospital patient room with overhead mixing ventilation." Hvac&R Research 18.4 (2012): 602-615

[3]   Cao, Guangyu, Kai Sirén, and Simo Kilpeläinen. "Modelling and Experimental Study of Performance of the Protected Occupied Zone Ventilation." *Energy and Buildings* 68 (2014): 515-31.

[4]   Xu, Chunwen. "Experimental Study of the Cross-infection Risk due to the Cross-flow of Exhaled Airflows and a Plane Jet with the Protected Occupied Zone Ventilation." ASHRAE Transactions 120 (2014): 1J.

[5]   Cook, G., & Int-Hout, D. (2009). Air motion control in the hospital operating room. ASHRAE Journal, 51(3), 30-34,36.

[6]   *ENØK I Bygninger: Effektiv Energibruk: Håndbok for Planlegging, Gjennomføring Og Oppfølging*. Oslo: SINTEF, 1996.

[7]   Carrer, Paolo, Pawel Wargocki, Annaclara Fanetti, Wolfgang Bischof, Eduardo De Oliveira Fernandes, Thomas Hartmann, Stylianos Kephalopoulos, Susanna Palkonen, and Olli Seppänen. "What Does the Scientific Literature Tell Us about the Ventilation–health Relationship in Public and Residential Buildings?" *Building and Environment* 94 (2015): 273-86.

[8]   Li, Y., G. M. Leung, J. W. Tang, X. Yang, C. Y. H. Chao, J. Z. Lin, J. W. Lu, P. V. Nielsen, J. Niu, H. Qian, A. C. Sleigh, H.-J. J. Su, J. Sundell, T. W. Wong, and P. L. Yuen. "Role of Ventilation in Airborne Transmission of Infectious Agents in the Built Environment - a Multidisciplinary Systematic Review." *Indoor Air* 17.1 (2007): 2-18.

[9]   Bivolarova, Mariya P., Arsen K. Melikov, Chiyomi Mizutani, Kanji Kajiwara, and Zhecho D. Bolashikov. "Bed-integrated Local Exhaust Ventilation System Combined with Local Air Cleaning for Improved IAQ in Hospital Patient Rooms." *Building and Environment* 100 (2016): 10-18.

[10]   Müller, Dirk. *Mixing Ventilation: Guide on Mixing Air Distribution Design*. Brussels: REHVA, 2013.

[11]   Memarzadeh, F., & Manning, A. P. (2002). Comparison of operating room ventilation systems in the protection of the surgical site / discussion. ASHRAE Transactions, 108, 3.

[12]   Yang, Bin, Chandra Sekhar, and Arsen K. Melikov. "Ceiling Mounted Personalized Ventilation System in Hot and Humid Climate—An Energy Analysis." *Energy and Buildings* 42.12 (2010): 2304-308.

[13]   Yang, B., S. C. Sekhar, and A. K. Melikov. "Ceiling-mounted Personalized Ventilation System Integrated with a Secondary Air Distribution System - a Human Response Study in Hot and Humid Climate." *Indoor Air* 20.4 (2010): 309-19.

[14]   Guyonnaud, L., C. Solliec, M. Dufresne De Virel, and C. Rey. "Design of Air Curtains Used for Area Confinement in Tunnels." *Experiments in Fluids* 28.4 (2000): 377-84.

[15] Cao, G., PhD., Nielsen, P. V., PhD., Xu, C., & Jensen, R. L., PhD. (2014). Experimental study of the cross-infection risk due to the cross-flow of exhaled airflows and a plane jet with the protected occupied zone ventilation. ASHRAE Transactions, 120, 8-1J,2J,3J,4J,5J,6J,7J,8J.

[16] Awbi, H. B. Ventilation of Buildings. London: Taylor & Francis, 2003. Print.

[17] Schlichting, Hermann, and J. Kestin. *Boundary- Layer Theory*. New York: McGraw-Hill, 1979.

[18] Namer, I., and M. V. Ötügen. "Velocity measurements in a plane turbulent air jet at moderate Reynolds numbers." *Experiments in Fluids* 6.6 (1988): 387-399.

[19] Rajaratnam, N. *Turbulent Jets*. Amsterdam: Elsevier, 1976.

Appendix A – Instrumentation

All equipment used in experiments was supplied by NTNU.

A.1 – Handheld anemometer: TSI 962 Thermoanemometer

The specifications to the handheld anemometer measuring probe, the TSI 962 Thermoanemometer are found at the webpage of TSI. Link to the specific resource used to obtain the data is found at the bottom of the page.

Spcifications:

Range

- 0 to 9,999 ft/min (0 to 50 m/s)
- 0 to 200°F (-18 to 93°C)

Accuracy

- ±3% of reading or ±3 ft/min
- (±0.015 m/s), whichever is greater
- ±0.5°F (±0.3°C)

Resolution

- 1 ft/min (0.01 m/s)
- 0.1°F (0.1°C)

Figure A.1 - TSI 962 Thermoanemometer

Probe Dimensions

- Length 40 in. (101.6 cm)
- Tip dia. 0.28 in. (7.0 mm)
- Base dia. 0.51 in. (13.0 mm)
- Articulating Section Length 6 in. (15.2 cm)
- Articulating Knuckle dia. 0.38 in. (9.5 mm)

Link: http://www.tsi.com/products/product-accessories/thermoanemometer-articulated-probe-962.aspx

A.2 – Air distribution measuring system "AirDistSys5000"

The air distribution measuring system consist of five anemometer probes, a barometer which correct the measurements of the anemometers according to changes in pressure, a wireless transmitter, wireless receiver which is connected to a computer and a power supply. The setup is demonstrated in figure A.2. Sensor-electronic also provided the software needed to record and analyze recorded data.
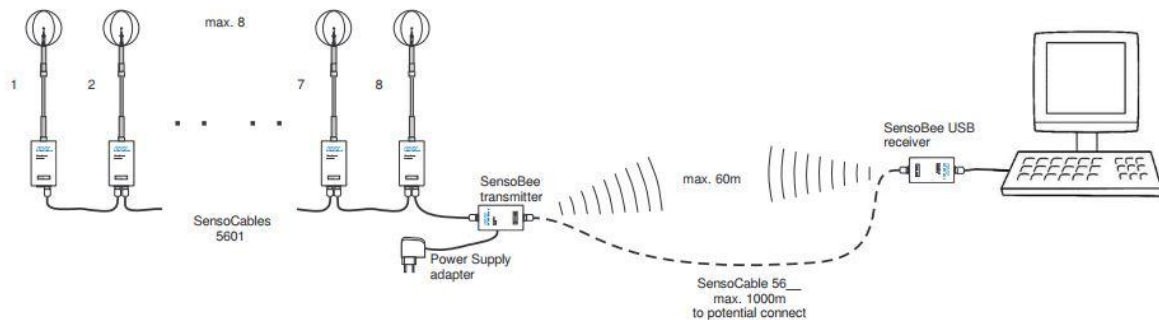
Figure A.2 - AirDistSys 5000 Setup, picture from the user manual found in the link at the end of the sub-chapter

Following are the technical specifications to each component described in the first paragraph. All data are collected from sensor-electronic directly, and a link to the used resource is at the end of chapter A.2.

A.2.1 – Anemometer probes: SensoAnemo series 5100LSF transducer

Technical data:

- type of speed sensor: omnidirectional, spherical
- diameter of speed sensor   2 mm
- measurement speed range: 0.05… 5 m/s
- accuracy of speed measurement: ±0.02 m/s ±1.5% of readings
- directional error above 2m/s: ±2.5%
- automatic temperature compensation: < than ±0.1%/K
- upper frequency f_{up}:   min. 1 Hz, typ. 1.5 Hz
- temperature range: -10…+50 °C
- accuracy of temperature: 0.2 °C
- sampling rate: 8 Hz
- interface: port RS485
- baud rate: 115000 bps
- optional analog output: current 0…20 mA, voltage 0-2V or 0-5V only for velocity, non-linear (set of equations) V [m/s]= f(Iv)
- max analog output resistance: 100 Ohm
- power supply: 3.3…9 VDC
- power consumption: max. 80mA, typ.60mA, peak. 110mA, economy mode 6mA

A.2.2 – Barometer: SensoBar 5301 transducer

Technical data:

- measurement range: 500…1500 hPa
- accuracy: ±3 hPa
- response time: 2s
- humidity measurement range: 0…100 % RH
- humidity accuracy: ±2% in range 10…90% RH
- long term stability of humidity: <1 % RH/year
- response time of humidity: <4s
- interface: port RS485
- baud rate: 115000 bps
- power supply: 3.3…9 VDC
- power consumption: max. 6mA, typ.60mA, economy mode 1mA

A.2.3 – Wireless transmitter: SensoBee wire-less transmitter

Technical data:

- indoor (urban) range: up to 60m
- outdoor line-of-sight range: up to 100m
- transmit power output: 100mW (20dB) EIRP
- operating frequency: 2.4GHz
- RF data rate: 250 kbps
- power supply: 6…9 VDC/1A

A.2.4 – Wireless receiver: SensoBee USB wire-less receiver

Technical data: There is no specific technical data. The receiver is connected to the computer using the USB interface which it is also powered through.

Link: http://www.sensor-electronic.pl/pdf/MAN_AirDistSys5000.pdf

Risk Assessment Report

Diffuser experiment with air curtain and co-flow

Prosjektnavn	performance of a combined downward jet for protected zone ventilation reducing exposure risk of occupants to indoor pollutants.
Apparatur	Klimarom VA-lab
Enhet	NTNU
Apparaturansvarlig	Guangyu Cao
Prosjektleder	Guangyu Cao
HMS-koordinator	Morten Grønli
HMS-ansvarlig (linjeleder)	Olav Bolland
Plassering	Klimarom, Varmetekniske laboratorier
Romnummer	C247C, 2. etg i klimalab, Varmetekniske laboratorier
Risikovurdering utført av	Inge Håvard Rekstad

Approval:

Apparatur kort (UNIT CARD) valid for:	3 måneder
Forsøk pågår kort (EXPERIMENT IN PROGRESS) valid for:	3 måneder

Rolle	Navn	Dato	Signatur
Prosjektleder	Guangyu Cao		*Guyu Cao*
HMS koordinator	Morten Grønli		
HMS ansvarlig (linjeleder)	Olav Bolland		

TABLE OF CONTENTS

1 INTRODUCTION

This experiments purpose is to investigate the performance of a combined downward jet for protected occupied zone ventilation. The air distribution and performance of the curtain will be measured. The experiment will be conducted in the middle of the small office in the Klimalab.

The experiment will be conducted in several steps:

- **Presetting** of the air curtain nozzle and "laminar air flow diffuser" by measuring the velocity at the outlet to be sure there is an even outflow and that their respective air speeds are at the right ratio to one another. Adjust the fan and valve to get the desired value for the flow velocity. **Calibrating** the anemometers.
- Conduct smoke test to reveal the air flow pattern and CO_2 experiment. CO_2 will be supplied at the opposite side of the LAF-diffuser in order to measure the protection efficiency.

2 ORGANISATION

Rolle	
Prosjektleder	Guangyu Cao
Apparaturansvarlig	Guangyu Cao
Romansvarlig	Lars Konrad Sørensen
HMS koordinator	Morten Grønli
HMS ansvarlig (linjeleder):	Olav Bolland

3 RISK MANAGEMENT IN THE PROJECT

Hovedaktiviteter risikostyring	Nødvendige tiltak, dokumentasjon	DATE
Prosjekt initiering	Prosjekt initiering mal	
Veiledningsmøte Guidance Meeting	Skjema for Veiledningsmøte med pre-risikovurdering	
Innledende risikovurdering	Fareidentifikasjon – HAZID	

Initial Assessment	Skjema grovanalyse	
Vurdering av teknisk sikkerhet Evaluation of technical security	Prosess-HAZOP Tekniske dokumentasjoner	
Vurdering av operasjonell sikkerhet Evaluation of operational safety	Prosedyre-HAZOP Opplæringsplan for operatører	
Sluttvurdering, kvalitetssikring Final assessment, quality assurance	Uavhengig kontroll Utstedelse av apparaturkort Utstedelse av forsøk pågår kort	

4   DESCRIPTIONS OF EXPERIMENTAL SETUP
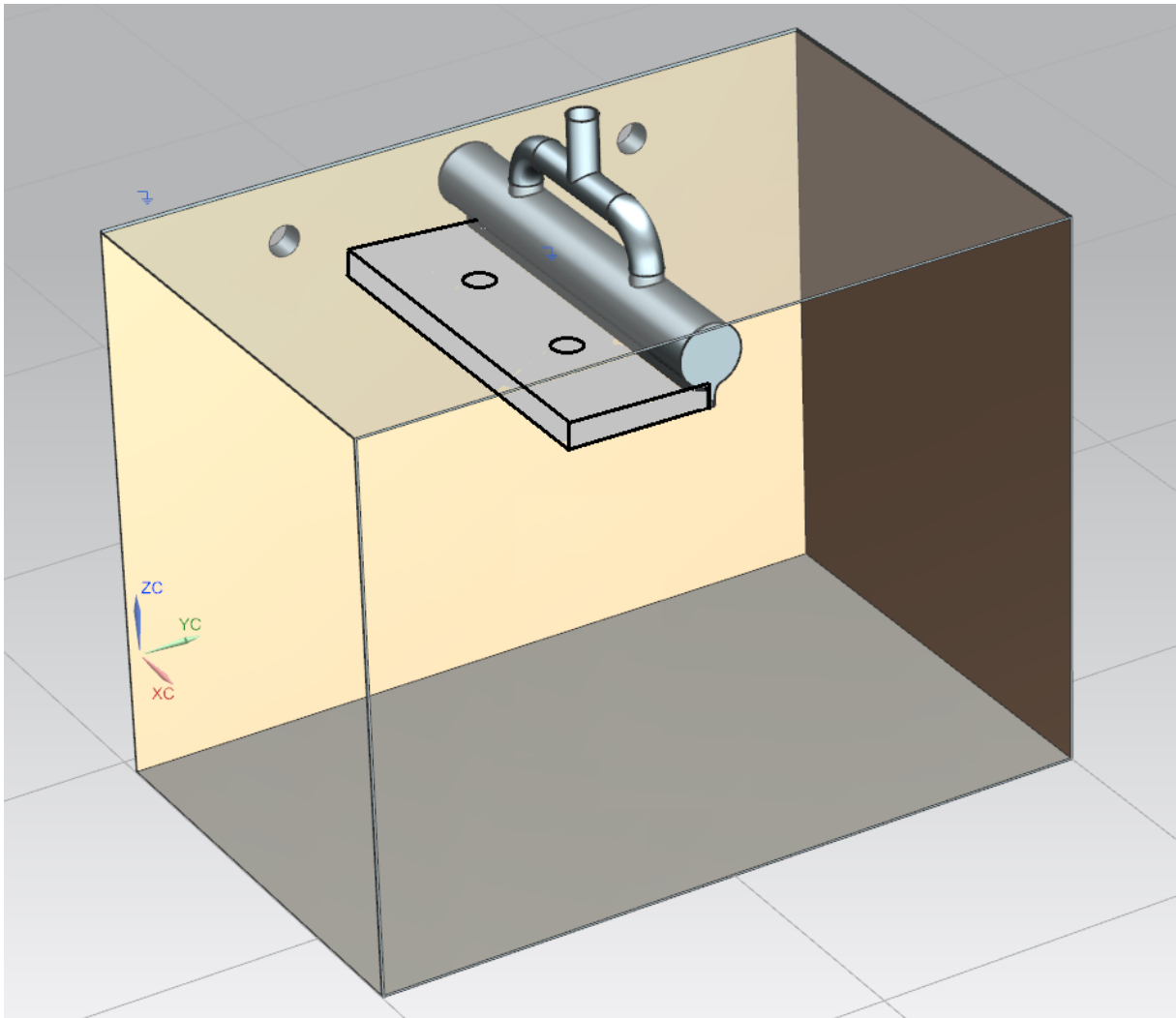
Location of the room, is the little room inside the KlimaLab at VAT, 2nd floor.

The experimental setup will be like the figure above. There will be measurements of the airflow distribution mainly underneath the diffusers. Air is exhausted by the fans on the back wall.

Instrumentation that will be used is:

- Anemometer
- Thermometer
- Diffusers
- Fan controlling the volume flow out of the diffusers

- Exhaust fan x2
- Smoke machine
- CO2 machine
- CO2-meter

5   EVACUATION FROM THE EXPERIMENTAL AREA

Evacuate at signal from the alarm system or local gas alarms with its own local alert with sound and light outside the room in question, see 6.2

Evacuation from the rigging area takes place through the marked emergency exits to the assembly point, (corner of Old Chemistry Kjelhuset or parking 1a-b.)

Action on rig before evacuation:

In case of evacuation, the fans and the thermal manikin should be switched off. The measurements stop.

6   WARNING

6.1   Before experiments

Send an e-mail with information about the planned experiment to:

iept-experiments@ivt.ntnu.no

The e-mail must include the following information:

- Name of responsible person:
- Experimental setup/rig:
- Start Experiments: (date and time)
- Stop Experiments: (date and time)

You must get the approval back from the laboratory management before start up. All running experiments are notified in the activity calendar for the lab to be sure they are coordinated with other activity.

6.2   Abnormal situation

FIRE

If you are NOT able to extinguish the fire, activate the nearest fire alarm and evacuate area. Be then available for fire brigade and building caretaker to detect fire place.
If possible, notify:

NTNU	SINTEF
Morten Grønli, Mob: 918 97 515	Harald Mæhlum, Mob: 930 14 986
Olav Bolland: Mob: 918 97 209	Petter Røkke, Mob: 901 20 221
NTNU – SINTEF Beredskapstelefon	800 80 388

GAS ALARM

If a gas alarm occurs, close gas bottles immediately and ventilate the area. If the level of the gas concentration does not decrease within a reasonable time, activate the fire alarm and evacuate the lab. Designated personnel or fire department checks the leak to determine whether it is possible to seal the leak and ventilate the area in a responsible manner.

Alert Order is in the above paragraph.

PERSONAL INJURY

- First aid kit in the fire / first aid stations
- Shout for help
- Start life-saving first aid
- **CALL 113** if there is any doubt whether there is a serious injury

OTHER ABNORMAL SITUATIONS

NTNU:

You will find the reporting form for non-conformance on:

https://innsida.ntnu.no/wiki/-/wiki/Norsk/Melde+avvik

SINTEF:

Synergi

7 ASSESSMENT OF TECHNICAL SAFETY

7.1 HAZOP

See Chapter 13 "Guide to the report template".

The experiment set up is divided into the following nodes:

Node 1	Test rig in Klimalab
Node 2	

Attachments, Form: Hazop_mal

Conclusion: (Safety taken care of)

7.2 Flammable, reactive and pressurized substances and gas

Are any flammable, reactive and pressurized substances and gases in use?

NO	

7.3 Pressurized equipment

Is any pressurized equipment in use?

NO	

7.4 Effects on the environment (emissions, noise, temperature, vibration, smell)

Will the experiments generate emission of smoke, gas, odour or unusual waste?

Is there a need for a discharge permit, extraordinary measures?

NO	

Attachments:

Conclusion:

7.5 Radiation

See Chapter 13 "Guide to the report template".

NO	

Attachments:

Conclusion:

7.6 Chemicals

Will any chemicals or other harmful substances be used in the experiments? Describe how the chemicals should be handled (stored, disposed, etc.) Evaluate the risk according to safety datasheets, MSDS. Is there a need for protective actions given in the operational procedure?

NO	

Attachments:

Conclusion:

7.7 Electricity safety (deviations from the norms/standards)

NO	

Attachments:

Conclusion: The use of electrical equipment in this experiment complies with the standards and regulations in terms of touch danger.

8   ASSESSMENT OF OPERATIONAL SAFETY

Ensure that the procedures cover all identified risk factors that must be taken care of. Ensure that the operators and technical performance have sufficient expertise.

8.1   Procedure HAZOP

See Chapter 13 "Guide to the report template".

The method is a procedure to identify causes and sources of danger to operational problems.

Attachments:: HAZOP_MAL_Prosedyre

Conclusion: Simple misunderstandings will not lead to dangerous situations. Form not filled.

8.2   Operation procedure and emergency shutdown procedure

See Chapter 13 "Guide to the report template".

The operating procedure is a checklist that must be filled out for each experiment.

 Emergency procedure should attempt to set the experiment set up in a harmless state by unforeseen events.

Attachments: Procedure for running experiments

Emergency shutdown procedure: In case of emergency, fans should be switched off and manikin turned off if possible before leaving the rig.

8.3   Training of operators

The operator should know how to use the anemometers, how to adjust the watt level on the thermal manikin and how to operate both exhaust fans and supply fan. Training should be completed before the actual measurements begin. The operator should also be responsible and tidy, so that no accidents occur. In case of evacuation, the operator should turn off the manikin and the fans and leave the building.

8.4   Technical modifications

- *Technical modifications made by the operator (e.g.Replacement of components, equal to equal)*
- *Technical modifications that must be made by Technical staff (for example, modification of pressure equipment).*
- *What technical modifications give a need for a new risk assessment(by changing the risk picture)?*

8.5 Personal protective equipment

• *Use gloves when there is opportunity for contact with hot/cold surfaces.*

8.6 General Safety

An operator should always be present to follow the measurements. However, there is no risk involved when leaving the rig for a few moments. Door to the room must always be closed during measurements. No entry allowed at that point.

8.7 Safety equipment

Not required

8.8 Special predations

9 QUANTIFYING OF RISK - RISK MATRIX

See Chapter 13 "Guide to the report template".

The risk matrix will provide visualization and an overview of activity risks so that management and users get the most complete picture of risk factors.

IDnr	Aktivitet-hendelse	Frekv-Sans	Kons	RV
	Rotating exhaust fans, danger of contact	1	C	C1
	Contact burn on the smoke machine	1	C	C1

Conclusion: The *Participants has to make a comprehensive assessment to determine whether the remaining risks of the activity/process is acceptable.*

10 REGULATIONS AND GUIDELINES

Se http://www.arbeidstilsynet.no/regelverk/index.html

- Lov om tilsyn med elektriske anlegg og elektrisk utstyr (1929)
- Arbeidsmiljøloven
- Forskrift om systematisk helse-, miljø- og sikkerhetsarbeid (HMS Internkontrollforskrift)
- Forskrift om sikkerhet ved arbeid og drift av elektriske anlegg (FSE 2006)
- Forskrift om elektriske forsyningsanlegg (FEF 2006)
- Forskrift om utstyr og sikkerhetssystem til bruk i eksplosjonsfarlig område NEK 420
- Forskrift om håndtering av brannfarlig, reaksjonsfarlig og trykksatt stoff samt utstyr og anlegg som benyttes ved håndteringen
- Forskrift om Håndtering av eksplosjonsfarlig stoff
- Forskrift om bruk av arbeidsutstyr.
- Forskrift om Arbeidsplasser og arbeidslokaler
- Forskrift om Bruk av personlig verneutstyr på arbeidsplassen
- Forskrift om Helse og sikkerhet i eksplosjonsfarlige atmosfærer
- Forskrift om Høytrykksspyling
- Forskrift om Maskiner
- Forskrift om Sikkerhetsskilting og signalgivning på arbeidsplassen
- Forskrift om Stillaser, stiger og arbeid på tak m.m.
- Forskrift om Sveising, termisk skjæring, termisk sprøyting, kullbuemeisling, lodding og sliping (varmt arbeid)
- Forskrift om Tekniske innretninger
- Forskrift om Tungt og ensformig arbeid
- Forskrift om Vern mot eksponering for kjemikalier på arbeidsplassen (Kjemikalieforskriften)
- Forskrift om Vern mot kunstig optisk stråling på arbeidsplassen
- Forskrift om Vern mot mekaniske vibrasjoner
- Forskrift om Vern mot støy på arbeidsplassen

Veiledninger fra arbeidstilsynet

se: http://www.arbeidstilsynet.no/regelverk/veiledninger.html

11 DOCUMENTATION

- Tegninger, foto, beskrivelser av forsøksoppsetningen
- Hazop_mal
- Sertifikat for trykkpåkjent utstyr
- Håndtering avfall i NTNU
- Sikker bruk av LASERE, retningslinje
- HAZOP_MAL_Prosedyre
- Forsøksprosedyre
- Opplæringsplan for operatører
- Skjema for sikker jobb analyse, (SJA)
- Apparaturkortet

- Forsøk pågår kort

12 GUIDANCE TO RISK ASSESSMENT TEMPLATE

Chapter 7 Assessment of technical safety.

Ensure that the design of the experiment set up is optimized in terms of technical safety.

Identifying risk factors related to the selected design, and possibly to initiate re-design to ensure that risk is eliminated as much as possible through technical security.

This should describe what the experimental setup actually are able to manage and acceptance for emission.

7.1 HAZOP

The experimental set up is divided into nodes (eg motor unit, pump unit, cooling unit.). By using guidewords to identify causes, consequences and safeguards, recommendations and conclusions are made according to if necessary safety is obtained. When actions are performed the HAZOP is completed.

(e.g. "No flow", cause: the pipe is deformed, consequence: pump runs hot, precaution: measurement of flow with a link to the emergency or if the consequence is not critical used manual monitoring and are written into the operational procedure.)

7.2 Flammable, reactive and pressurized substances and gas.

According to the Regulations for handling of flammable, reactive and pressurized substances and equipment and facilities used for this:

Flammable material: Solid, liquid or gaseous substance, preparation, and substance with occurrence or combination of these conditions, by its flash point, contact with other substances, pressure, temperature or other chemical properties represent a danger of fire.

Reactive substances: Solid, liquid, or gaseous substances, preparations and substances that occur in combinations of these conditions, which on contact with water, by its pressure, temperature or chemical conditions, represents a potentially dangerous reaction, explosion or release of hazardous gas, steam, dust or fog.

Pressurized : Other solid, liquid or gaseous substance or mixes having fire or hazardous material response, when under pressure, and thus may represent a risk of uncontrolled emissions

Further criteria for the classification of flammable, reactive and pressurized substances are set out in Annex 1 of the Guide to the Regulations "Flammable, reactive and pressurized substances"

http://www.dsb.no/Global/Publikasjoner/2009/Veiledning/Generell%20veiledning.pdf

http://www.dsb.no/Global/Publikasjoner/2010/Tema/Temaveiledning_bruk_av_farlig_stoff_Del_1.pdf

Experiment setup area should be reviewed with respect to the assessment of Ex zone
• Zone 0: Always explosive atmosphere, such as inside the tank with gas, flammable liquid.
• Zone 1: Primary zone, sometimes explosive atmosphere such as a complete drain point
• Zone 2: secondary discharge could cause an explosive atmosphere by accident, such as flanges, valves and connection points

7.4 Effects on the environment

With pollution means: bringing solids, liquid or gas to air, water or ground, noise and vibrations, influence of temperature that may cause damage or inconvenience effect to the environment.

Regulations: http://www.lovdata.no/all/hl-19810313-006.html#6

NTNU guidance to handling of waste:http://www.ntnu.no/hms/retningslinjer/HMSR18B.pdf

7.5 Radiation

Definition of radiation

Ionizing radiation: Electromagnetic radiation (in radiation issues with wawelength <100 nm) or rapid atomic particles (e.g. alpha and beta particles) with the ability to stream ionized atoms or molecules.

Non ionizing radiation: Electromagnetic radiation (wavelength >100 nm), og ultrasound[1] with small or no capability to ionize.

Radiation sources: All ionizing and powerful non-ionizing radiation sources.

Ionizing radiation sources: Sources giving ionizing radiation e.g. all types of radiation sources, x-ray, and electron microscopes.

Powerful non ionizing radiation sources: Sources giving powerful non ionizing radiation which can

harm health and/or environment, e.g. class 3B and 4. MR_2 systems, UVC_3 sources, powerful IR $sources_4$.

$_1$Ultrasound is an acoustic radiation ("sound") over the audible frequency range (> 20 kHz). In radiation protection regulations are referred to ultrasound with electromagnetic non-ionizing radiation.

$_2$MR (e.g. NMR) - nuclear magnetic resonance method that is used to "depict" inner structures of different materials.

$_3$UVC is electromagnetic radiation in the wavelength range 100-280 nm.

$_4$IR is electromagnetic radiation in the wavelength range 700 nm - 1 mm.

For each laser there should be an information binder (HMSRV3404B) which shall include:

- General information
- Name of the instrument manager, deputy, and local radiation protection coordinator
- Key data on the apparatus
- Instrument-specific documentation
- References to (or copies of) data sheets, radiation protection regulations, etc.
- Assessments of risk factors
- Instructions for users
- Instructions for practical use, startup, operation, shutdown, safety precautions, logging, locking, or use of radiation sensor, etc.
- Emergency procedures
- See NTNU for laser: http://www.ntnu.no/hms/retningslinjer/HMSR34B.pdf

7.6 The use and handling of chemicals.

In the meaning chemicals, a element that can pose a danger to employee safety and health

See: http://www.lovdata.no/cgi-wift/ldles?doc=/sf/sf/sf-20010430-0443.html

Safety datasheet is to be kept in the HSE binder for the experiment set up and registered in the database for chemicals.

Chapter 8 Assessment of operational procedures.

Ensures that established procedures meet all identified risk factors that must be taken care of through operational barriers and that the operators and technical performance have sufficient expertise.

8.1 Procedure Hazop

Procedural HAZOP is a systematic review of the current procedure, using the fixed HAZOP methodology and defined guidewords. The procedure is broken into individual operations (nodes) and analyzed using guidewords to identify possible nonconformity, confusion or sources of inadequate performance and failure.

8.2 Procedure for running experiments and emergency shutdown.

Have to be prepared for all experiment setups.

The operating procedure has to describe stepwise preparation, startup, during and ending conditions of an experiment. The procedure should describe the assumptions and conditions for starting, operating parameters with the deviation allowed before aborting the experiment and the condition of the rig to be abandoned.

Emergency procedure describes how an emergency shutdown have to be done, (conducted by the uninitiated),

what happens when emergency shutdown, is activated. (electricity / gas supply) and

which events will activate the emergency shutdown (fire, leakage).

Chapter 9 Quantifying of RISK

Quantifying of the residue hazards, Risk matrix

To illustrate the overall risk, compared to the risk assessment, each activity is plotted with values for the probability and consequence into the matrix. Use task IDnr.
Example: If activity IDnr. 1 has been given a probability 3 and D for consequence the risk value become D3, red. This is done for all activities giving them risk values.
In the matrix are different degrees of risk highlighted in red, yellow or green. When an activity ends up on a red risk (= unacceptable risk), risk reducing action has to be taken

CONSEQUENCES	Catastrophic	E1	E2	E3	E4	E5
	Major	D1	D2	D3	D4	D5

	Moderate	C1	C2	C3	C4	C5
	Minor	B1	B2	B3	B4	B5
	Insignificant	A1	A2	A3	A4	A5
		Rare	Unlikely	Possible	Likely	Almost
		PROBABILITY				

Table 8. Risk's Matrix

COLOUR		DESCRIPTION
Red		Unacceptable risk Action has to be taken to reduce risk
Yellow		Assessment area. Actions has to be considered
Green		Acceptable risk. Action can be taken based on other criteria

Table 9. The principle of the acceptance criterion. Explanation of the colors used in the matrix

Attachment to Risk Assessment report

Diffuser experiment with air curtain and co-flow

Prosjektnavn	performance of a combined downward jet for protected zone ventilation reducing exposure risk of occupants to indoor pollutants.
Apparatur	Klimarom VA-lab
Enhet	NTNU
Apparaturansvarlig	Guangyu Cao
Prosjektleder	Guangyu Cao
HMS-koordinator	Morten Grønli
HMS-ansvarlig (linjeleder)	Olav Bolland
Plassering	Klimarom, Varmetekniske laboratorier
Romnummer	C247C, 2. etg i klimalab, Varmetekniske laboratorier
Risikovurdering utført av	Inge Håvard Rekstad

TABLE OF CONTENTS

13 ATTACHMENT A: PROCESS AND INSTRUMENTATION DIAGRAM

14   ATTACHMENT B: HAZOP TEMPLATE

Project: performance of a combined downward jet for protected zone ventilation reducing exposure risk of occupants to indoor pollutants. Node: 1						Page	
Ref	**Guideword**	**Causes**	**Consequences**	**Safeguards**	**Recommendations**	**Action**	**Date/Sign**
Not likely	No flow	Pipe is blocked/bent	Fan wear. Will create under pressure in working part of pipe	Use flow meter by fan and at outlet. Make sure the flow levels are approximately the same	Check the duct set up before turning on the fan. Check flow meters	Turn off the fan again and follow the recommendations	
Not likely	Reverse flow	Fan runs the wrong way	Faulty measurements during experiment	Check that the flow from the fan is correct	Adjust the fan speed and direction of rotation to the desired setting	Turn off the fan again and follow the recommendations	
Low risk	More flow	Fan runs too fast	Faulty measurements during experiment		Adjust the fan speed to the correct speed	Adjust the fan speed to the correct speed	
Low risk	Less flow	Fan runs too slow	Faulty measurements during experiment		Adjust the fan speed to the correct speed	Adjust the fan speed to the correct speed	

Project: performance of a combined downward jet for protected zone ventilation reducing exposure risk of occupants to indoor pollutants. Node: 1						Page	
Ref	Guideword	Causes	Consequences	Safeguards	Recommendations	Action	Date/Sign

Project: performance of a combined downward jet for protected zone ventilation reducing exposure risk of occupants to indoor pollutants. Node: 1						Page	
Ref	Guideword	Causes	Consequences	Safeguards	Recommendations	Action	Date/Sign

15 ATTACHMENT C: TEST CERTIFICATE FOR LOCAL PRESSURE TESTING

Trykkpåkjent utstyr:	
Benyttes i rigg:	
Design trykk for utstyr (bara):	
Maksimum tillatt trykk (bara): (i.e. burst pressure om kjent)	
Maksimum driftstrykk i denne rigg:	

Prøvetrykket skal fastlegges i følge standarden og med hensyn til maksimum tillatt trykk.

Prøvetrykk (bara):			
X maksimum driftstrykk: I følge standard			
Test medium:			
Temperatur (°C)			
Start tid:		Trykk (bara):	
Slutt tid:		Trykk (bara):	
Maksimum driftstrykk i denne rigg:			

Eventuelle repetisjoner fra atm. trykk til maksimum prøvetrykk:……………

Test trykket, dato for testing og maksimum tillatt driftstrykk skal markers på (skilt eller innslått)

_____   _____

Sted og dato   Signatur

16 ATTACHMENT D: HAZOP PROCEDURE (TEMPLATE)

Project:						Page	
Node: 1							
Ref#	Guideword	Causes	Consequences	Safeguards	Recommendations	Action	Date/Sign
	Not clear procedure	Procedure is to ambitious, or confusingly					
	Step in the wrong place	The procedure can lead to actions done in the wrong pattern or sequence					
	Wrong actions	Procedure improperly specified					
	Incorrect information	Information provided in advance of the specified action is wrong					
	Step missing	Missing step, or step requires too much of operator					
	Step unsucessful	Step has a high probability of failure					
	Influence and	Procedure's performance can					

Project:						Page	
Node: 1							
Ref#	Guideword	Causes	Consequences	Safeguards	Recommendations	Action	Date/Sign
	effects from other	be affected by other sources					

17 ATTACHMENT E: PROCEDURE FOR RUNNING EXPERIMENTS

Prosjekt		Signatur
Energilabprosjekt : EKB-Lab: Diffuser co flow (Jonas Fuglseth)		
performance of a combined downward jet for protected zone ventilation reducing exposure risk of occupants to indoor pollutants.	**Dato**	
Apparatur		
Diffuser experiment with air curtain and LAF co-flow		
Prosjektleder		
Guangyu Cao		

	Conditions for the experiment:	Completed
	Experiments should be run in normal working hours, 08:00-16:00 during winter time and 08.00-15.00 during summer time. Experiments outside normal working hours shall be approved.	
	One person must always be present while running experiments, and should be approved as an experimental leader.	
	An early warning is given according to the lab rules, and accepted by authorized personnel.	
	Be sure that everyone taking part of the experiment is wearing the necessary protecting equipment and is aware of the shut down procedure and escape routes.	
	Preparations	**Carried out**
	Post the "Experiment in progress" sign.	
	Hang up black blanket (to be able to see smoke profile)	
	Turn on the fan to supply air through the diffuser nozzle, and check outlet velocity at 10 different locations that the flow has an even velocity	

	Measure initial air temperature in the room. Check at 3-4 different heights to be sure there is little thermal stratification	
	Set LAF speed to 0.75m/s (or 1m/s – multiple speeds tested)	
	Set curtain speed to 1.5m/s	
	During the experiment	
	Measure velocity at all relevant locations	
	Check that the temperature in the room is the same as the air curtain temperature.	
	End of experiment	
	Turn off fans and heat source	
	Remove all obstructions/barriers/signs around the experiment.	
	Tidy up and return all tools and equipment.	
	Tidy and cleanup work areas.	
	Return equipment and systems back to their normal operation settings (fire alarm)	
	To reflect on before the next experiment and experience useful for others	
	Was the experiment completed as planned and on scheduled in professional terms?	
	Was the competence which was needed for security and completion of the experiment available to you?	
	Do you have any information/ knowledge from the experiment that you should document and share with fellow colleagues?	

Operator(s):

Navn	Dato	Signatur

18 ATTACHMENT F: TRAINING OF OPERATORS

Prosjekt	Dato	Signatur
Apparatur		
Prosjektleder		

	Knowledge about EPT LAB in general	
	Lab • Access • routines and rules • working hour	
	Knowledge about the evacuation procedures.	
	Activity calendar for the Lab	
	Early warning, **iept-experiments@ivt.ntnu.no**	
	Knowledge about the experiments	
	Procedures for the experiments	
	Emergency shutdown.	
	Nearest fire and first aid station.	

I hereby declare that I have read and understood the regulatory requirements has received appropriate training to run this experiment and are aware of my personal responsibility by working in EPT laboratories.

Operator(s):

Navn	Dato	Signatur

19   ATTACHMENT G: FORM FOR SAFE JOB ANALYSIS

SJA name:	
Date:	Location:
Mark for completed checklist:	

Participators:		
SJA-responsible:		

Specification of work (What and how?):
Risks associated with the work:
Safeguards: (plan for actions, see next page):
Conclusions/comments:

Recommended/approved	Date/Signature:	Recommended/approved	Date/Signature:
SJA-responsible:		HSE responsible:	

Responsible for work:		Other, (position):	

HSE aspect	Yes	No	NA	Comments / actions	Resp.
Documentation, experience, qualifications					
Known operation or work?					
Knowledge of experiences / incidents from similar operations?					
Necessary personnel?					
Communication and coordinating					
Potential conflicts with other operations?					
Handling of an eventually incident (alarm, evacuation)?					
Need for extra assistance / watch?					
Working area					
Unusual working position					
Work in tanks, manhole?					
Work in ditch, shaft or pit?					
Clean and tidy?					
Protective equipment beyond the personal?					
Weather, wind, visibility, lighting, ventilation?					
Usage of scaffolding/lifts/belts/ straps, anti-falling device?					
Work at hights?					
Ionizing radiation?					
Influence of escape routes?					
Chemical hazards					
Usage of hazardous/toxic/corrosive chemicals?					
Usage of flammable or explosive chemicals?					
Risk assessment of usage?					

Biological materials/substances?					
Dust/asbestos/dust from insulation?					
Mechanical hazards					
Stability/strength/tension?					
Crush/clamp/cut/hit?					
Dust/pressure/temperature?					
Handling of waste disposal?					
Need of special tools?					
Electrical hazards					
Current/Voltage/over 1000V?					
Current surge, short circuit?					
Loss of current supply?					
Area					
Need for inspection?					
Marking/system of signs/rope off?					
Environmental consequences?					
Key physical security systems					
Work on or demounting of safety systems?					
Other					

20 APPARATURKORT / UNITCARD

Dette kortet SKAL henges godt synlig på apparaturen!

This card MUST be posted on a visible place on the unit!

Apparatur (Unit)	
Diffuser experiment with air curtain and LAF co-flow	
Prosjektleder (Project Leader)	**Telefon mobil/privat** (Phone no. mobile/private)
Guangyu Cao	+4791897689
Apparaturansvarlig (Unit Responsible)	**Telefon mobil/privat** (Phone no. mobile/private)
Guangyu Cao	+4747361023

Sikkerhetsrisikoer (Safety hazards)
Ingen nevneverdige

Sikkerhetsregler (Safety rules)
Vifter og dukke skal være avskrudd når de ikke er i bruk

Nødstopp prosedyre (Emergency shutdown)
Skru av vifter og termisk dukke

Her finner du (Here you will find):

Prosedyrer (Procedures)	I rommet

Bruksanvisning (Users manual)	I rommet

Nærmeste (Nearest)

Brannslukningsapparat (fire extinguisher)	1. etasje VVSLab(syd)
Førstehjelpsskap (first aid cabinet)	1. etasje VVSLab(syd)

NTNU

Institutt for energi og prosessteknikk

SINTEF Energi

Avdeling energiprosesser

Dato

Dato

Signert

Signert

21   FORSØK PÅGÅR /EXPERIMENT IN PROGRESS

Dette kortet SKAL henges opp før forsøk kan starte!

This card MUST be posted on the unit before the experiment startup!

Apparatur (Unit)	
Diffuser experiment with air curtain	
Prosjektleder (Project Leader)	**Telefon mobil/privat** (Phone no. mobile/private)
Guangyu Cao	+4791897689
Apparaturansvarlig (Unit Responsible)	**Telefon mobil/privat** (Phone no. mobile/private)
Guangyu Cao	+4791897689
Godkjente operatører (Approved Operators)	**Telefon mobil/privat** (Phone no. mobile/private)
Jonas Fuglseth	+4792461567

Prosjekt (Project)

Energilabprosjekt : EKB-Lab: Diffuser co-flow (Jonas Fuglseth)

Performance of a combined downward jet for protected zone ventilation reducing exposure risk of occupants to indoor pollutants.

Forsøkstid / Experimental time (start - stop)

08.12.16 - 01.07.17

Kort beskrivelse av forsøket og relaterte farer (Short description of the experiment and related hazards**)**

Måling av hastighetsprofil til luftgardin med medstrøm luft på èn side. Ingen relaterte farer. Dør skal være lukket under forsøket.

NTNU

Institutt for energi og prosessteknikk

Dato

Signert

SINTEF Energi

Avdeling energiprosesser

Dato

Signert

Appendix C – Outlet velocities

Measurement results in all tables are [m/s]

Avg=0,41m/s	P1	P2	P3	P4	P5	P6	P7	P8	P9
S1 (70cm)	0,61	0,38	0,37	0,54	0,72	0,72	0,61	0,43	0,67
S2 (40cm)	0,11	0,27	0,15	0,26	0,48	0,18	0,26	0,33	0,35
S3 (5cm)	0,62	0,3	0,41	0,48	0,38	0,26	0,25	0,27	0,68
Slot	0,61	0,65	0,65	0,67	0,7	0,64	0,61	0,56	0,62
AVG=	0,63								

Table C.1 - Vr=1.5

Avg=0,41	p1	p2	p3	p4	p5	p6	p7	p8	p9
S1 (70cm)	0,61	0,38	0,37	0,54	0,72	0,72	0,61	0,43	0,67
S2 (40cm)	0,11	0,27	0,15	0,26	0,48	0,18	0,26	0,33	0,35
S3 (5cm)	0,62	0,3	0,41	0,48	0,38	0,26	0,25	0,27	0,68
Slot	0,93	0,99	1	0,99	1,05	1,01	0,91	0,99	1,03
Avg=0,99									

Table C.2 - Vr=2.5

Avg=0,44	p1	p2	p3	p4	p5	p6	p7	p8	p9
S1 (70cm)	0,61	0,38	0,55	0,53	0,34	0,31	0,2	0,3	0,72
S2 (40cm)	0,17	0,44	0,14	0,31	0,6	0,17	0,15	0,32	0,4
S3 (5cm)	0,53	0,48	0,45	0,51	0,56	0,72	0,66	0,56	0,82
Slot	1,48	1,56	1,54	1,44	1,45	1,55	1,54	1,44	1,39
Avg=1,49									

Table C.3 - Vr=3

Avg=0,21	p1	p2	p3	p4	p5	p6	p7	p8	p9
S1 (70cm)	0,3	0,15	0,18	0,2	0,25	0,19	0,13	0,14	0,27
S2 (40cm)	0,06	0,2	0,1	0,16	0,22	0,12	0,13	0,28	0,18
S3 (5cm)	0,22	0,18	0,2	0,21	0,29	0,32	0,26	0,28	0,37
Slot	1,55	1,48	1,59	1,55	1,58	1,57	1,45	1,4	1,5
Avg=1,52									

Table C.4 - Vr=7.5 1

Avg=0,92	p1	p2	p3	p4	p5	p6	p7	p8	p9
S1 (70cm)	1,47	0,79	0,9	0,94	1,13	0,65	0,4	0,74	1,59
S2 (40cm)	0,19	0,65	0,3	0,72	1,13	0,21	0,35	0,75	0,5
S3 (5cm)	1,51	0,71	0,92	1,06	1,55	0,94	1,33	1,31	2,09

Table C.5 - Perforated plate, 1.0 m/s

Avg=0,63	p1	p2	p3	p4	p5	p6	p7	p8	p9
S1 (70cm)	0,82	0,44	0,65	0,83	0,81	0,54	0,34	0,4	1,1
S2 (40cm)	0,15	0,45	0,2	0,5	0,76	0,2	0,24	0,59	0,39
S3 (5cm)	0,78	0,43	0,6	0,75	0,94	0,99	0,8	0,85	1,45

Table C.6 - Perforated plate, 0.75 m/s

Avg=0,47	p1	p2	p3	p4	p5	p6	p7	p8	p9
S1 (70cm)	0,52	0,4	0,4	0,61	0,52	0,4	0,23	0,3	0,83
S2 (40cm)	0,2	0,43	0,19	0,45	0,59	0,14	0,24	0,41	0,31
S3 (5cm)	0,68	0,42	0,56	0,54	0,55	0,8	0,45	0,65	0,95

Table C.7 - Perforated plate, 0.5 m/s

Avg=0,2	p1	p2	p3	p4	p5	p6	p7	p8	p9
S1 (70cm)	0,23	0,14	0,21	0,19	0,19	0,21	0,13	0,16	0,25
S2 (40cm)	0,06	0,19	0,11	0,15	0,27	0,15	0,17	0,2	0,19
S3 (5cm)	0,21	0,2	0,2	0,23	0,27	0,3	0,23	0,22	0,28

Table C.8 - Perforated plate, 0.2 m/s

Avg=1,54	P1	P2	P3	P4	P5	P6	P7	P8	P9
Slot	1,45	1,48	1,63	1,52	1,72	1,64	1,47	1,42	1,49

Table C.9 - Slot diffuser, 1.5 m/s

Appendix D – Photos

Following are photos taken in preparation to and during experiments.
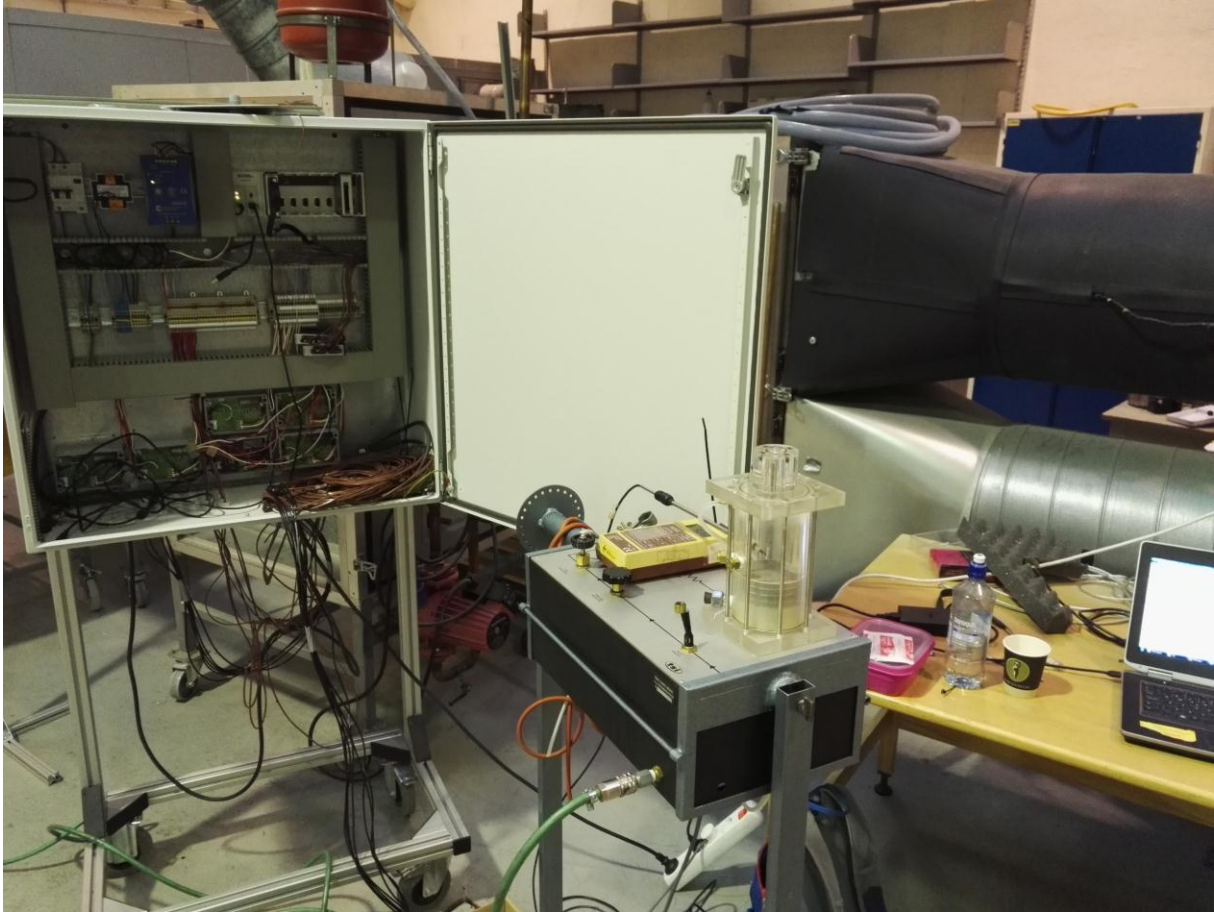

Figure D.1 - Calibration of anemometers that were not used during measurements

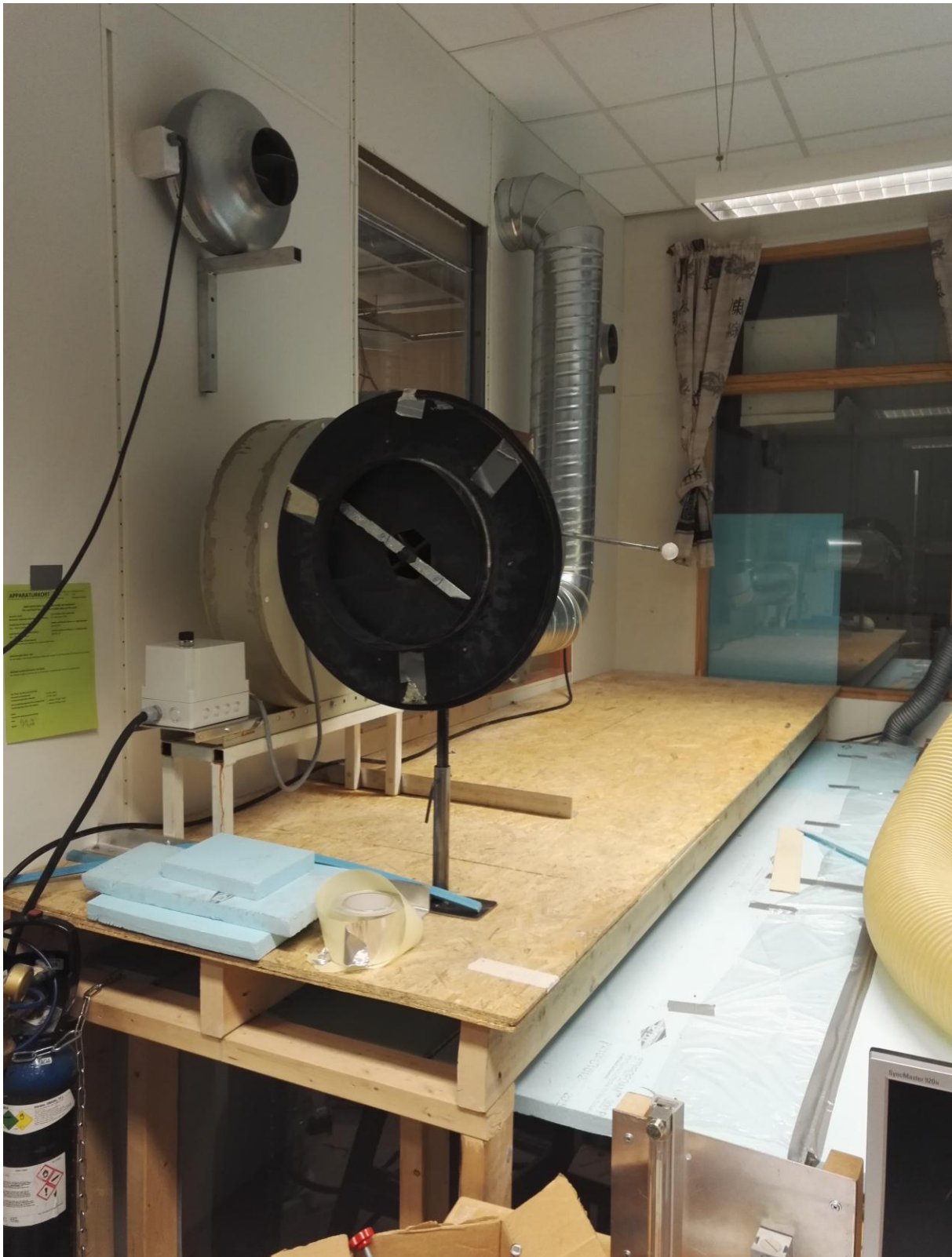*Figure D.2 - Configuration of the two diffusers*

Figure D.3 - Supply fan for the perforated plate diffuser with its aperture set to its lowest setting of 0.2 m/s

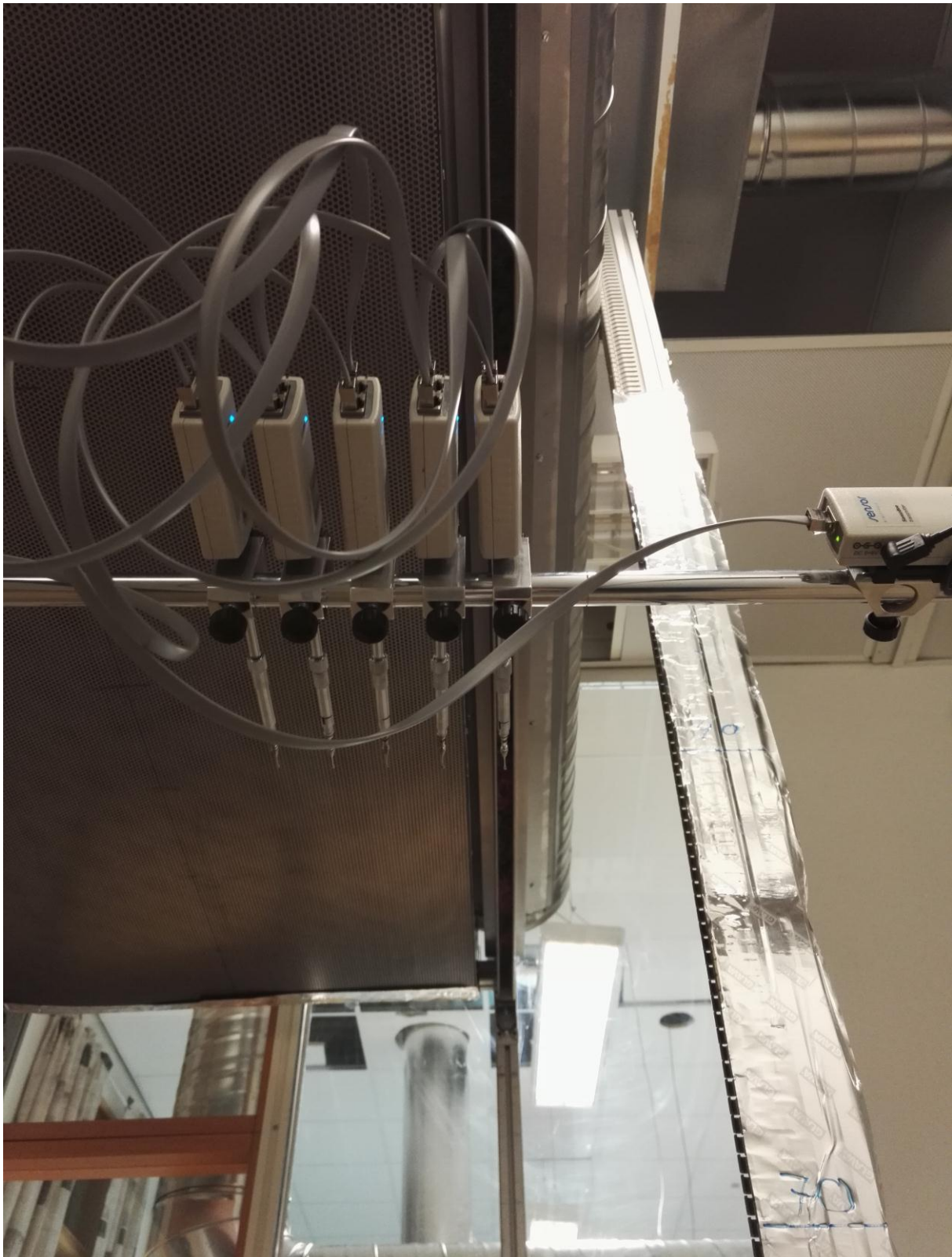*Figure D.4 - Placement of the air distribution measurement equipment*

Figure D.5 - Allignment of probes to the center axis of the plane jet